ABSTRACT

Title of Thesis:	IMPACT OF PERIODIC HIGH CONCENTRATIONS OF SALTS ON BIORETENTION NUTRIENTS PERFORMANCE
	Meigan McManus, Master of Science, 2018
Thesis Directed By:	Dr. Allen P. Davis, Civil and Environmental Engineering

Bioretention is a stormwater control measure commonly used to remove pollutants, including nitrogen (N) and phosphorus (P), from urban runoff. This project seeks to evaluate the impacts of high concentrations of sodium chloride (NaCl) deicer on bioretention N and P removal performances. Bioretention mesocosm studies were conducted to examine N and P removal efficiencies following periodic 2,000, 5,000, and 10,000 mg/L NaCl salt applications. Episodic washouts of TSS, N and P, likely due to ion exchange with the sodium and chloride ions, were observed for all three columns and mass export of P was observed for the 2,000 and 5,000 mg/L NaCl columns after 26 m and 7 m applied water, respectively. No mass N export was observed. Based on a mass balance of N and P, it is recommended to limit the use of deicers to prevent long-term P export.

IMPACT OF PERIODIC HIGH CONCENTRATIONS OF SALTS ON BIORETENTION NUTRIENTS PERFORMANCE

by

Meigan McManus

Thesis submitted to the Faculty of the Graduate School of the
University of Maryland, College Park, in partial fulfillment
of the requirements for the degree of
Master of Science
2018

Advisory Committee:
Professor Allen P. Davis, Chair
Professor Alba Torrents
Assistant Professor Birthe Kjellerup

Acknowledgements

I would like to thank the Maryland State Highway Administration for their financial support of this project and the University of Maryland, specifically the Research Greenhouse Complex and the Inorganic Pollutants Research Laboratory, for the use of their facilities and resources. I would like to thank Stancills Inc. and Pope Farm Nursery for their donations of materials.

Thank you to my peers, family, and friends who have provided advice and support for this project. Thank you to my committee members, Dr. Torrents and Dr. Kjellerup, for providing guidance.

Lastly, I would like to thank Dr. Davis, who has provided unwavering support and mentorship since the beginning of this project.

Table of Contents

List of Tables

List of Figures

Chapter 1: Introduction

The Federal Clean Water Act requires states to establish water quality standards (WQS) and total maximum daily loads (TMDLs) for water bodies that do not meet WQS (Maryland State Highway Administration 2017a). A TMDL is the maximum amount of a pollutant a water body can assimilate and still meet WQS. The United States Environmental Protection Agency enforces the standards through the National Pollutant Discharge Elimination System program (NPDES), which regulates pollutant discharges (Maryland State Highway Administration n.d.). Pollutants of particular interest in the Chesapeake Bay watershed include nitrogen and phosphorus, and additional pollutant reduction goals can include heavy metals. Stormwater control measures (SCMs) are practices used to meet TMDL pollutant reductions. Maryland State Highway Administration (SHA) is required to adhere to MD water quality standards under a Municipal Separate Storm Sewer (MS4) permit and uses SCMs in order to decrease pollutant loads from impervious highways (Maryland State Highway Administration 2017a, n.d.).

As a result of urbanization, increased impervious areas have resulted in increased runoff and decreased water quality (Dietz 2007). Urban stormwater contains nitrogen (N) and phosphorus (P) from fertilizers, automobile exhaust, and detergents; as a result of excess N and P inputs, eutrophication and algal blooms may occur in receiving water bodies. N and P concentrations in urban areas have been reported to be around 2.9 mg-N/L and 0.3 mg-P/L, respectively. In particular, road highway N and P runoff concentrations have been reported as 5.5 mg-N/L and 0.6

mg-P/L (Stagge et al. 2012). Bioretention studies report 41% mass load reductions for TN and 55% for TP (Li and Davis 2014; Liu and Davis 2014).

Bioretention systems are among the most common SCMs, since bioretention systems mitigate peak flows and reduce runoff volumes in addition to reducing pollutant loads from influent runoff (Davis et al. 2009). Bioretention systems contain an engineered bioretention soil media (BSM), comprised of sand, soil, and organic matter, and the BSM reduces pollutant loads by filtering influent stormwater (Figure 1). As polluted influent infiltrates through the BSM, many pollutants are removed via sedimentation, adsorption, and biological processes (Davis et al. 2009; Maryland State Highway Administration 2017a). Depending on the design of the bioretention system, effluent may be returned to the conveyance system or infiltrate through the surrounding soils.

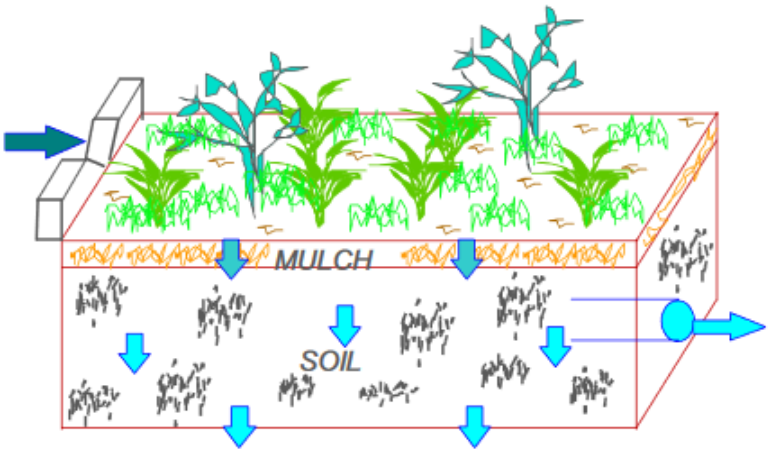

Figure 1. Schematic of a bioretention system (Davis et al. 2009).

However, much of the research related to bioretention performance in the past decade has not focused specifically on performance during winter months. In the winter, roadway deicers are applied preceding and during snow, ice, and freezing

roadway events in order to ensure the safety of highway networks, Right-of-Way surroundings, and supporting infrastructure. The US EPA (2010) estimates approximately 15 million tons of deicing salts are used each year, and sodium chloride (NaCl) is the most common as it is the cheapest option for municipalities. While NaCl is effective in melting ice and snow, its impact on bioretention systems and performance is not clear.

The effects of salts on soil structure are well-documented in sodic/saline soil literature. Sodic conditions occur when there are high levels of exchangeable sodium and are associated with a decline of soil structure (Wong et al. 2010). When there is a large concentration of sodium ions in a soil, the resulting electrical repulsive forces increase the diffuse double layer and result in clay dispersion (Qadir and Schubert 2002). Colloid-assisted transport of pollutants may occur as a result. In addition, the cations may be released due to ion exchange between positively charged pollutants and sodium ions (Nelson et al. 2009; Norrström and Bergstedt 2010; Tedoldi et al. 2016). Unlike sodium ions, as an anion, chloride is not held in soils as soils typically carry a net negative charge. Chloride can create complexes with metals and organic matter (Norrström 2005; Nelson et al. 2009), likewise causing mobilization. The persistence of chloride from winter road salts in SCMs has been observed to last through to late summer months (Borst and Brown 2014; Drake et al. 2014; Winston et al. 2016; Robinson et al. 2017), which demonstrates the need to better understand and quantify year-long performance of SCMs in cold climates.

Many previous studies concerning SCMs and high salt concentrations focused on the effects of pH and temperature on heavy metals removal. Heavy metals may

enter stormwater from car brake pads, engine parts, tire wear, and fuel combustion (Nelson et al. 2009). Some studies have found that salt will increase metal mobility in bioretention systems (Endreny et al. 2012; Paus et al. 2014), although other studies have found that salt did not (Denich et al. 2013). Interestingly, Paus et al. (2014) notes that while sorbed metals may be released due to increased salt applications, the released metals are "not expected to be a significant problem."

Existing studies related to SCMs and high salt concentrations in winter months reveal little about nitrogen and phosphorus removal. Denich et al. (2013) spiked bioretention columns with an equivalent of two years' loading of salt (2,430 g of a locally used deicer) and flushed the columns with deionized water. No phosphorus removal from the stormwater was observed while nitrate was the only nitrogen species found to be removed, with removal efficiencies as high as 88%. In a study of roadside wetlands, a decrease in denitrification rates was observed when chloride dosages were greater than 2500 mg/L, although there was not a significant difference in rates where wetlands had been previously exposed to high concentrations of chloride (Lancaster et al. 2016). Based on the limited scope of previous research, the effect of elevated levels of salts on the concentration and the speciation of nitrogen and phosphorus species in SCM effluent can provide an understanding of seasonal variations and improve SCM design recommendations.

1.1 Research Goals and Hypotheses

This project has two primary goals: 1) To quantify and speciate nitrogen, phosphorus and total metals release in bioretention mesocosms impacted by high salt applications and 2) To understand the impact of high salt concentrations on nutrient and metal release across different types of applied salts.

To assess these goals, three individual bioretention mesocosms received salt doses of 2,000 mg/L, 5,000 mg/L, and 10,000 mg/L NaCl, followed by synthetic stormwater applications with non-winter salt concentrations ("baseline" storms). Effluent was collected and tested for total nitrogen, total phosphorus, and various species in order to determine the relationship between applied salt concentration and nutrient and metal release. Effluent from small columns filled with BSM received different salt applications of various salts, and effluent was collected to compare release of total nitrogen and total phosphorus. The results from the mesocosm and small column studies were compared with other studies that evaluated SCM winter performance.

It is hypothesized that road salt will cause releases of N and P, and continued application of salt will prevent mass removal of the pollutants. Mesocosms receiving higher concentrations of applied NaCl will release more N, P, and metals than the 2,000 mg/L NaCl column and control column, a column that received no salt applications. Ultimately, the mesocosm and small column studies will be used to provide an understanding of the mechanisms of salt interactions and to provide MD

SHA and other MS4 permitters that use bioretention with recommendations for winter practices.

Chapter 2: Materials and Methodology

2.1 Bioretention Mesocosm Construction

An acrylic column was purchased from Piedmont Plastics in Elkridge, MD. The column has 19.1 cm inner diameter and is 122 cm long. The bottom of the column has a 14.7-degree slope leading to a 3.8 cm discharge port to prevent pooling and to allow for sample collection. At the University of Maryland Research Greenhouse Complex in College Park, Maryland, based on SHA bioretention construction recommendations (Maryland Department of the Environment 2000), the column was packed with a 7 cm layer of washed #7 gravel, a 7 cm layer of washed concrete sand, and 77 cm of State Highway 920.01.05 bioretention soil media (BSM, Appendix A-1), all from Stancills Inc., Waldorf, Maryland and Perryville, Maryland. To remove fine particles, the sand and soil were washed using tap water until the water ran clear. Each media layer was separated by a 1 mm diameter mesh fabric purchased from a local home supply store in order to reduce the migration of media and sand into subsequent layers.

A mature *Juncus effuses*, grown by Pope Farm Nursery in Gaithersburg, Maryland, was planted directly into the BSM (Figure 1). Ambient temperature in the greenhouse is kept at 24 °C for the day and night. To mimic conditions in the ground, aluminum foil was wrapped around the column to inhibit algal growth from sunlight. Periodically, the aluminum foil was peeled away to check for algal growth.

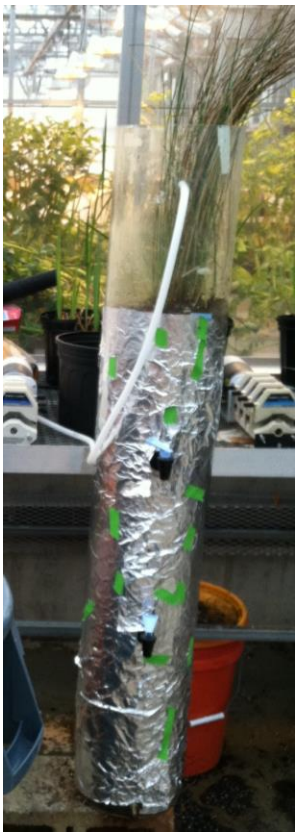

Figure 2. The bioretrention column setup in the University of Maryland Greenhouse.

2.1.1 BSM Analysis

BSM used for the 2,000 and 5,000 mg/L NaCl columns was sent to the University of Delaware Testing Program. A soil texture analysis by the Boyoucos hydrometer method (Bouyoucos 1962) and Mehlich 3 extraction (Mehlich 1984) were performed in order to determine the soil texture and cation exchange capacity (CEC) of the BSM.

Additionally, loss on ignition (LOI, Heiri et al. 2001) was determined for the BSM used for the 2,000 and 5,000 mg/L NaCl columns. The LOI method was run in triplicate and the average LOI and standard deviation were calculated. LOI for the BSM used for the control and 10,000 mg/L NaCl columns were not available and were not tested for any of the soils parameters. .

2.2 Mini Column Construction

Kimble Kontes FlexColumn Economy borosilicate glass columns were purchased from Fisher Scientific. The columns have a 2.5 cm inner diameter and are 20 cm long. The polyethylene disks at the end of each column were removed and replaced with 1 mm diameter mesh purchased from a local home supply store. The 20 cm columns were filled with 15 cm of State Highway 920.01.05 BSM and the remaining headspace was filled with washed sand, all from Stancills Inc., Waldorf, Maryland and Perryville, Maryland. The columns were kept at room temperature at the University of Maryland Environmental Engineering Laboratory Research Facility. Masterflex Precision tubing was attached to the end caps, and the columns were taped against a ring stand to allow for sufficient room above and below the columns for sample collection (Figure 3).

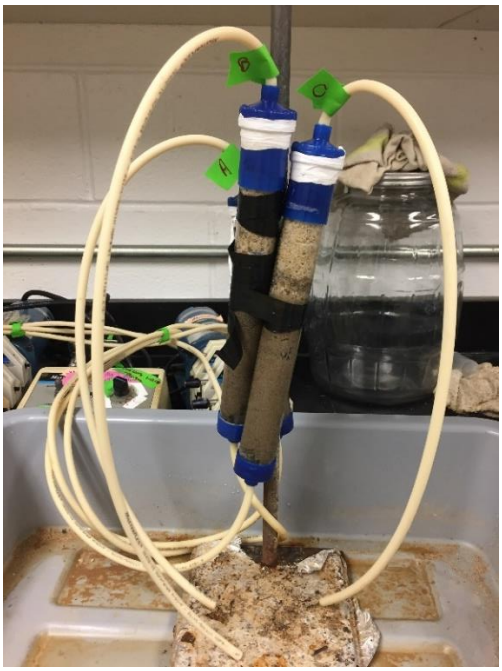

Figure 3. Mini column construction in the University of Maryland Environmental Engineering Laboratory Research Facility.

2.3 Synthetic Stormwater Preparation

Synthetic stormwater based on the recipe by O'Neill and Davis (2012) was mixed prior to each mesocosm trial. Tap water from the University of Maryland Greenhouse Research Complex was used to make synthetic stormwater. Additional N and zinc (Zn) were added based on tap water concentrations in order to reproduce the concentrations from the original recipe (Table 1). Sodium bisulfate ($NaHSO_3$) was added to minimize effects of chlorine in the tap water. Diamond Crystal Salt, a water softener NaCl purchased at a local home supply store, was used for road salt events. NaCl concentrations applied to the mesocosms were 2,000 mg/L, 5,000 mg/L, and 10,000 mg/L NaCl.

Table 1. Makeup of synthetic stormwater used in this study (O'Neill and Davis 2012).

Component	**Value**	**Source**	**Manufacturer**
pH	7.0	HCl or NaOH	Fisher Science
Inorganic nitrogen: NO_3^-	1 mg/L as N	$NaNO_3$	AMRESCO
Organic N	2 mg/L as N	Glycine	Alfa Aesar
Phosphorus	0.2 mg/L as P	Na_2HPO_4	N/A
Copper	0.06 mg/L	$CuCl_2$	N/A
Zinc	0.5 mg/L	$ZnCl_2$	AMRESCO
Dissolved solids (salts)	20 mg/L to 10,000 mg/L	NaCl	Diamond Crystal (high salt), Fisher Science (baseline)

Mini columns received the same synthetic stormwater recipe based on O'Neill and Davis (2012). Tap water from the University of Maryland Environmental Engineering Laboratory Research Facility was used to make the synthetic stormwater,

with N, Zn, copper (Cu), and sodium bisulfite ($NaHSO_3$). All salt applications were run in triplicate, with each set of columns receiving different salts of NaCl, KCl, LiCl, $MgCl_2$, $CaCl_2$, NaBr, and NaF. Influent salt concentrations were adjusted to be the equivalent ionic strength of 0.09 M (5,000 mg/L) NaCl using

$$I = \frac{1}{2}\sum_{i=1}^{n} c_i z_i^2 \qquad \text{[Eq 1.]}$$

where I is ionic strength, c is the molar concentration of the ion, and z is the charge of the ion. A summary of the salts used for high salt events is provided in Table 2.

Table 2. Masses of salts used in mini column studies for high salt events. 1 L of synthetic stormwater was prepared based on the recipe by O'Neill and Davis (2012).

Salt	**Mass (g)**	**Manufacturer**
NaCl	5.0	Diamond Crystal (high salt), Fisher Science (baseline)
KCl	6.4	VWR International
LiCl	3.6	Alfa Aesar
$MgCl_2$	2.7	JT Baker
$CaCl_2$	3.2	Fisher Science
NaBr	8.8	Sigma Aldrich
NaF	3.6	Alfa Aesar

2.4 Mesocosm Trials and Sampling

The median rainfall duration in Maryland is 6 hours and the median depth is 0.71 cm (Kreeb 2003). To analyze the system under stressed conditions, a 5 cm rainfall depth was used. Over 6 hours, the rainfall rate is 0.83 cm/hour which is increased to 16.7 cm/hour to account for an assumed 20:1 drainage area-to-SCM ratio.

Mesocosms received influent synthetic stormwater at the rate of 16.7 cm/hour for six hour intervals, with each six hour interval representing a storm event. The first four storm events used 20 mg/L NaCl ("baseline" storms) in order to determine effluent concentrations prior to high salt events. After the first four baseline events, the mesocosms received synthetic stormwater sets of one high salt event followed by five baseline storms. The five baseline storms were done to simulate runoff conditions after road salt applications.

Initially, samples were collected immediately after effluent exited the port at the bottom of the column, 30 minutes and 60 minutes after the exit time, and subsequently every hour for the remaining duration of the storm. After the influent stopped, an additional sample was collected beyond the period of the 6-hour storm. Eight to ten samples were collected during each storm.

Following the 15^{th} and 14^{th} m of applied water for the 2,000 and 5,000 mg/L NaCl columns, respectively, effluent characteristics followed similar enough patterns to reduce sampling size to four samples per storm. Sampling times were reduced to the initial effluent, 30 minutes after the exit time, halfway through the six hour storm, and at the end of the six hour storm. If influent pooled in the column to the point where the column may overflow, the inflow rate was adjusted to equal the outflow rate. If the outflow rate was less than 0.1 mL/s, then the influent was stopped until the head had dropped at least an inch.

The pH, conductivity, and temperature were recorded using a VWR sympHony multi-meter model B40PCID and accompanying conductivity electrode model 89231-618 and RedRod pH electrode model 89231-586. The flow rate was

measured with a graduated cylinder and stopwatch. Tap water samples and synthetic stormwater samples taken at the beginning, halfway point, and end of the 6-hour period were collected to analyze the composition of the influent throughout the storm. All samples were frozen in the University of Maryland Environmental Laboratory Research Facility in College Park, Maryland until analyzed. Analytical methods for runoff analysis are presented in Table 3.

Table 3. Analytical methods for analysis of synthetic stormwater influent and effluent samples.

Parameter	**Method**	**Standard method**	**Detection limit**	**Accuracy**
pH	pH probe and meter	4500-H+B	pH range 2-11	0.01 unit
Conductivity	Conductivity probe and meter	2510-B	Conductivity range 0 to 3000 mS/cm	0.01 µS/cm
Total suspended solids (TSS)	Gravimetric	2540-D	1 mg/L	1 mg/L
Turbidity	Turbidimeter	ISO 7027	0.001 NTU	0.01 NTU
Total phosphorus	Digestion and spectrophotometry; ICP	4500-P B.5 4500-P E; ICPE-9000, SHIMADZU	0.01 mg/L as P ICP detection limit, 1 µg/L as P	0.01 mg/L as P
Dissolved phosphorus	Filtration, digestion, and spectrophotometry; ICP	4500-P B.5 4500-P E; ICPE-9000, SHIMADZU	0.01 mg/L as P	0.01 mg/L as P
Soluble reactive phosphorus (phosphate)	Filtration and spectrophotometry	4500-P E	0.01 mg/L as P	0.01 mg/L as P
Total nitrogen	Digestion and spectrophotometry	4500-N C	0.1 mg/L as N	0.01 mg/L as N

Total dissolved nitrogen	Filtration, digestion, and spectrophotometry	4500-N C	0.1 mg/L as N	0.01 mg/L as N
Nitrate	Ion chromatography	4110-NO_3-B	0.1 mg/L as N	0.01 mg/L as N
Nitrite	Spectrophotometry	4500-NO_2^-B	0.01 mg/L as N	0.01 mg/L as N
Ammonium	Spectrophotometry	4500-NH_3 F	0.05 mg/L as N	0.01 mg/L as N
Total organic carbon	Digestion and spectrophotometry	5310-TOC B	4 µg/L	4 µg/L
Total dissolved organic carbon	Filtration, digestion, and spectrophotometry	5310-TOC B	4 µg/L	4 µg/L
Copper, Zinc, Calcium, Sodium	ICP	ICPE-9000, SHIMADZU	1 µg/L for copper, zinc, and calcium 10 mg/L for sodium	

2.5 Mini Column Trials and Sampling

Mini columns were analyzed under the same stressed conditions as the mesocosms. The depth of water applied to the mini columns was scaled based on their length relative to the mesocosms. As a result of the scaling, the storm duration for the columns was 71 minutes per storm. The mini columns received 0.20 m of synthetic stormwater per storm, and similar to the mesocosms, received four baseline storms before alternating between a high salt event and five baseline storms. The columns received synthetic stormwater at least every two days to allow for intermittent draining.

For baseline storms, samples were collected when effluent initially exited the column, and approximately an hour before the storm ended for a total of two samples per column. Since collecting 125 mL of sample took approximately an hour, one sample was collected during high salt events. All samples were frozen in the University of Maryland Environmental Laboratory Research Facility in College Park, Maryland until analyzed. Analytical methods for total N and total P are presented in Table 3.

2.6 Organic Carbon Procedures

Total organic carbon (TOC) was measured on a Shimadzu TOC-L Analyzer using the TOC Measuring Unit with a detection limit of 4 µg-C/L. 40 mL samples were placed in baked glass vials (Eaton et al. 2005a). Dissolved organic carbon (DOC) was measured using samples filtered through 0.22 µm filters. Particulate organic carbon (POC) was calculated by

$$POC = TOC - DOC \quad \text{[Eq. 2]}$$

If calculations resulted in a negative concentration, the concentration was assumed to be zero.

2.7 Metals Procedures

Total metals were measured according to Eaton et al. (2005f). 70% trace metal grade nitric acid was added to 50 mL unfiltered samples and digested. Samples were diluted to 50 mL before analysis on a Shimadzu ICPE-9000, with detection limits of 1 µg/L for copper, zinc, and calcium and 10 µg/L for sodium. The Shimadzu ICPE-9000 was run under axial conditions for copper, zinc, and phosphorus. Radial

conditions were run for sodium and calcium in order to account for a higher standard range. Effluent samples from the 2,000 and 5,000 mg/L NaCl columns were analyzed for total metals every other storm event.

All influent and effluent samples from the 10,000 mg/L NaCl column did not undergo a nitric acid digestion. Instead, unfiltered samples received 0.3 mL 70% trace metal nitric acid in 10 mL of sample, resulting in a 2% acidified sample. The sample was run on the ICP-OES.

2.8 Nitrogen Procedures

For total nitrogen (TN), standards were diluted from a 1000 ppm nitrogen as nitrate stock from Fisher Scientific (CAT #:5459-16). For all storms, 40 mL of samples and standards were analyzed on a Shimadzu SSM-5000A with Total Nitrogen Measuring Unit with a detection limit of 0.01 mg-N/L (Eaton et al. 2005c).

Dissolved nitrogen (DN) measurements followed the TN procedure, using samples filtered through a 0.22 µm filter. Particulate nitrogen (PN) was calculated by

$$\mathrm{TN} - \mathrm{DN} = \mathrm{PN} \qquad \text{[Eq. 3]}$$

If calculations resulted in a negative concentration, the concentration was assumed to be zero.

To measure ammonium (NH_4^+), 10 mL samples were filtered through a 0.22 µm filter to remove suspended particles and diluted to fit the linearization of the standard curve. 10 mL standards were diluted from 5 mg/L ammonium chloride stock solution. The 4500-NH_3 F Phenate Method was used to determine the ammonium concentrations (Eaton et al. 2005d). Samples were read on a Shimadzu UV 160 UV Visible Reading Spectrophotometer with a detection limit of 0.01 mg-N/L.

To measure nitrite (NO_2^-), 10 mL of samples were filtered through a 0.22 µm filter to remove suspended particles, and prepared with 10 mL of standards, from sodium nitrite. The 4500-NO_2^--B Colorimetric Method was used to determine nitrite concentrations (Eaton et al. 2005e). Samples were read on a Shimadzu UV1560U UV Visible Recording Spectrophotometer with a detection limit of 0.01 mg-N/L NO_2^--N. NO_2^- measurements were discontinued due to interference from turbidity in samples post-salt application.

To measure nitrate (NO_3^-), samples were filtered through a 0.22 µm filter to remove suspended particles. 5 mL of samples were poured into 5.0 mL polyvials and sealed with filter caps. Nitrate standards were prepared from a 1000 ppm nitrogen as nitrate stock from Fisher Scientific (CAT #:5459-16). A 2 L anion eluent solution was prepared with 4.5 mM Na_2CO_3 from Fisher Scientific (CAT #:S223-500) and 1.4 mM $NaHCO_3$ from Fisher Scientific (CAT #:S263-500). The anion eluent solution was connected to the Dionex ICS-1100 with ASRS 4 mm suppressor and Dionex IonPac AS22 column. The samples were placed an autosampler and analyzed with the maximum sample measuring time set to 8.5 minutes. Standard checks were analyzed every eight to ten samples to monitor the consistency of the Dionex ICS-1100. If the standard checks failed (error exceeded ±10%), samples were re-tested using a new standard curve. The eluent flow in the instrument was set to 1.2 mL/min with a suppressing current of 34 mA. After the sample analysis, the baselines of peaks were adjusted if necessary.

As a result of effluent samples containing high concentrations of salts, large chloride peaks prevented detection of nitrate peaks. Effluent samples from the 5,000

mg/L Nacl column had to be diluted using a 1:10 ratio in order to detect nitrate peaks. As a result, the detection limit for the measurements increased from 0.01 to 1 mg-N/L. 10,000 mg/L NaCl effluent samples could not be diluted to produce a significant nitrate peak. 2,000 mg/L NaCl column effluent samples did not have to be diluted.

Since effluent samples from the mesocosms became turbid, NH_4^+ and NO_2^- measurements were discontinued. Dissolved Kjeldahl Nitrogen (DKN) measurements were added and calculated by

$$DN - NO_3^- = DKN \quad \text{[Eq. 4]}$$

DKN is assumed to be the summation of all dissolved organic N and ammonium. If $DN - NO_3^- \leq 0$, then DKN was assumed to be 0 mg-N/L.

2.9 Phosphorus Procedures

For all storms, the persulfate oxidation method was used to determine total phosphorus (TP), dissolved phosphorus (DP), and soluble reactive phosphorus (SRP). In addition to the samples, 40 mL standards were prepared using a stock solution of 5-ppm phosphate and digested (Eaton et al. 2005f). The samples and standards were read on a Shimadzu UV160U UV Visible Recording Spectrophotometer with a method detection limit of 0.01 mg-P/L (Murphy and Riley 1962).

To determine DP, effluent samples were filtered using a 0.22 µm filter and the same procedure for TP was used. 25 mL of filtered samples were not digested and tested with the Murphy and Riley (1962) colorimetric method to determine SRP.

Total particulate phosphorus (PP, Eq. 5) and dissolved organic phosphorus (DOP, Eq. 6) were calculated from TP, DP, and SRP measurements. If calculations resulted in a negative concentration, the concentration was assumed to be zero.

$$TP - DP = PP \quad \text{[Eq 5]}$$

$$DP - SRP = DOP \quad \text{[Eq. 6]}$$

Since samples after applying salt became turbid, TP and DP effluent samples from the 2,000 and 5,000 mg/L NaCl columns were read on the ICP after the 6th and 7th m applied water, respectively. 50 mL samples were digested with 0.5 mg potassium persulfate, diluted to 50 mL, and analyzed using a Shimadzu ICPE-9000 with a detection limit of 1 µg-P/L. Missing ICP data is a result of the samples below detection limits, which was determined to be an unknown issue with the sample that is related to an inability to produce a peak. Since SRP could not be measured on the ICP since unfiltered samples may have clogged the machine, SRP and DOP measurements were discontinued due to turbidity in samples post-salt application.

2.10 Mass Balance

A mass balance was calculated for each column in order to determine net retention or export of TN, TP, NO_3^-, Zn, Cu, TSS, and NaCl. For NaCl concentrations, a linear relationship between conductivity and NaCl concentration was assumed. Based on a 20 mg/L NaCl storm producing a conductivity reading of 300 µS/cm and a 5,000 mg/L NaCl storm producing a conductivity reading of 9000 µS/cm, the following equation was applied to all storms to determine the NaCl concentration:

$$y = 0.5724x - 151.72 \quad \text{[Eq. 7]}$$

where y is the NaCl concentration (mg/L) and x is the conductivity (µS/cm).

NaCl, TN, and TP influent and effluent masses for each storm were calculated as

$$m = \sum_{i=1}^{n}(c * Q * \Delta t)_i \quad \text{[Eq. 8]}$$

where m is total mass (mg), c is concentration (mg/L), Q is flow rate (mL/s), and Δt is the time between samples (min). The total masses of each storm were summed in order to calculate the total mass in and out of the column.

A water balance was calculated using

$$Volume = \sum_{i=1}^{n}(Q * \Delta t) \quad \text{[Eq. 9]}$$

in order to determine the influent and effluent volumes of water.

TP and TN mass balances were estimated from the initial 9 m applied water control column data from Owen (2016). For the influent and effluent data, a linear relationship between mass and applied water was assumed. Based on the relationship, TN and TP masses were estimated for 9 – 40 m applied water.

2.11 EMCs

An average event mean concentrations (EMCs) were calculated for TSS, Cu, Zn, TN, and TP using

$$EMC = \frac{m}{V} \quad \text{[Eq. 10]}$$

where m is the total mass of the pollutant (mg) and V is the total volume of water that exited the column (L). Calculations of m and V are provided in the mass balance section.

2.12 Statistical Methods

Student's t-test and F-test on variance were performed on effluent from the control, 2,000, and 5,000 mg/L NaCl columns in order to determine whether the effluent from the baseline storms were comparable. A two-tailed t-test was used in

order to determine if the data were statistically identical and a null hypothesis stated that the two sample means were not statistically different. The F-test was used to verify the homogeneity of variances. If the baseline storms for the two columns were statistically different, then the baseline storm data for each individual column were compared with its respective effluent after high salt events.

Additionally, the same statistical methods were applied to the effluent from the mini columns. Effluent turbidity, TP, and TN concentrations after 0.9 m applied water were compared pairwise in order to determine statistically significant differences between types of salts. The null hypothesis was rejected when the calculated critical value was greater than the critical values at the 95% confidence interval ($p<0.05$). All statistical analyses were done on RStudio Desktop ver.1.1.453.

2.13 Quality Assurance and Quality Control Measures

All laboratory analytical measurements underwent calibrations every time they were used. Linear calibrations had no less than 0.999 correlation coefficients. For mesocosm samples that underwent spectrophotometric analyses, a random sample was selected and ran in duplicate in order to determine concentration variation. If the samples were not within ±10%, the samples are marked in text and figures. On the TN, IC, and ICP instruments, standard checks were performed every 10 – 15 samples. If standard checks failed (error exceeded ±10%), samples were re-tested using a new standard curve.

Standards additions were performed on turbid samples in order to determine the accuracy of the spectrophotometric analyses. If the standard addition failed

(expected concentration exceeded ±10%), the method was either discontinued (in the case of NH_4^+, NO_2^-, SRP) or modified (in the case of TP and speciation).

Chapter 3: Results and Discussion

3.1 BSM Analysis Results

The BSM characterization based on the LOI and University of Delaware Soil Testing program is provided in Table 4. Based on the soil texture results, the BSM is classified as a loamy sand and the BSM used meets the Maryland SHA BSM specifications (Appendix A-1). Although the percent clay was at the maximum value for BSM, no infiltration issues or ponding were observed during the mesocosm trials. Extractable nutrient results are discussed in the TSS and Turbidity Results (3.2).

Table 4. BSM characterization for the BSM used for the 2,000 and 5,000 mg/L NaCl columns.

LOI (%)	**LOI standard deviation (%)**	**Sand (%)**	**Silt (%)**	**Clay (%)**
3.0	1.2	84.0	6.0	10.0
Ca (mg/kg)	**Mg (mg/kg)**	**Na (mg/kg)**	**CEC (meq/100 g)**	
684	112	5.62	4.58	

3.2 TSS and Turbidity Results

3.2.1 Particulate Matter Results

Influent TSS remained less than 1 mg/L for all storms. Effluent samples for the 2,000, 5,000, and 10,000 mg/L NaCl columns were collected until the 26th, 40th, and 7th m applied water, respectively. Effluent samples from the initial 0 – 4 m applied water were captured every other storm. After the first high salt event, effluent was collected for all columns and analyzed for TSS and N and P species. Average effluent TSS for the 2,000, 5,000, and 10,000 mg/L NaCl columns exceed 80 mg/L (Table 5). Standard deviations for the effluent from each column are roughly equivalent to that of the respective average.

Table 5. Summary of effluent TSS for the 2,000, 5,000, and 10,000 mg/L NaCl columns.

	2,000 mg/L NaCl	**5,000 mg/L NaCl**	**10,000 mg/L NaCl**
Average	103	83.6	128
Standard deviation	90.2	75.3	126

Effluent from mesocosms consistently exhibited similar patterns on a storm-by-storm basis. For all mesocosms, the effluent TSS peak occurs approximately 30 minutes into the storm event, and effluent TSS decreases until the end of the storm event. This "sawtooth" pattern varied in magnitude depending on the concentration of high salt and on the number of baseline storms after the high salt event. Following high salt events, the TSS peaks decrease until the next high salt application. Of the three NaCl columns, the 10,000 mg/L NaCl column had the highest initial TSS concentration after the first salt application (540 mg/L, Figure 4), and the TSS peaks of the 5,000 and 2,000 mg/L NaCl columns decreased in magnitude (285 mg/L and 257 mg/L, respectively). By the fifth storm after a high salt event, effluent TSS from the 2,000 and 5,000 mg/L NaCl columns was less than 30 mg/L.

The 10,000 mg/L NaCl column experienced clogging after the first salt application (Appendix B-1). After the high salt spike, the effluent velocity rapidly decreased until it was less than 0.1 cm/hour, which occurred at around 7.2 m of applied stormwater (Appendix B-2), and as a result, the experiment was terminated. Media clogging as a result of high suspended solids release caused by road salt and reduction of infiltration rates have been reported in mesocosm studies with maximum applied NaCl concentrations ranging from 1,200 mg/L to 2,275 mg/L NaCl (Denich and Bradford 2008; Denich et al. 2013; Kakuturu and Clark 2015a; b).

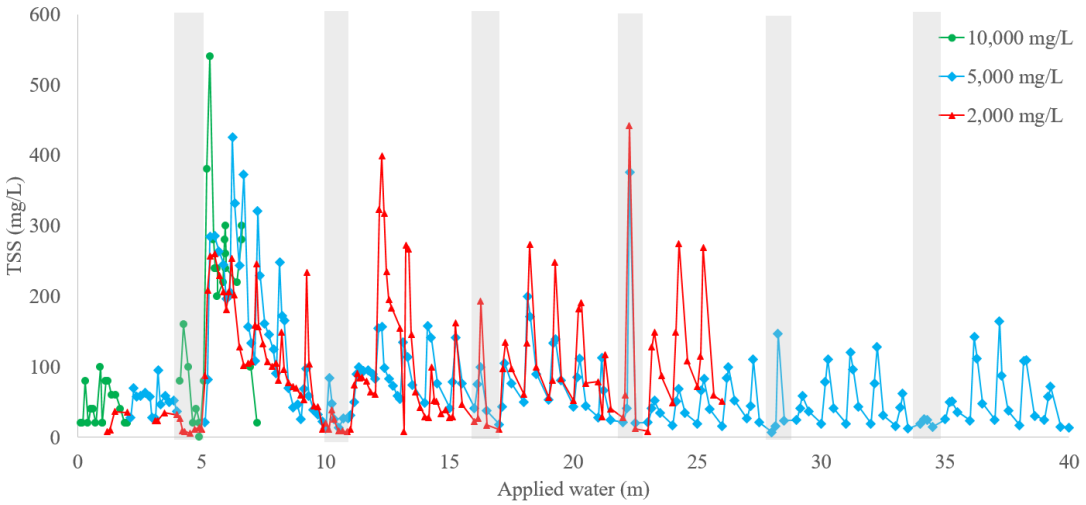

Figure 4. TSS in effluent from the 10,000, 5,000, and 2,000 mg/L NaCl bioretention columns. High salt events occurred every sixth event, indicated by gray boxes. Intermediate baseline events contained 20 mg/L NaCl. Applied velocity was 16.7 cm/hour to all columns. The 10,000 mg/L NaCl column was terminated at 7.2 m due to clogging.

The effluent TSS from the 2,000 mg/L NaCl column remained less than those from the 5,000 mg/L NaCl column after the first high salt event. It is hypothesized that the greater TSS concentrations from the 5,000 mg/L NaCl column are likely related to the amount of sodium ions applied to the column. Rengasamy and Olsson (1991) state that the proportion of clay particles separated from aggregates is proportional to the sodium adsorption ratio (SAR), which is a measure of sodium ions relative to calcium and magnesium ions and may be used to describe sodicity in a soil. The SAR is defined as

$$SAR = \frac{C_{Na}}{\sqrt{\frac{C_{Ca}C_{Mg}}{2}}} \qquad \text{[Eq. 11]}$$

where C represents the concentrations mmol/L of the cation identified as subscripts (Qadir and Schubert 2002). As high salt events contributed to an excess of sodium ions, cation exchange between sodium and soil cations takes place, and sodium preferentially replaces calcium (Rengasamy and Olsson 1991; Winston et al. 2016).

As the concentration of sodium ions increases, electrical repulsive forces between clay particles become dominant, causing clay swelling and deflocculation (Qadir and Schubert 2002).

Based on the extractable nutrient results from the University of Delaware Soil Testing Program and assuming a soil bulk density of 1.3 g/cm^3, the SAR of the virgin BSM used for the 2,000 and 5,000 mg/L NaCl columns was estimated to be 1.20. Using the classification proposed by Sumner et al. (1998), the virgin BSM was classified as a non-sodic soil.

SAR for the 2,000 and 5,000 mg/L NaCl columns can be estimated (Eq. 11) with the assumption that the concentration of magnesium ions is negligible compared to the sodium and calcium ions. The SAR during 5,000 mg/L NaCl salt events produced maximum SAR values ranging from 31.7 to 39.8 (Figure 5). The maximum SAR observed during the 2,000 mg/L NaCl salt event was 14.6. For both columns, the SAR continued to decrease, and the minimum SAR after high salt events observed for the 2,000 and 5,000 mg/L NaCl were 2.5 and 0.5, respectively.

Although it was hypothesized that the greater TSS concentrations from the 5,000 mg/L NaCl column are likely related to the amount of sodium ions applied to the column, effluent SAR measurements did not reflect that larger SAR values were related to high TSS concentrations. The correlation coefficients comparing TSS and SAR are 0.13 and 0.05 for the 5,000 and 2,000 mg/L NaCl columns, respectively (Appendix B-3). Since SAR is an index used to describe soil sodicity, which are described in terms of the relative amounts of sodium ions available on exchange sites (Qadir and Schubert 2002). Since there are a variety of soil degradation mechanisms

that occur under sodic conditions, including clay swelling, slaking, and deflocculation, the SAR value does not provide a holistic measure of soil dispersion alone. Therefore comparing the SARs of the effluent 5,000 and 2,000 mg/L NaCl columns is not an indirect measurement of the TSS concentrations.

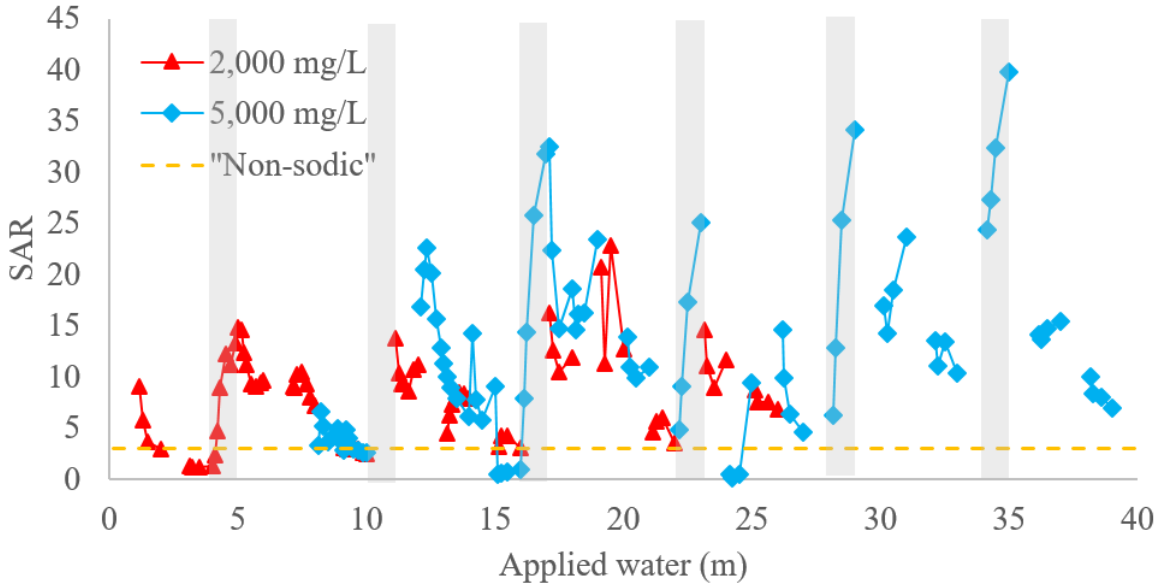

Figure 5. Estimated SAR for effluent from the 2,000 and 5,000 mg/L NaCl bioretention columns. High salt events occurred every sixth event, indicated by gray boxes. Intermediate baseline events contained 20 mg/L NaCl. Applied velocity was 16.7 cm/hour to all columns. The non-sodic classification is from Sumner et al. (1998), which classifies a non-sodic soil as one with an SAR < 3.

After the 11th meter of applied water, which occurred after the second salt spike, the TSS concentrations from the 2,000 mg/L NaCl column exceeded the concentrations from the 5,000 mg/L NaCl column (Figure 4). It is hypothesized that the greater concentrations from the 2,000 mg/L NaCl column are due to the column releasing greater amounts of NaCl. Taking the area under the conductivity plot (Appendix B-4) to represent the mass of NaCl in the column, the 2,000 mg/L NaCl column released a greater amount of NaCl than the 5,000 mg/L column in the later half of the five baseline storms after the second and third high salt events. For

example, during the 14th m applied water, the 2,000 mg/L NaCl column released an estimated 4,960 mg NaCl compared to 3,700 mg NaCl from the 5,000 mg/L NaCl column. The storm events where effluent conductivity from the 2,000 mg/L NaCl column was greater than that of the 5,000 mg/L NaCl column coincide with greater influent conductivity, measuring around 800 µS/cm.

The influent conductivity appeared to reflect the amount of NaCl discharged and the hypothesis is supported based on the fact that the 2,000 mg/L NaCl column released greater masses of NaCl than the 5,000 mg/L NaCl column during periods where effluent conductivity was greater in the 2,000 mg/L NaCl column. The amount of NaCl discharged is likely tied to cation exchange/adsorption mechanisms between influent divalent cations, which are more preferably held than monovalent cations by clays (Qadir and Schubert 2002), and residual sodium ions. Cation exchange mechanisms are discussed in the turbidity section.

Effluent TSS concentrations continued to remain greater than influent TSS, suggesting that the effects of the salt application continue through at least 5 m of applied water following a high salt event. Denich et al. (2013) conducted a mass balance of NaCl through bioretention mesocosms and found that after applying up to 122 g of a local salt mix, mesocosms continued to release Na^+ when flushed 10 times with 10 L DI. The lasting salt effect is consistent with field studies citing TSS and chloride release continuing through the summer months (Borst and Brown 2014; Drake et al. 2014; Robinson et al. 2017), with TSS concentrations around or less than 10 mg/L by the fall (Géhéniau Nicolas et al. 2015; Winston et al. 2016; Doan and Davis 2017).

The TSS peaks after the fourth high salt event in the 5,000 mg/L NaCl column remain below 170 mg/L (Figure 4), suggesting that a quasi-steady state of cation exchange has been reached. Despite perturbations of the high salt events, the TSS response is consistent for storms following the fourth salt spike in the 5,000 mg/L NaCl column, which corresponds to approximately 560,000 mg NaCl applied. Within each storm event, the sawtooth pattern remains, suggesting that the baseline storms remove sodium on clay adsorption sites. Based on roadside soil core studies, Robinson et al. (2017) found that sodium and chloride retention capacity can be depleted through "sufficient salt application," which occurred after 2,000 mg chloride was constantly applied as NaCl to the cores, with each core containing approximately 75 cm^3 of BSM, for five weeks. However, sodium retention continued to be non-conservative by the end of the study, where sodium moves through the soil slower than the porewater due to interaction with soil particles, plants, and microbes, suggesting that cation exchange contributed to the increased retention. Robinson et al. (2017) hypothesize that ion exchange sites are more likely to be occupied by ions from previous winters, lowering the capacity of the soil to retain ions. The occupation of adsorption sites on soil media from previous salt events may explain why a quasi-steady state has been reached in the 5,000 mg/L NaCl column.

3.2.2 TSS Mass Balance

The 2,000, 5,000, and 10,000 mg/L NaCl columns exported 5,300, 54,000, and 60,000 mg TSS after 7, 26, and 40 m applied water, respectively (Figure 6). The TSS EMCs for the 2,000, 5,000, and 10,000 mg/L NaCl columns were 110, 73.1, and 59.1 mg/L. By the 26^{th} m applied water, the 2,000 mg/L NaCl column had exported

more TSS mass than the 5,000 mg/L NaCl column, which can be explained by the greater EMC for the 2,000 mg/L NaCl column. The greater EMC for the 2,000 mg/L NaCl column is likely related to the column releasing more NaCl at the end of the second and third sets of high salt events and baseline storms. In contrast, the 5,000 mg/L NaCl column TSS export remained relatively constant after the first high salt event, which may be related to the soil's capacity to retain ions after continued exposure to high salt events (Robinson et al. 2017). Compared to the 0 – 4 m applied water, the increased rate of TSS export after high salt events supports prolonged NaCl release, which contributes to continuous soil deflocculation and increased TSS concentrations.

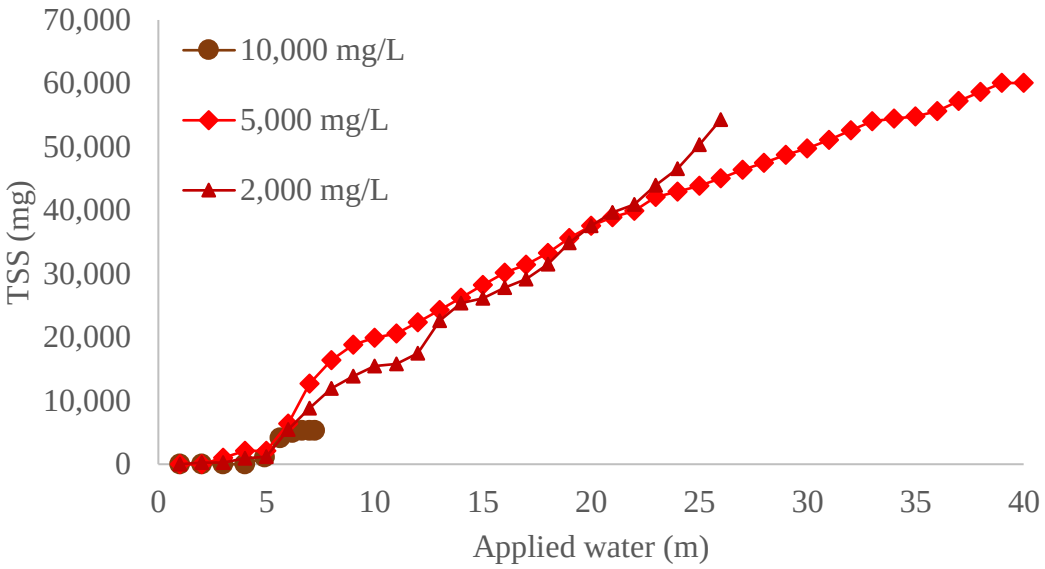

Figure 6. Effluent TSS mass balances for the 10,000, 5,000, and 2,000 mg/L NaCl bioretention columns. High salt events occurred every six storm events. Intermediate baseline events contained 20 mg/L NaCl. Influent TSS was less than 1 mg/L. Applied velocity was 16.7 cm/hour to all columns. Storm events continued until 26, 40, and 7 m applied water for the 2,000, 5,000, and 10,000 mg/L NaCl columns, respectively.

After the third high salt event (17 m applied water), the rate of TSS export of the 2,000 mg/L NaCl column exceeded that of the 5,000 mg/L NaCl column (Figure

6). At that time, the 5,000 mg/L NaCl column had retained nearly triple the mass of NaCl as the 2,000 mg/L NaCl column (133,000 vs 55,700 mg NaCl). Based on the assumption that more sodium occupied adsorption sites on the soil media in the 5,000 than the 2,000 mg/L NaCl column, it is hypothesized that TSS export rates from the 2,000 mg/L NaCl column will decrease once a sufficient mass of NaCl is retained.

Since the average annual rainfall in Maryland is 1.04 m (Papenfuse 2016) and 1:20 is the assumed SCM-to-drainage area ratio, 20 m applied water is roughly equivalent to 1 year of applied MD rainfall. Therefore, the 2,000 and 5,000 mg/L NaCl columns received the equivalent of 1 year and 4 months and 2 years of applied MD rainfall, respectively. From a short-term perspective, the greater rate of TSS export from the 2,000 mg/L NaCl column implies that areas that received lower amounts of road salt may export greater loads of TSS into receiving waterbodies after one winter season. In contrast, areas that received higher amounts of road salt may export lesser quantities of TSS into receiving waterbodies over multiple years. Since the time for the rate of TSS removal in the 2,000 mg/L NaCl column to equal that of the 5,000 mg/L NaCl column is equivalent to 2.5 years, long-term TSS removal performance is not an issue given that bioretention design life is predicted to be 25 years (Willard 2014).

3.2.3 Turbidity Results

Influent turbidity consistently remained less than 1 NTU. Effluent turbidity was measured for the 2,000 and 5,000 mg/L NaCl samples. Average effluent turbidity for both columns exceeded the US EPA WQS of 150 NTU (US EPA 2015), as averages were greater than 300 NTU (Table 6). Standard deviations for each column

exceeded the respective averages. Effluent turbidity patterns exhibited sawtooth patterns similarly observed with effluent TSS, although the maximum turbidity measurement typically occurred during the second baseline storm following a high salt event (Figure 7). After high salt events, samples contained brown effluent (Figure 8A), with turbidities greater than 1500 NTU. As the 2,000 mg/L and 5,000 mg/L NaCl columns continued to receive baseline storms, the turbidity would reduce and ultimately reach <1 NTU during the following high salt event (Figure 8B).

Table 6. Summary of effluent turbidity for the 2,000 and 5,000 mg/L NaCl columns, with all units in NTU.

	2,000 mg/L NaCl	**5,000 mg/L NaCl**
Average	423	321
Standard deviation	480	349

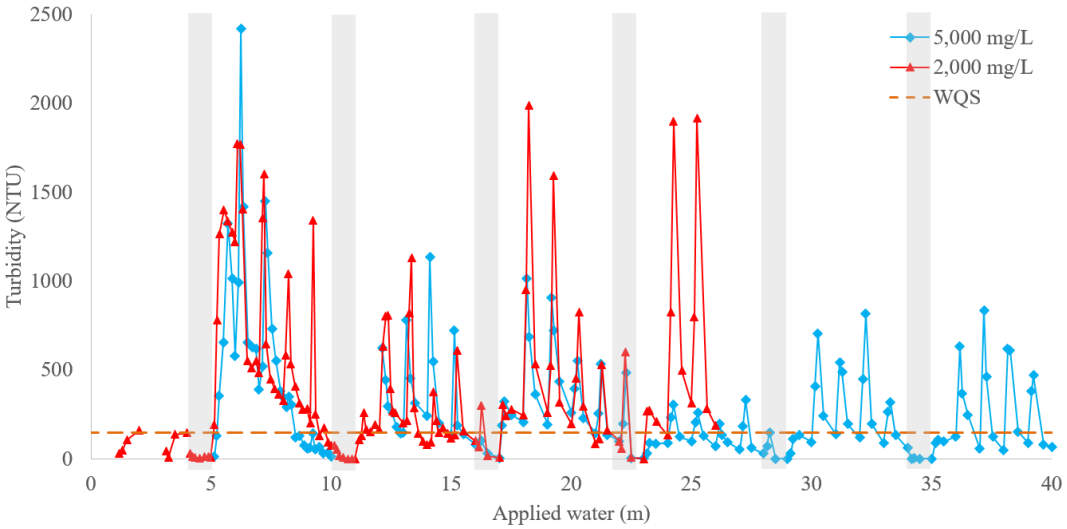

Figure 7. Effluent turbidity from the 5,000 and 2,000 mg/L NaCl bioretention columns. High salt events occurred every sixth event, indicated by gray boxes. Intermediate baseline events contained 20 mg/L NaCl. Applied velocity was 16.7 cm/hour to all columns. The WQS is 150 NTU (US EPA 2015).

A 

B 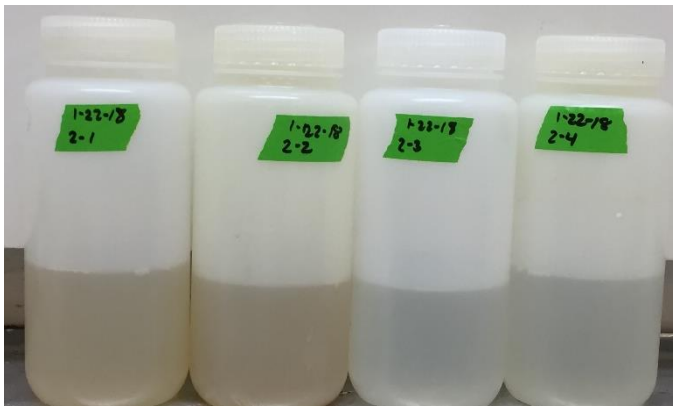

Figure 8. Effluent samples from the 5,000 mg/L NaCl column taken during A) the third baseline storm after the first high salt application (7 – 8 m applied water) and B) the fifth high salt event (28 – 29 m applied water).

The effects of soil dispersion as measured by TSS are moderately correlated to turbidity, with a correlation coefficient of 0.66 and 0.60 for the 5,000 mg/L and 2,000 mg/L NaCl columns, respectively (Appendix B-5). NaCl and other deicers have been found to cause soil deflocculation and resulting high TSS concentrations in effluent (Qadir and Schubert 2002; Winston et al. 2016). When adsorbed sodium ions on clay surfaces come into contact with water, the enlarged hydrated ionic radius increases distance between clay particles. The thickness of the diffuse double layer increases to the point where the repulsive forces overcome the attractive forces, causing clay particle dispersion (Rengasamy and Olsson 1991; Parameswaran and Sivapullaiah 2017). In addition to clay dispersion contributing to increased turbidity, release of organic matter due to increased chloride concentrations may contribute as well. The

relationship between organic matter release and chloride is discussed in the TOC section.

The US EPA WQS for turbidity states that turbidity shall not exceed 150 NTU at any time or 50 NTU as a monthly average (US EPA 2015). With the exception of samples taken at the end of baseline events and samples taken during high salt events, effluent from the 2,000 and 5,000 mg/L NaCl columns exceeded the WQS. Since turbidity is moderately correlated to TSS release, bioretention designs in cold weather areas may need to be modified in order to improve sediment filtration after salt applications. Brown and Hunt (2012) found that excavating the top 75 mm of media in two bioretention cells moderately increased TSS removal efficiencies by 5-8% compared to pre-repair. Although the bulk of captured solids is expected at the surface of the BSM (Davis et al. 2010), further investigation is needed to assess salt distribution vertically through the BSM in order to improve filtering abilities of the BSM.

3.2.3 pH and Colloid Charge

Average influent pH for all columns ranged from 6.96 to 7.0, with standard deviations ranging 0.2 to 0.4 (Table 8, Appendix B-6). Across all columns, the average influent pH was 7.0. Average effluent pH ranged from 6.63 to 6.74 with standard deviations ranging from 0.3 to 0.4. The pH 8.2 occurred at the end of the 18^{th} storm in the 5,000 mg/L NaCl column and is likely due to pH probe error since the initial influent measurement was 7.0. Effluent pH decreased by approximately one order of magnitude from the average effluent pH during each high salt event for the 10,000, 5,000, and 2,000 mg/L NaCl columns. During high salt events, effluent pH

ranged from 5.8 to 7.5, and pH decreased to a minimum, which occurred during the middle of each salt event, before increasing approximately 0.3 pH units.

Table 7. Summary of influent and effluent pH for the 2,000, 5,000, and 10,000 mg/L NaCl columns.

	2,000 mg/L NaCl		**5,000 mg/L NaCl**		**10,000 mg/L NaCl**	
	Influent	**Effluent**	**Influent**	**Effluent**	**Influent**	**Effluent**
Average	6.98	6.67	7.0	6.74	6.98	6.63
Standard deviation	0.4	0.3	0.3	0.4	0.2	0.3

Similar impacts on pH as a result of salt applications equivalent to 3,700 mg/L NaCl on soil were observed in roadside cores taken by Robinson et al. (2017), who cited proton displacement via cation exchange as the cause. (Zhang et al. 2011) report the surface charge of conventional BSM (defined as a mixture of soil, sand, and mulch) is slightly negative at pH 7. Assuming that the zero point charge has not been surpassed to significantly alter the soil colloid charge, chloride and other anions may be assumed to be mobile through the soil in the mesocosm experiments. Therefore it is unlikely that chloride was adsorbed to soil particles and likely the case that excess sodium ions contributed to soil deflocculation, which in turn resulted in increased TSS concentrations after high salt events.

3.3 TOC Results

Influent TOC consistently remained around 5 mg-C/L with the averages for each column around 5.9 mg-C/L and standard deviation 1.9 mg-C/L (Table 7). Effluent TOC data for the 10,000 mg/L were not collected. During 5 – 19 m applied water, no effluent TOC was measured from the 5,000 mg/L NaCl column and during 3 – 5 m applied water for the 2,000 mg/L NaCl column. Average effluent TOC

ranged from 15.8 to 30.2 mg-C/L and standard deviations were roughly equivalent to the average. The effluent TOC concentrations displayed sawtooth patterns, as described in the TSS section. During a high salt event, effluent TOC was of the same magnitude of influent TOC (<10 mg-C/L, Figure 9). Following a high salt event, the maximum TOC concentration within five baseline storms occurred during the second baseline storm event for both columns. Similar effluent maxima patterns were exhibited in the effluent for TSS and turbidity, as discussed in the previous section.

Table 8. Summary of influent and effluent TOC concentrations for the 2,000 and 5,000 mg/L NaCl columns, with all values in mg-C/L.

	2,000 mg/L NaCl		**5,000 mg/L NaCl**	
	Influent	**Effluent**	**Influent**	**Effluent**
Average	5.79	15.8	5.93	30.2
Standard deviation	1.86	16.2	1.99	30.0

However, the maximum TOC concentration occurred at around 24 m of applied water in the 2,000 mg/L NaCl column, with a TOC concentration of 102.6 mg-C/L, and at 18 m of applied water in the 5,000 mg/L column, with a TOC concentration of 136 mg-C/L (Figure 9). The delay in the maximum TOC concentration in the 2,000 mg/L NaCl column may be a consequence of the difference in NaCl mass exiting the columns. By the 18^{th} m applied water, approximately 330,000 mg NaCl had exited the 5,000 mg/L NaCl column whereas 224,000 mg NaCl had exited the 2,000 mg/L NaCl column by the 24^{th} m applied water. Based on the previous discussion how more sodium adsorption sites on media become occupied with increased NaCl mass applied, the lesser mass of NaCl may influence TOC removal from adsorption sites.

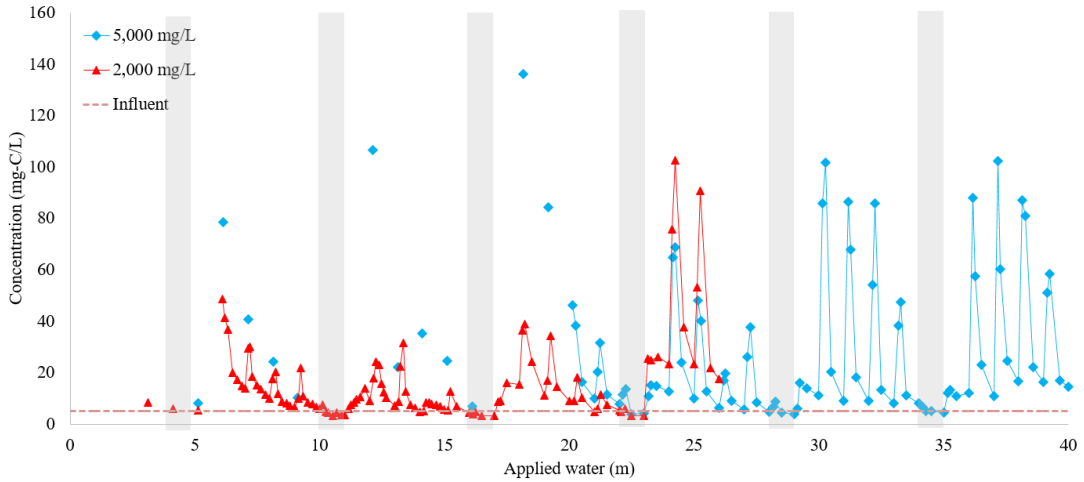

Figure 9. Effluent TOC from the 5,000 and 2,000 mg/L NaCl bioretention columns. High salt events occurred every sixth event, indicated by gray boxes. Intermediate baseline events contained 20 mg/L NaCl. Influent TOC averaged 5 mg-C/L with a standard deviation of 1.9 mg-C/L. Effluent averages ranged from 15.8 to 30.2 mg-C/L with standard deviations ranging from 16.2 to 30.0 mg-C/L. Applied velocity was 16.7 cm/hour to all columns.

Effluent TOC is more strongly correlated to turbidity (R^2 = 0.66 and 0.60 for the 5,000 mg/L and 2,000 mg/L NaCl column, respectively, Appendix C-1) than with TSS (R^2 = 0.31 and 0.28 for the 5,000 mg/L and 2,000 mg/L NaCl column, respectively, Appendix C-2). The brown-colored effluent be due to colloid dispersion as a result of the salt application, but also associated with release of organic matter (Figure 8A).

With the exception of occasional high concentrations of particulate organic carbon (21.5 and 85.8 mg-C/L as maxima for the 2,000 and 5,000 mg/L NaCl columns, respectively), which coincide with TSS peaks (Figure 4), dissolved organic carbon makes up over 88% of TOC in the 2,000 mg/L and 5,000 mg/L NaCl effluent (Figure 10). In soils with a high ESP, organic matter is highly soluble (Nelson and Oades 1998), and the continued release of dissolved organic carbon may be due to a solvation effect of the salt as the salt alters the composition of exchange sites on clays

(Kaiser et al., 1996; Wiklander, 1975; Wong et al., 2010). Since dissolved organic carbon was the primary form of TOC release, elevated TOC concentrations are mostly a result of the release of dissolved organic matter from the media, although deflocculation of clays may contribute to the release of particulate organic matter.

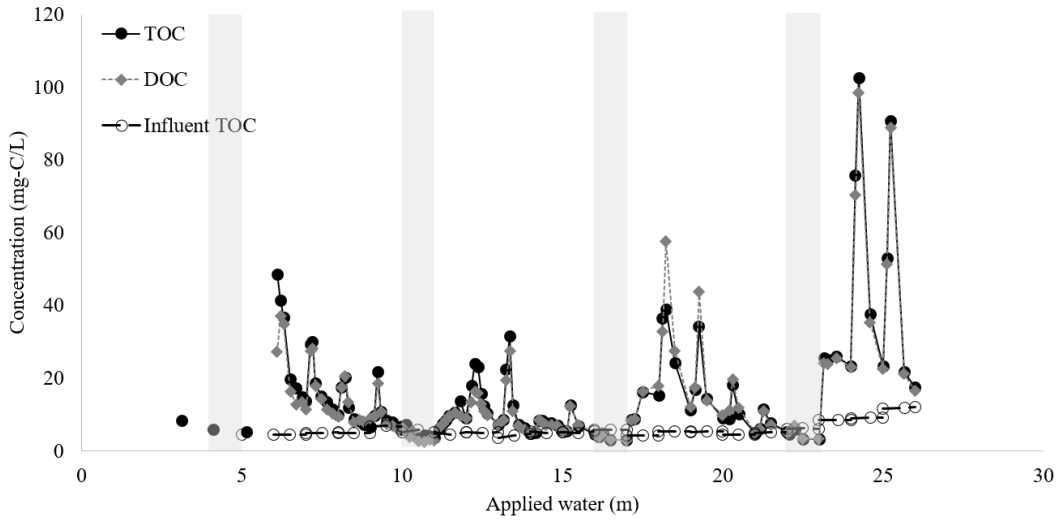

A

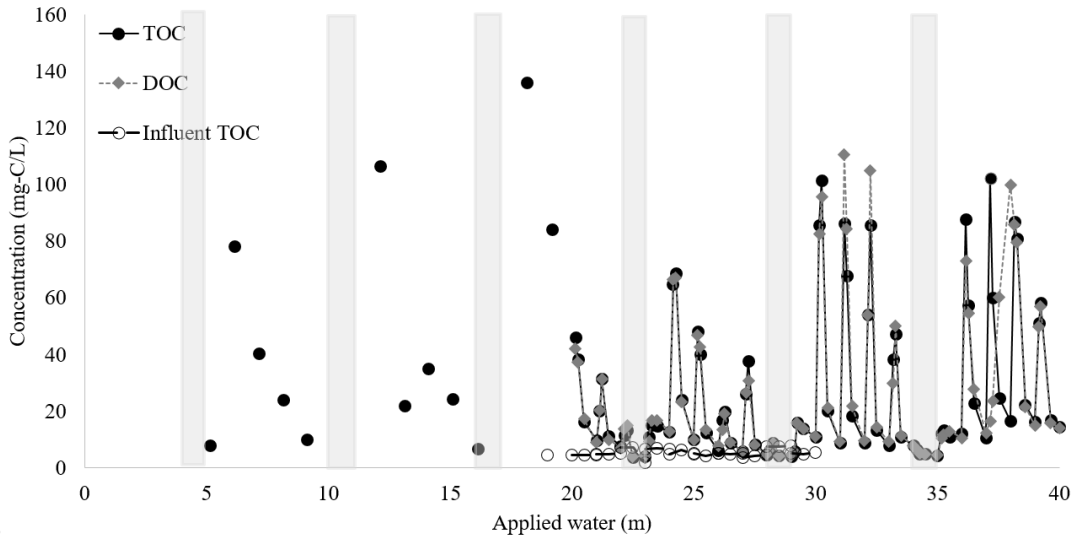

B

Figure 10. Effluent TOC and DOC from the 2,000 (A) and 5,000 (B) mg/L NaCl bioretention columns. High salt events occurred every sixth event, indicated by gray boxes. Intermediate baseline events contained 20 mg/L NaCl. Influent TOC averaged 5 mg-C/L. Applied velocity was 16.7 cm/hour to all columns.

3.4 Metals Results

3.4.1 Temperature Effects

Influent and effluent temperatures ranged from 13.0 to 32.5 °C (Appendix D-1). The average influent temperature ranged from 18.5 to 22.0 °C, with standard deviations ranging from 2.2 to 4.4 °C, and the average effluent temperature ranged from 21.8 to 24.2 °C, with standard deviations ranging from 1.5 to 3.3°C (Table 8). Despite the greenhouse thermostats set to 24 °C, the range of temperatures reflect that the air temperature was subject to variations due to outdoor conditions. Colder months resulted in lower temperatures as well with summer months and higher temperatures. As a result, water properties such as viscosity, and reaction rates were not constant throughout the trials.

Table 9. Summary of influent and effluent temperatures for the 2,000, 5,000, and 10,000 mg/L NaCl columns, with all units in °C.

	2,000 mg/L NaCl		**5,000 mg/L NaCl**		**10,000 mg/L NaCl**	
	Influent	**Effluent**	**Influent**	**Effluent**	**Influent**	**Effluent**
Average	19.9	21.8	22.0	24.2	18.5	22.6
Standard deviation	3.1	1.8	4.4	3.3	2.2	1.5

Lower temperatures have been reported to decrease the rate of sorption and filtration as a result of increased water viscosity (Paus et al. 2014). In a study conducted by Søberg et al. (2014), metal capture by bioretention mesocosms was studied under high and low temperatures (17.1 °C and 4.6 °C) and with and without the addition of salt. The low temperature conditions with the addition of salt resulted in lower metal removal rates than mesocosms that did not receive salt. In regards to the temperatures, the t-test revealed no significant difference existed and the authors concluded that temperature changes were not the primary variable in regards to

removal performance. The authors hypothesize that since salt increases metal solubility, a higher fraction of metals remains in the dissolved phase and therefore a lower removal efficiency under cold temperatures. Based on the findings by Søberg et al. (2014), the temperature impacts on the metal removals were lesser than the salt impacts for the mesocosm study.

3.4.2 Copper Results

All influent concentrations ranged from 45 to 128 µg/L Cu, with averages ranging from 37 to 55 µg/L Cu, and standard deviations ranging from 16 to 34 µg/L Cu (Table 9). Across all three columns, the average influent concentration was 56 µg/L Cu with a standard deviation of 33 µg/L Cu (Figure 11). Average effluent concentrations ranged from 20 to 30 µg/L Cu, with standard deviations ranging from 16 to 23 µg/L Cu.

Table 10. Summary of influent and effluent copper concentrations for the 2,000, 5,000, and 10,000 mg/L NaCl columns, with units in µg/L Cu.

	2,000 mg/L NaCl		**5,000 mg/L NaCl**		**10,000 mg/L NaCl**	
	Influent	**Effluent**	**Influent**	**Effluent**	**Influent**	**Effluent**
Average	52	20	55	24	37	30
Standard deviation	30	16	34	23	16	36

Baseline storms (0 – 4 m applied water) for all columns exhibited similar patterns of copper concentrations in the effluent on an individual storm basis and effluent Cu concentrations were typically less than influent concentrations. As opposed to previously observed sawtooth effluent patterns, the maximum effluent copper concentration started at the beginning of the storm and concentrations decreased through the storm. At the beginning of each storm, the maximum peaks

occurred at 30 – 50 µg/L Cu. By the end of each baseline storm, effluent concentrations decreased to below 5 µg/L Cu. With the exception of three storm events from the 5,000 mg/L NaCl column, effluent copper concentrations remained below influent concentrations.

Salt applications of 2,000 mg/L NaCl did not greatly impact patterns in effluent copper compared to the initial baseline storms (0 – 4 m applied water). Storms immediately following a salt application had concentrations less than 15 µg/L Cu (Figure 11). However, the decreases in effluent concentration through storm events were observed in subsequent baseline storms. Since data are missing from the second baseline storm following a salt spike, it is inconclusive whether deviations from observed the effluent patterns occurred. Overall, effluent copper concentrations always remained below influent concentrations.

High salt events of 5,000 mg/L NaCl deviated from baseline storm patterns, but copper concentrations in the following baseline storms were similar in magnitude to the 0 - 4 m baseline events (Figure 11). After high salt events, the maximum effluent copper concentrations immediately after were greater than the average influent (56 µg/L Cu), but effluent concentrations after the maxima became less than the average influent. For instance, after the first high salt event, during the 6^{th} m applied water, an effluent spike of 151 µg/L Cu was observed. Effluent concentrations throughout the rest of the storm event were less than 10 µg/L Cu. After the third high salt event, during the 17^{th} m applied water, the effluent peak was 100 µg/L Cu, and effluent concentrations decreased to 48 µg/L Cu. During the 27^{th}, 29^{th}, and 35^{th} m applied water, high concentrations in effluent ranged from 88 to 97

µg/L Cu , which may be explained by elevated Cu concentrations of 150 µg/L Cu in tap water, compared to normal instances with concentrations around 50 µg/L Cu.

Similar to the 2,000 mg/L NaCl column, a delay in the appearance of an effluent peak (109 µg/L Cu) was observed in the 7th m applied water in the 10,000 mg/L NaCl column (Figure 11). After the high salt storm, effluent peaks at the beginning of each storm increased to a peak maximum of 201 µg/L Cu, which occurred at 6.4 m applied water, and the following effluent peak decreased to 89 µg/L Cu. The closeness of the effluent concentration peaks is related to the decreased effluent velocity as a result of the media clogging. Since none of the samples were digested for this column, the effluent Cu data are unrepresentative of total metals that could have washed out in the effluent.

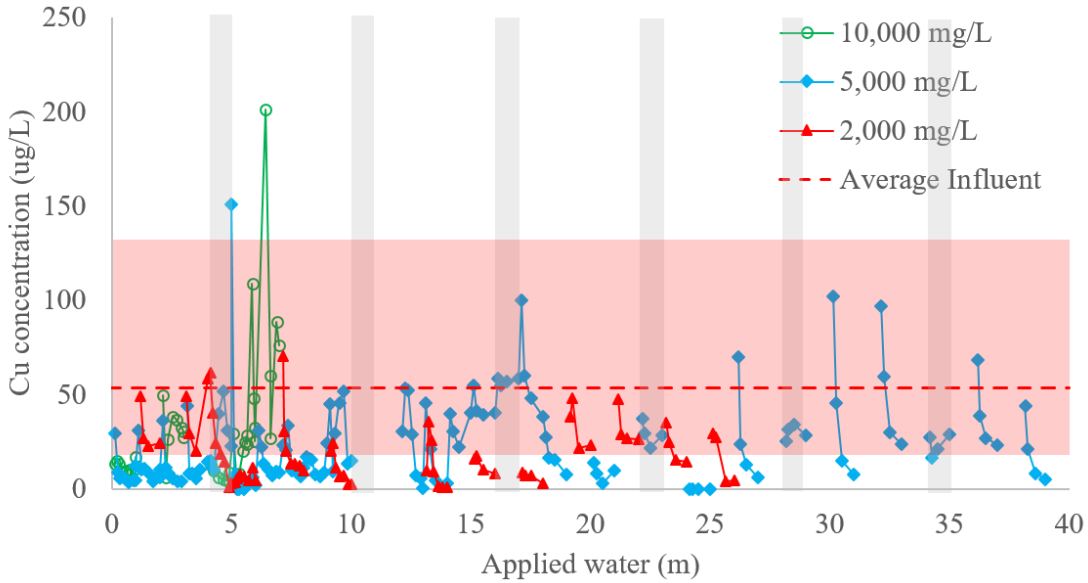

Figure 11. Copper in effluent from the 10,000, 5,000, and 2,000 mg/L NaCl bioretention columns. Undigested 10,000 mg/L NaCl effluent samples are represented by open symbols. High salt events occurred every sixth event, indicated by gray boxes. Intermediate baseline events contained 20 mg/L NaCl. Influent concentration range is within the red box (45.5 µg/L – 128 µg/L Cu), with the red dashed line representing the average copper concentration (55.9 µg/L Cu). Applied velocity was 16.7 cm/hour to all columns.

The large decrease in copper concentrations following high salt events is most likely a result organic matter dispersion and ion exchange taking place in the media. Based on correlation coefficients for effluent copper and TOC for the 2,000 and 5,000 mg/L NaCl columns (0.09 and 0.10, respectively, Appendix D-2), effluent copper and TOC do not appear to be strongly related. The small correlation coefficients are likely due to the different effluent patterns observed for the pollutants, as copper concentrations did not display sawtooth patterns like effluent TOC. However, the mechanism responsible the effluent copper maximum occurring after the TOC maximum is unknown.

Leaching experiments using roadside soils similarly observed copper release simultaneously with organic matter dispersion under conditions of high exchangeable sodium (Amrhein et al. 1992). Nelson et al. (2009) similarly conclude through laboratory experiments using highway soils exposed to 0.1 M chloride, used to represent high first flush events, that copper releases are likely tied to mobilization of organic matter. Bäckström et al. (2004) found that as a result of roadside salts, the dissolved copper fraction increases, allowing more copper to be removed through ion exchange (Warren and Zimmerman 1994; Bäckström et al. 2004). Increasing ionic strength may explain why copper washouts in effluent increased with increased NaCl concentration (Zehetner et al. 2009; Tedoldi et al. 2016), but further research is necessary to explain why effluent copper peaks occurred after TOC peaks.

3.4.3 Copper Mass Balance

For all mesocosms, copper was retained despite periodic high salt events. Influent and effluent masses were only calculated for storm events where data were

collected. Copper mass removals for the 2,000, 5,000, and 10,000 mg/L NaCl columns were 74.3%, 65.4%, and 70.6%, respectively. Laboratory and short-term bioretention field studies find similar removal copper efficiencies, ranging from 72 to 98% (Muthanna et al. 2007; Paus et al. 2014; Søberg et al. 2014), although the range of effiencies may be attributed to the addition of organic matter amendments to the BSM. Since the 2,000 and 5,000 mg/L NaCl columns demonstrated similar rates of Cu mass release (Figure 12), road salt applications up to 5,000 mg/L NaCl may produce comparable results as smaller concentrations. Based on this study, the use of NaCl as a deicer does not impair the capture of copper in SCMs.

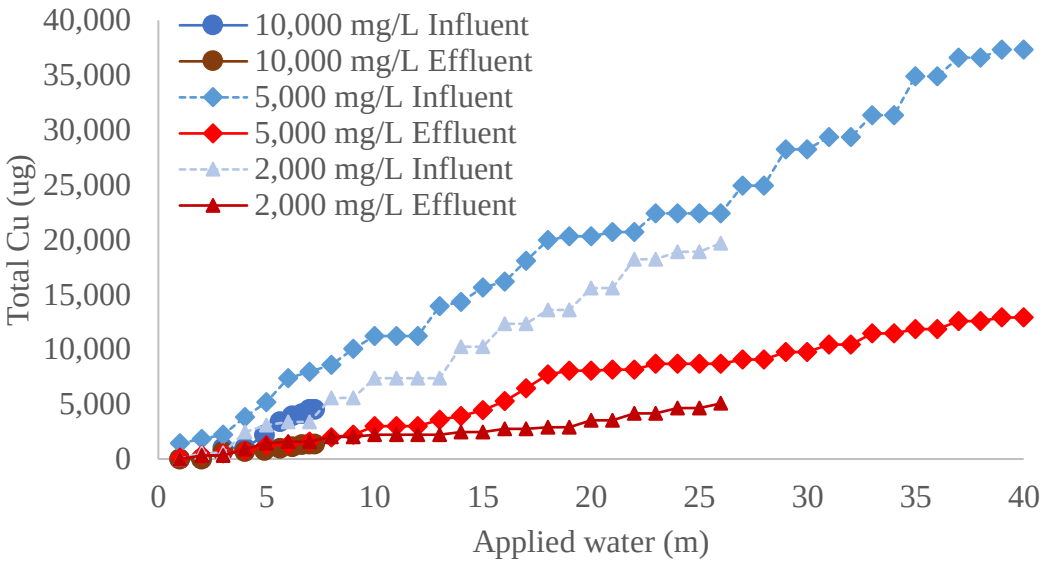

Figure 12. Copper mass balances for the 10,000, 5,000, and 2,000 mg/L NaCl bioretention columns. High salt events occurred every six storm events. Intermediate baseline events contained 20 mg/L NaCl. Average influent copper was 56 µg/L Cu. Applied velocity was 16.7 cm/hour to all columns. Storm events continued until 26, 40, and 7 m applied water for the 2,000, 5,000, and 10,000 mg/L NaCl columns, respectively.

Maryland Department of the Environment (2005 p. 26) sets the acute and chronic freshwater thresholds for copper at 13 and 9 µg/L Cu, respectively. Copper

EMCs for the 2,000, 5,000, and 10,000 mg/L NaCl columns were 10, 16, and 15 µg/L Cu, respectively. Evidently NaCl concentrations greater than 2,000 mg/L NaCl produced effluent greater than the acute WQS, and all applied NaCl concentrations did not meet the chronic threshold. Since the US EPA (2002) defines chronic exposure as a period of 4 days, bioretention effluent during winter is likely to violate the freshwater chronic threshold as well.

3.4.4 Zinc Results

Influent zinc concentration ranged from 142 to 459 µg/L Zn, with an average concentration of 304 µg/L Zn across all columns and a standard deviation of 0.06 µg/L Zn (Figure 13). Individual influent averages for each column ranged from 294 to 348 µg/L Zn, with standard deviations ranging from 87 to 103 µg/L Zn (Table 10). With the exception of the high zinc peak of 539 µg/L Zn during the 3rd m applied water in the 10,000 mg/L NaCl column, the baseline storms for all columns exhibited effluent zinc patterns similar to effluent copper. Maximum concentrations occurred at the first sample, ranging from 61 to 251 µg/L Zn. By the end of each baseline storm, effluent concentrations ranged from 23 to 49 µg/L Zn. Individual effluent averages for each column ranged from 91 to 197 µg/L Zn, with standard deviations from 79 to 324 µg/L Zn.

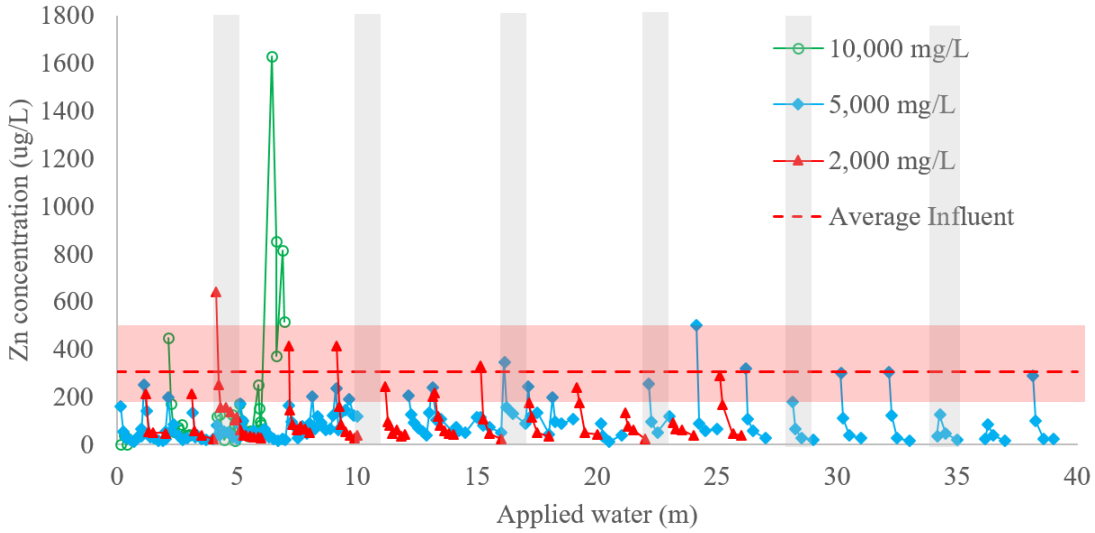

Figure 13. Zinc in effluent from the 10,000 mg/L, 5,000 mg/L, and 2,000 mg/L NaCl bioretention columns. High salt events occurred every sixth event, indicated by gray boxes. Intermediate baseline events contained 20 mg/L NaCl. Influent concentration range is within the red box (142 – 459 µg/L Zn), with the red dashed line representing the average zinc concentration (304 µg/L). Applied velocity was 16.7 cm/hour to all columns.

Table 11. Summary of influent and effluent zinc concentrations for the 2,000, 5,000, and 10,000 mg/L NaCl columns, with all units in µg/L Zn.

	2,000 mg/L NaCl		**5,000 mg/L NaCl**		**10,000 mg/L NaCl**	
	Influent	**Effluent**	**Influent**	**Effluent**	**Influent**	**Effluent**
Average	294	110	304	91	348	197
Standard deviation	87	108	67	79	10	324

During the first salt spike in the 5,000 mg/L NaCl column, effluent zinc concentration decreased from 642 µg/L Zn to 117 µg/L Zn (Figure 13). The subsequent baseline storm released zinc at similar levels to the 0 – 4 m baseline events. However, effluent from the 7th, 9^{th,}, 14th and 25th m of applied water had higher initial zinc concentrations, with the maximum concentrations around 414 µg/L Zn. Influent zinc concentrations during these events were slightly higher than average, ranging from 337 to 408 µg/L Zn, which may explain the slightly higher concentrations. Disregarding the events with slightly elevated influent zinc

concentrations, effluent between salt events were of the same magnitude of the 0 – 4 m baseline storms.

By the 29th m applied water in the 5,000 mg/L NaCl column, peak effluent zinc concentrations remained below 310 µg/L Zn and decrease to less than 20 µg/L Zn(Figure 13). In a column study that alternated 0.1 M NaCl (equivalent to 5,844 mg/L NaCl) and deionized water applications to highway infiltration trench soils, Norrström (2005) hypothesizes the difference between zinc leaching in the initial and final stages of a column leaching experiment is a result of the exhaustion of available mobilized zinc. Although deviations from the baseline storm patterns occurred only when influent Zn was higher than normal, the effluent data do not suggest a difference between zinc concentrations from the initial and final stages of the 5,000 mg/L NaCl column. However, Zn effluent data are unavailable for all storm events, and a full dataset may provide better insight into Zn removal differences between beginning and final leaching experiments.

Effluent zinc data are unavailable until the 8th m applied water for the 10,000 mg/L NaCl column. However, the 10,000 mg/L NaCl column effluent patterns exhibit similar behavior to that of the copper in that during the 8th m applied water; similar to Cu effluent patterns after the high salt event, Zn peaks occurred at the beginning of every storm event with the greatest concentration of 1,630 µg/L Zn occurring at 6.4 m applied water and the next peak at 6.9 m applied water (817 µg/L Zn, Figure 13). In the infiltration trench soil column study as mentioned above, Norrström (2005) found that most leachate zinc was dissolved (83%) after simulating three high salt events. Warren and Zimmerman (1994) likewise concluded through metal extractions on

roadside samples near Toronto, Canada that NaCl is likely to cause zinc partitioning to the leachable phase. Although effluent samples from the 10,000 mg/L NaCl column did not undergo a nitric acid digestion, previous studies suggest that effluent zinc is likely to be mostly in the dissolved phase and therefore the data collected for the 10,000 mg/L NaCl column may be sufficient to represent total zinc.

Zinc is likely to be released in association with organic matter and ion exchange (Bäckström et al. 2004; Paus et al. 2014), although Norrström (2005) cites chloride complexes are a likely cause for zinc mobilization as well. High concentrations of NaCl are likely to cause an increase in the Zn dissolved phase, coupled with a simultaneous decrease in the organic fraction (Warren and Zimmerman 1994; Bäckström et al. 2004; Søberg et al. 2017). However, effluent zinc and TOC were not strongly correlated (correlation coefficients for the 2,000 and 5,000 mg/L NaCl columns were 0.02 and 0.10, respectively, Appendix D-3). The effluent zinc peak occurring after the TOC peak may partially explain the weak correlation, although as mentioned in the copper section, it is unknown why the delay occurred. Since there was no clear distinction in effluent patterns between baseline storms and high salt events, characterization of effluent zinc in the 2,000 mg/L and 5,000 mg/L NaCl may provide further insight as to when the organic fraction is the primary source of zinc after a salt application.

To minimize organic matter loss from sodic soils, Wong et al. (2010) suggest replacing sodium ions with polyvalent cations on clay adsorption sites in order to create linkages between clays and organic matter. As a result, the polyvalent cation-organic matter linkages are less soluble than Na-organic linkages and will decrease

organic matter content in runoff. Further investigation is necessary to determine appropriate amelioration strategies for sodic soils that allow for organic matter and zinc accumulation.

3.4.5 Zinc Mass Balance

Overall, zinc retention in all mesocosms was observed. Mass balances for zinc were calculated for storms where influent and effluent data were available. All mesocosms demonstrated zinc uptake, with mass removals of 79.5%, 79.5%, and 76.5% for the 10,000, 5,000, and 2,000 mg/L NaCl columns, respectively. Similarly to the copper mass balance, the 2,000 and 5,000 mg/L NaCl columns demonstrated similar rates of zinc release (Figure 14). Additionally, Maryland Department of the Environment (2005) and US EPA (2017) cite the chronic zinc threshold in freshwaters at 120 µg/L Zn. Zinc EMCs for the 2,000, 5,000, and 10,000 mg/L NaCl columns were 57, 73, 1 µg/L Zn. Since the chronic zinc threshold was not exceeded and the mass balances for all columns exhibited no zinc export, zinc export from SCMs exposed to high concentrations of road salt does not appear to be an issue.

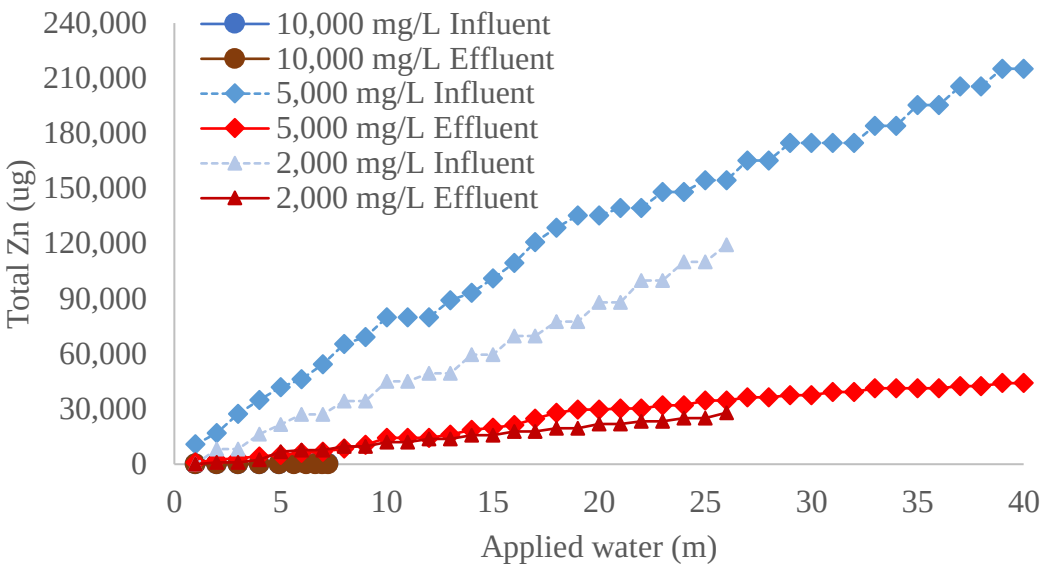

Figure 14. Zinc mass balances for the 10,000, 5,000, and 2,000 mg/L NaCl bioretention columns. High salt events occurred every six storm events. Intermediate baseline events contained 20 mg/L NaCl. Average influent copper was 306 µg/L Zn. Applied velocity was 16.7 cm/hour to all columns. Storm events continued until 26, 40, and 7 m applied water for the 2,000, 5,000, and 10,000 mg/L NaCl columns, respectively.

3.4.6 Sodium and Calcium Results

Effluent sodium and calcium data are not available for the 10,000 mg/L NaCl column. Samples from the 2,000 mg/L and 5,000 mg/L NaCl columns were measured for sodium and calcium, and samples every other storm event. Sodium and calcium analysis began after the 9th m applied water in the 5,000 mg/L NaCl column and at the start of the 2,000 mg/L NaCl study. During the 0 – 4 m baseline storm events, effluent Na concentrations ranged from 43 to 86 mg/L Na (Figure 15), with average concentrations ranging from 182 to 313 mg/L Na, and standard deviations from 208 to 496 mg/L Na (Table 11). With the exception of high salt events, influent concentrations ranged from 15.5 mg/L to 38.9 mg/L Na. During 2,000 mg/L and 5,000 mg/L NaCl events, influent Na was approximately 650 mg/L and 1900 mg/L

Na, respectively. Effluent sodium was strongly correlated to conductivity (R^2 = 0.88 and 0.99 for the 2,000 mg/L and 5,000 mg/L NaCl columns, respectively, Appendix D-3), so effluent sodium washouts strongly mirrored those of conductivity measurements. Even after five baseline storm events following a salt event, effluent sodium concentrations remained greater than influent concentrations.

Table 12. Influent and effluent sodium concentrations for the 2,000 and 5,000 mg/L NaCl columns, with units in mg/L Na.

	2,000 mg/L NaCl		**5,000 mg/L NaCl**	
	Influent	**Effluent**	**Influent**	**Effluent**
Average	77	182	345	313
Standard deviation	161	208	652	496

During the first high salt event, the greatest sodium concentration of 912 mg/L Na was observed in the 2,000 mg/L NaCl column (Figure 15), although the concentration decreased to 117 mg/L by the end of the following baseline storm. Future baseline storms after high salt events (11^{th} and 17^{th} m applied water) exhibited similar high initial effluent concentrations (246 mg/L and 177 mg/L Na) but concentrations decreased close to baseline levels by the end of the event. The 5,000 mg/L NaCl column exhibited similar sodium release except the maximum concentrations during high salt events were greater than 1,200 mg/L Na.

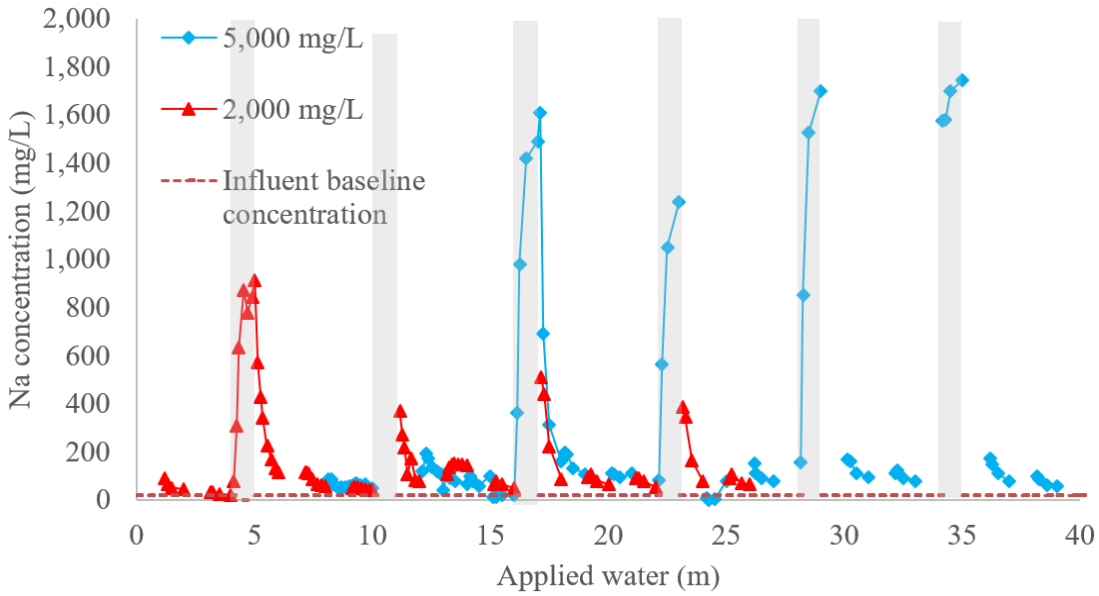

Figure 15. Sodium in effluent from the 5,000 and 2,000 mg/L NaCl bioretention columns. High salt events occurred every sixth event, indicated by gray boxes. Intermediate baseline events contained 20 mg/L NaCl. Average influent concentration range is represented by the dashed red line (20 mg/L Na). Applied velocity was 16.7 cm/hour to all columns.

Baseline effluent calcium concentrations were less than 45 mg/L Ca, and influent concentrations ranged from 11 to 54 mg/L, with an average of 41.9 mg/L Ca across all columns (Figure 16). Individual effluent averages ranged from 46 to 58 mg/L Ca, with standard deviations from 80 to 81 mg/L Ca (Table 12). During the first high salt event in the 2,000 mg/L NaCl column, the maximum effluent calcium concentration was 339 mg/L. By the 8th m applied water, the effluent concentration returned to baseline effluent levels. The first two high salt events were not monitored for the 5,000 mg/L NaCl column, but the calcium concentrations in the remaining high salt events had maximum peaks between 312 and 259 mg/L Ca.

Table 13. Summary of influent and effluent calcium concentrations for the 2,000 and 5,000 mg/L NaCl columns, with units in mg/L Ca.

	2,000 mg/L NaCl		**5,000 mg/L NaCl**	
	Influent	**Effluent**	**Influent**	**Effluent**
Average	27	46	49	48
Standard deviation	5	80	55	81

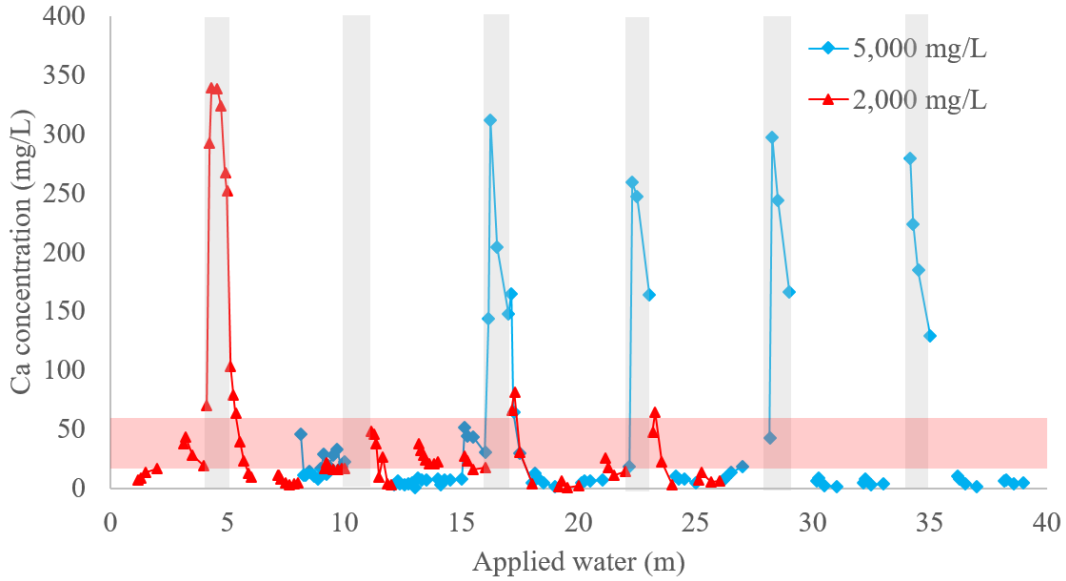

Figure 16. Calcium in effluent from the 5,000 and 2,000 mg/L NaCl bioretention columns. High salt events occurred every sixth event, indicated by gray boxes. Intermediate baseline events contained 20 mg/L NaCl. Influent concentration range is within the red box (11.2 mg/L – 54.0 mg/L Ca), and average concentration is 41.9 mg/L Ca. Applied velocity was 16.7 cm/hour to all columns.

Cation exchange between calcium and sodium is likely occurring during the high salt events and during baseline events. Sodium ions preferentially replace calcium from exchange sites via cation exchange (Norrström and Bergstedt 2010; Winston et al. 2016; Parameswaran and Sivapullaiah 2017), which is evidenced by the strongly correlated relationship between the two ions (R^2 = 0.74 and 0.70 for the 2,000 mg/L and 5,000 mg/L NaCl columns, respectively, Appendix D-4). As a result of increased concentrations of sodium ions in media, soil dispersion occurs, as

discussed in the TSS section. However, reintroduction of calcium ions may replace adsorbed sodium and as a result, the physical effects of NaCl on soil structure may be mitigated (Shainberg et al. 1989; Ilyas et al. 1997; Qadir and Oster 2002; Wong et al. 2010; Gao et al. 2016). Based on this knowledge, sufficient amounts of calcium may have been added to the columns during baseline storm events, evidenced by high concentrations of sodium rapidly decreasing to concentrations observed during the 0 – 4 m applied water (approximately 100 mg/L Na), to the point where the soil deflocculation ceased and effluent ran clear by the fifth baseline storm and following high salt event (Figure 8b). The implications of a prolonged recovery of calcium pools in soil suggest the need for an additional source of calcium in order to replace sorbed sodium faster than relying on influent stormwater as a calcium source.

As previously discussed in the TSS section, the estimated SAR values (Eq. 11) for the 2,000 and 5,000 mg/L NaCl columns are typically greater than 10 during and initially after a high salt application (Figure 5). By the end of five baseline storms, SAR values are generally ≤ 3. Qadir and Schubert (2002) summarize different categorizations of salt-affected soils based on parameters such as electrolyte concentration, exchangeable sodium percentage (ESP), and SAR. ESP incorporates values of exchangeable sodium and cation exchange capacity, which was not evaluated in this study. Sumner et al. (1998) proposed three levels of classification: non-sodic (SAR ≤ 3, ESP ≤ 6), sodic (SAR = 3 – 10, ESP = 6 – 15), and very sodic (SAR > 10, ESP > 15). Based on this classification, the media tended to return to a non-sodic state after all baseline storm events. The return to a non-sodic classification is supported by the low NTU and TSS measurements, as described in their respective

sections. Through cation exchange between sodium and calcium ions, soil deflocculation continued through baseline storm events until enough sodium had been washed out of the columns, which is evidenced by the decrease in SAR.

3.5 Nitrogen Results

3.5.1 TN and DN Results

Influent TN ranged from 2.5 - 4.3 mg-N/L as a result of variable TN in the tap water (Figure 17). Average TN was 3.4 mg-N/L across all columns and standard deviation was 0.84 mg-N/L. Average influent TN for individual columns ranged from 3.1 to 3.5 mg-N/L, with standard deviations from 0.6 to 0.8 mg-N/L (Table 13). During the first baseline storms, 0 – 4 m applied water, effluent from the 2,000, 5,000, and 10,000 mg/L NaCl columns was within a range of 0.2 - 3.0 mg-N/L (Figure 17). Average effluent TN for individual columns ranged from 1.7 to 2.6 mg-N/L with standard deviations from 0.8 to 1.4 mg-N/L. Effluent TN for the baseline storms for the 2,000 mg/L NaCl column were statistically different than the baseline effluent from the control and 5,000 mg/L NaCl columns. Therefore, effluent observations within the 0 – 4 m were made relative to the respective column.

Table 14. Summary of influent and effluent TN concentrations for the 2,000, 5,000, and 10,000 mg/L NaCl columns, with units in mg-N/L.

	2,000 mg/L NaCl		**5,000 mg/L NaCl**		**10,000 mg/L NaCl**	
	Influent	**Effluent**	**Influent**	**Effluent**	**Influent**	**Effluent**
Average	3.4	2.6	3.5	2.4	3.1	1.7
Standard deviation	0.8	0.9	0.6	1.4	0.8	1.7

TN data from a control column by Owen (2016) had effluent ranging from 0.6 – 3.6 mg-N/L. Average effluent TN from the control column was approximately 2.0 mg-N/L and the applied velocity and stormwater recipe were the same as in this study.

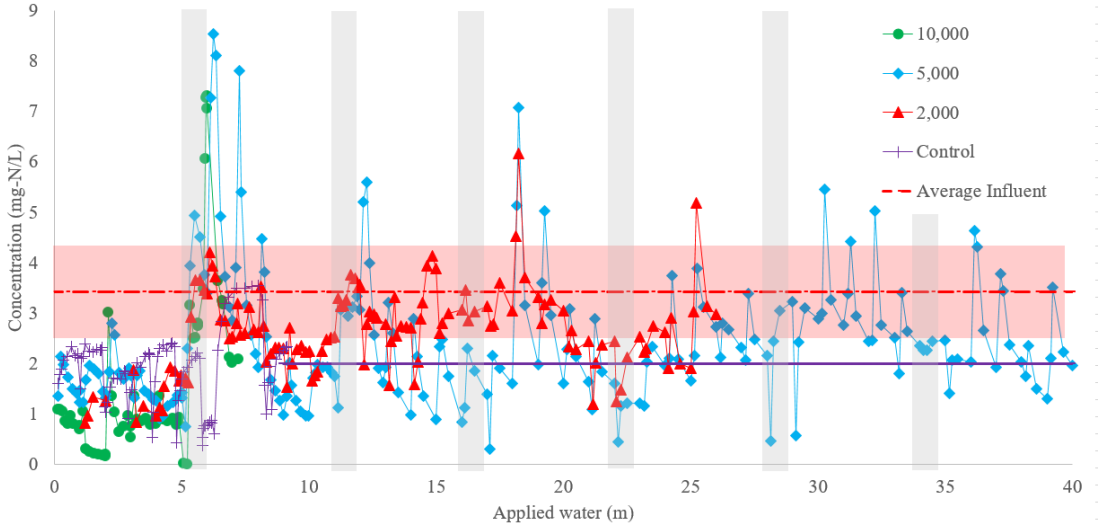

Figure 17. TN in effluent from the 10,000, 5,000, and 2,000 mg/L NaCl bioretention columns. Data for the control column are from Owen (2016), and effluent data after 8 m is extrapolated. High salt events occurred every sixth event, indicated by gray boxes. Intermediate baseline events contained 20 mg/L NaCl. Influent TN ranged from 2.5 – 4.3 mg-N/L, indicated by the red box, and influent TN averaged 3.4 mg-N/L. Applied velocity was 16.7 cm/hour to all columns.

Effluent TN from the 10,000 mg/L NaCl column reached a maximum concentration of 7.3 mg-N/L, which occurred at 6.0 m applied water, immediately after the high salt event (Figure 17). As the effluent flow rate continued to decline as a result of the salt application, effluent TN concentration decreased to 2.0 mg-N/L by 6.9 m applied water, and remained at 2.0 mg-N/L until the experiment was terminated.

Effluent TN from the 5,000 mg/L NaCl column exhibited sawtooth patterns similarly observed with TSS and turbidity (Figure 17). TN peaks occurred every

storm during the second sample collection and TN concentrations decreased until the end of the storm. Within each set of salt application and five baseline storms, TN maxima occurred during the second baseline storm and the individual storm peaks decreased in the following storms. The TN maxima decreased with continued applications of synthetic stormwater, with the first maximum having a concentration of 8.5 mg-N/L, and the last maximum having a concentration of 4.6 mg-N/L. By the end of the five baseline storms for any set of salt and baseline storms, all effluent TN concentrations were less than the average influent concentration.

Effluent TN from individual storms from the 2,000 mg/L NaCl column exhibited similar sawtooth patterns to the 5,000 mg/L NaCl column (Figure 17). Effluent concentrations until the 16^{th} m applied water remained within or below the influent TN range. However, the maximum effluent TN concentration of 6.2 mg-N/L occurred after the third high salt event, although effluent concentrations in the following baseline storms were within the influent TN range. After the fourth high salt event, an effluent peak of 5.2 mg-N/L occurred during the third baseline storm.

DN measurements for the 2,000 and 5,000 mg/L NaCl columns began after the 7^{th} and 20^{th} m applied stormwater, respectively. 3.7% of all samples measured for DN were less than 98% of TN. DN samples from the 2,000 and 5,000 mg/L NaCl columns were greater than 80% and 60% of TN, respectively, indicating that a majority of the effluent TN is consistently in the dissolved form. Effluent with DN less than 98% of TN typically occurred during the first baseline storm following a salt event. Blecken et al. (2010) observed over 93% of effluent TN as DN in biofilters kept at 2, 7, and 20°C. The mechanisms that result in dissolved inorganic N species

and dissolved organic N comprising a majority of TN are discussed in the following subsections.

Since effluent flow rates were consistently less than influent flow rates, stormwater was retained in columns during storm events (Appendix E-1)and allowed for TN retention even during periods when effluent concentrations were greater than influent concentrations. However, Denich et al. (2013) did not observe TN removal in mesocosms loaded with 2- and 15-years worth of road salt as NaCl and noted N release occurred at different rates and times. Notably, the 2-years loading of 2,430 g of a salt mix is more than 2.5 times the amount of NaCl applied in this study. The greater NaCl mass used in the study by Denich et al. (2013) may explain why TN removal was not observed. Additionally, the mesocosms in the study by Denich et al. (2013) received synthetic stormwater containing the entire loadings of road salts and then were flushed 10 times with 10 L of DI, which contrasts to the one salt event/five baseline storms pattern. Applying baseline storms between high salt events may be more representative of how SCMs receive winter runoff, so TN removal in bioretention under winter loading conditions is possible.

3.5.2 TN Mass Balance

TN mass balances for the mesocosms are shown in Figure 18. For the 10,000 mg/L NaCl column, flow rate measurements were unavailable for 0 – 1 m applied water (the first storm event) and therefore estimates of influent and effluent N are unavailable. However, based on rates of N loadings from the other 0 – 4 m baseline storms, it is assumed that the TN effluent mass do not exceed the TN influent mass for the first storm event.

Effluent N mass from the 10,000 mg/L NaCl column remained below influent N and remained around 99 mg-N by the end of the experiment (Figure 18). Effluent N did not increase after the 6th m applied water as a result of the column clogging. By the end of the experiment, approximately 424 mg-N had been sequestered in the column out of 523 mg-N applied.

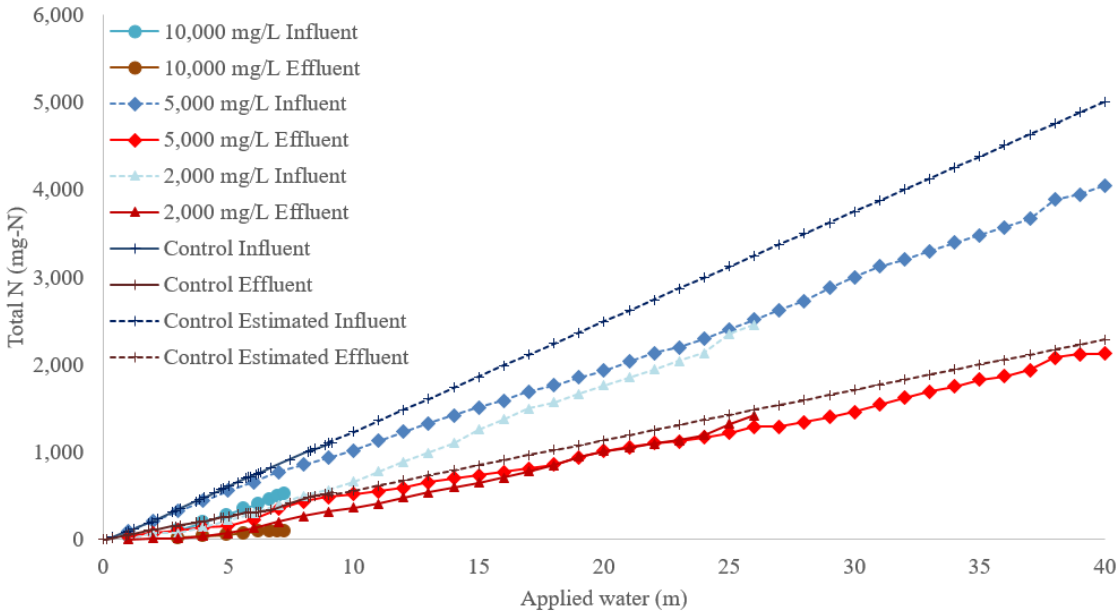

Figure 18. TN mass balances for the control, 10,000, 5,000, and 2,000 mg/L NaCl bioretention columns. High salt events occurred every six storm events. Intermediate baseline events contained 20 mg/L NaCl. Influent TN ranged from 2.5 – 4.3 mg-N/L, with an average of 3.4 mg-N/L. Applied velocity was 16.7 cm/hour to all columns. Storm events continued until 9, 26, 40, and 7 m applied water for the control, 2,000, 5,000, and 10,000 mg/L NaCl columns, respectively. Data for the control column are from Owen (2016) and after 9 m applied water, influent and effluent data for the control column are extrapolated assuming a linear relationship between TN mass and applied water.

By 40 m applied water, influent TN that had exited the 5,000 mg/L NaCl column was 3,747 mg-N (Figure 18). Effluent TN increased linearly and consistently remained less than the mass of influent TN. By 40 m applied water, effluent TN was 2,125 mg-NL with a net removal of 1,622 mg-N by the end of the experiment.

A mass balance was estimated for the 2,000 mg/L NaCl column, although samples from the two of the four initial baseline storms were not collected. Based on TN mass loading rates from observed 0 – 4 m applied water, it was also assumed that TN was not exported during the initial baseline events. Influent TN by the end of 26 m applied water was 2,456 mg-N, and effluent TN was 1,418 mg-N (Figure 18). Net N retained by the column was 1,038 mg-N.

After 9.1 m applied water, 1,110 mg-N had been applied to the control column and 541 mg-N had exited (Owen 2016, Figure 18). Based on the available data and assuming a linear relationship, it was estimated that by 40 m applied water, 5000 mg-N would have been applied and 2290 mg-N would have exited the column.

As discussed in the TSS mass balance section, the 2,000 and 5,000 mg/L NaCl columns received the equivalent of 1 year and 4 months and 2 years of applied MD rainfall, respectively. TN EMCs for the control, 2,000, 5,000, and 10,000 mg/L NaCl columns were 2.1, 2.9, 2.6, and 1.1 mg-N/L, respectively. Despite the increased effluent concentrations, the EMC for the 10,000 mg/L NaCl column is likely due to the clogging, which decreased the effluent volume.

Mechanisms for N mobility are related to ionic exchange and mobilization of organic matter, as discussed in detail below. The decreased EMC with increasing salt concentration may be related to increased occupancy of sodium on BSM adsorption sites, as discussed in the TSS section. Under the different NaCl loading conditions, mesocosms exhibited TN mass retention which demonstrates short-term capabilities of N removal. In addition to the simulated 15-year loading by Denich et al. (2013),

long-term studies of bioretention N performance under winter conditions are needed to further evaluate the lifetime performance of bioretention systems.

3.5.3 Ammonium and DKN Results

DKN measurements for the 2,000 and 5,000 mg/L NaCl columns began after the 7th and 20th m applied water, respectively. Effluent from the 2,000 and 5,000 mg/L NaCl columns exhibited sawtooth patterns previously described for effluent TSS (Figure 19). DKN maxima typically occurred during the second storm following a high salt event, and maximum DKN concentrations for the 2,000 and 5,000 mg/L NaCl column were 4.6 and 4.2 mg-N/L, respectively. Following a DKN spike, effluent concentrations would typically decrease to less than 2 mg-N/L. Average effluent DKN concentrations ranged from 1.2 to 1.3 mg-N/L with standard deviations from 0.8 to 1.0 mg-N/L (Table 14).

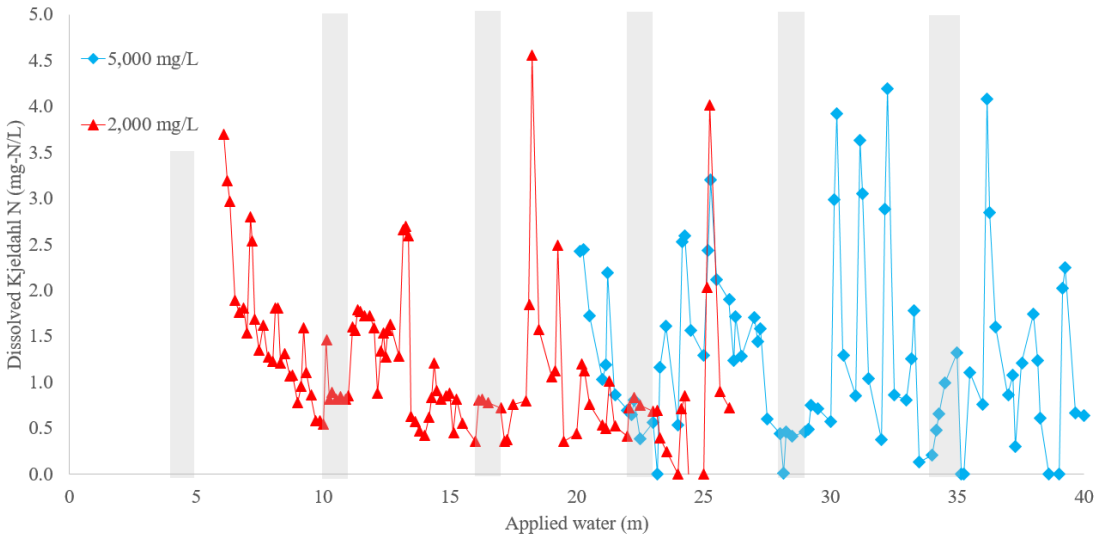

Figure 19. Dissolved Kjedhal Nitrogen (DKN = DN – NO_3^-) in effluent from the 10,000, 5,000, and 2,000 mg/L NaCl bioretention columns. High salt events occurred every sixth event, indicated by gray boxes. Intermediate baseline events contained 20 mg/L NaCl. Effluent DKN was not measured until the 7th and 20th m applied water for the 2,000 and 5,000 mg-N/L NaCl columns, respectively. If DN – NO_3^- < 0, DKN was assumed to be 0 mg-N/L. Applied velocity was 16.7 cm/hour to all columns.

Table 15. Summary of effluent DKN for the 2,000 and 5,000 mg/L NaCl columns, with units in mg-N/L.

	2,000 mg/L NaCl	**5,000 mg/L NaCl**
	Effluent	**Effluent**
Average	1.2	1.3
Standard deviation	0.8	1.0

Effluent DKN is more strongly correlated to turbidity (R^2 = 0.55 and 0.41 for the 2,000 and 5,000 mg/L NaCl columns, respectively, Appendix E-2) than to TOC (R^2 = 0.21 and 0.49 for the 2,000 and 5,000 mg/L NaCl columns, respectively, Appendix E-3). The positive correlation among DKN, turbidity, and TOC is likely related to chloride's solvating effect on organic matter (Kaiser et al., 1996; Wiklander, 1975; Wong et al., 2010), as discussed in the TOC section, in addition to cation exchange between ammonium and sodium ions. Since the relationship between effluent DKN is moderately correlated to turbidity, ammonium removal mechanisms unrelated to turbidity may further explain the DKN washouts.

The average influent ammonium concentration across all columns was 0.2 mg-N/L, with a standard deviation of 0.03 mg-N/L, and concentrations ranged from <0.1 mg-N/L to 0.5 mg-N/L (Figure 20). Individual average influent ammonium concentrations were from 0.1 to 0.2 mg-N/L with standard deviations from less than 0.1 to 0.2 mg-N/L (Table 15). Effluent ammonium could not be measured following salt applications once effluent samples became too discolored. Effluent ammonium from all columns in the four initial baseline storms ranged from 0.1 – 0.6 mg-N/L

with the exception of a peak of 1.6 mg-N/L occurring at 2.1 m applied water from the 10,000 mg/L NaCl column. For individual columns, average effluent ammonium concentrations ranged from 0.1 to 0.6 mg-N/L with standard deviations from 0.2 to 1.4 mg-N/L. During the 10,000 mg/L NaCl salt event, effluent concentrations decreased from 1.0 to 0.5 mg-N/L whereas effluent from the 2,000 and 5,000 mg/L NaCl columns remained within the baseline ammonium range. Effluent ammonium from the 10,000 mg/L NaCl column increased to 2.9 mg-N/L after 5.9 m applied water, or the second baseline storm after the high salt event, before decreasing to 0.6 mg-N/L at 6.4 m applied water. The final ammonium samples from the 10,000 NaCl column that could be measured were 1.5 and 1.7 mg-N/L.

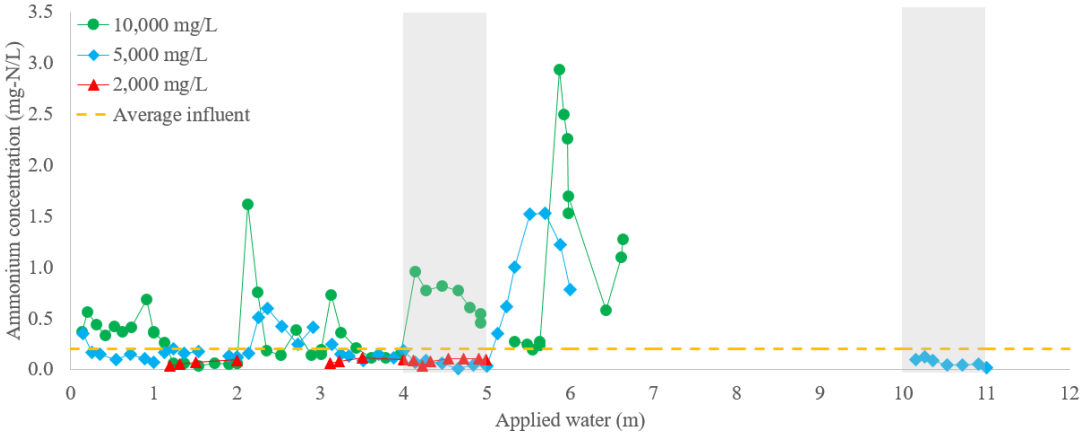

Figure 20. Ammonium in effluent from the 10,000, 5,000, and 2,000 mg/L NaCl bioretention columns. High salt events occurred every sixth event, indicated by gray boxes. Intermediate baseline events contained 20 mg/L NaCl. Missing data are due to discoloration of samples, which could not be measured on the UV-Vis. Applied velocity was 16.7 cm/hour to all columns.

Following the 5,000 mg/L NaCl salt application, effluent ammonium increased to 5.5 mg-N/L before decreasing to 0.8 mg-N/L over the course of 1 m applied water (Figure 20). The remaining four baseline storms were too discolored to measure ammonium. However, by the 10th m applied water, most effluent, except the

first two samples, was clear enough to measure ammonium. The effluent concentrations were less than 0.1 mg-N/L. Effluent ammonium from the 2,000 mg/L NaCl column following the high salt event was unable to be read.

Table 16. Summary of influent and effluent ammonium concentrations for the 2,000, 5,000, and 10,000 mg/L NaCl columns, with units in mg-N/L.

	2,000 mg/L NaCl		**5,000 mg/L NaCl**		**10,000 mg/L NaCl**	
	Influent	**Effluent**	**Influent**	**Effluent**	**Influent**	**Effluent**
Average	0.1	0.1	0.2	2.5	0.2	0.6
Standard deviation	<0.1	<0.1	0.2	1.4	0.1	0.6

Increased ammonium concentrations from the 10,000 and 5,000 mg/L NaCl columns is likely a result of cation exchange between ammonium and sodium ions. Khorsha and Davis (2017) observed clear competition between ammonium and sodium on exchange sites in clinoptilolite zeolite, and competition may be assumed to occur in BSM. Similar to hypotheses relating ionic strength to mobilized metals (Zehetner et al. 2009; Tedoldi et al. 2016), the magnitude of the released ammonium may be correlated to increased salt concentrations (Green and Cresser 2008). In a field study in Cumbria, UK conducted by Green and Cresser (2008), the proportion of ammonium in roadside soil samples was found to decrease with distance from the road likely due to road salt applications. The authors postulate that ammonium mobility may lead to ammonium limitations, affecting plant stress. Ammonium occupancy of cation exchange sites were found to be reduced over time in the roadside soils. The observed low concentrations of ammonium at 10 m applied water in the 5,000 mg/L NaCl column, which coincide with the second high salt event, may be a result of ammonium occupying few exchange sites on the BSM after exposing the column to elevated NaCl concentrations.

A second pathway of ammonium removal is through aerobic nitrification. Li and Davis (2014) observed lower ammonium concentrations and higher nitrate concentrations in bioretention effluent, suggesting nitrification during drying periods. Due to limited ammonium data, it is inconclusive if, and to what extent, ammonium was nitrified during and following high salt events. However, low nitrate concentrations reported for the 5,000 and 10,000 mg/L NaCl columns (to be discussed later) do not coincide with the elevated ammonium concentrations. Therefore, it is likely the observed elevated ammonium concentrations are likely due to cation exchange.

3.5.4 Nitrite and Nitrate Results

Effluent nitrite could not be measured following salt applications once effluent samples became too discolored. Effluent from the four initial baseline storms released nitrite typically less than 0.1 mg-N/L (Figure 21), although the 10,000 mg/L NaCl column exhibited elevated concentrations of 0.3 mg-N/L at 1.1 m applied water. For each column, average effluent nitrite was less than 0.1 mg-N/L with standard deviations also less than 0.1 mg-N/L (Table 16). During the 10,000 mg/L NaCl salt event, effluent nitrite increased from 0.1 mg-N/L and remained around 0.2 mg-N/L for the remainder of the storm. Effluent from the 2,000 and 5,000 mg/L NaCl columns remained below 0.1 mg-N/L. Effluent nitrite concentrations from the 10,000 mg/L NaCl exhibited a similar pattern observed for ammonium, with the peak nitrite concentration of 0.6 mg-N/L occurring at 5.6 m applied water. The final ammonium samples from the 10,000 NaCl column that could be measured was below detection limits (0.01 mg-N/L).

Table 17. Summary of influent and effluent nitrite concentrations for the 2,000, 5,000, and 10,000 mg/L NaCl columns, with units in mg-N/L.

	2,000 mg/L NaCl		**5,000 mg/L NaCl**		**10,000 mg/L NaCl**	
	Influent	**Effluenet**	**Influent**	**Effluent**	**Influent**	**Effluent**
Average	<0.1	<0.1	<0.1	<0.1	<0.1	0.1
Standard deviation	<0.1	<0.1	<0.1	<0.1	<0.1	0.1

Effluent nitrite from the 5,000 mg/L NaCl column remained below 0.1 mg-N/L following the high salt event (Figure 21), and effluent from the second high salt event were below detection limits. Effluent nitrite from the 2,000 mg/L NaCl column following the salt application could not be measured.

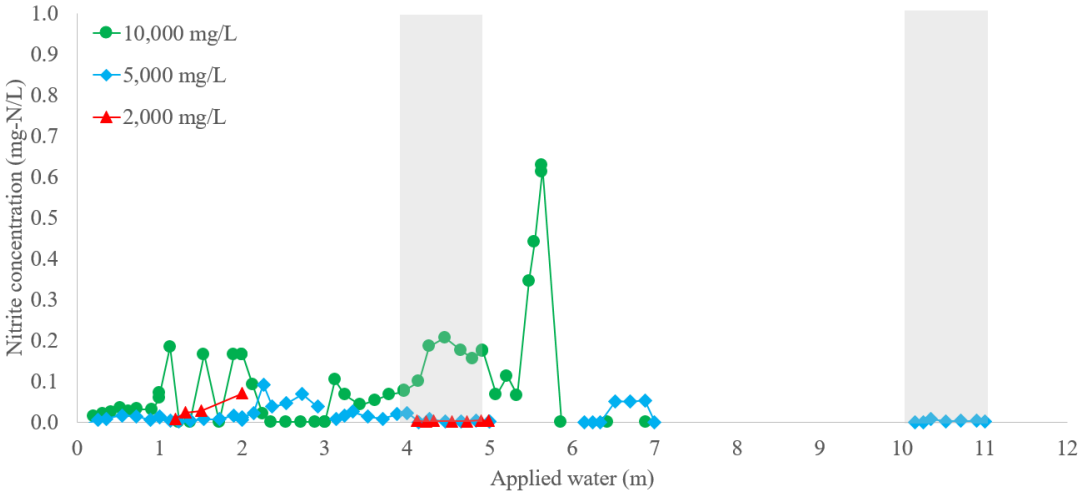

Figure 21. Nitrite in effluent from the 10,000, 5,000, and 2,000 mg/L NaCl bioretention columns. High salt events occurred every sixth event, indicated by gray boxes. Intermediate baseline events contained 20 mg/L NaCl. Missing data are due to discoloration of samples, which could not be measured on the UV-Vis. Applied velocity was 16.7 cm/hour to all columns.

Influent nitrate ranged from 1.2 – 3.1 mg-N/L as a result of variable tap water concentrations. (Figure 22). Average influent nitrate across all columns was 2.0 mg-N/L. For individual columns, average influent nitrate ranged from 1.3 to 3.4 mg-N/L, with standard deviations from 0.6 to 0.8 mg-N/L (Table 17). Effluent from the initial

baseline storms ranged between 0.3 – 2.1 mg-N/L. Average effluent nitrate for individual columns ranged from 0.1 to 1.8 mg-N/L with standard deviations from 0.1 to 0.7 mg-N/L. Missing effluent nitrate data are due to chloride peak interference, as discussed in the methodology.

Table 18. Summary of influent and effluent nitrate concentrations for the 2,000, 5,000, and 10,000 mg/L NaCl columns, with units in mg-N/L.

	2,000 mg/L NaCl		**5,000 mg/L NaCl**		**10,000 mg/L NaCl**	
	Influent	**Effluent**	**Influent**	**Effluent**	**Influent**	**Effluent**
Average	2.1	1.8	3.4	1.1	1.3	0.1
Standard deviation	0.6	0.7	0.7	0.7	0.8	0.1

Effluent nitrate from the 2,000 mg/L NaCl column generally increased to concentrations greater than the baseline storms (Figure 22). After the first 2,000 mg/L NaCl event, effluent nitrate increased to 2.0 mg-N/L, although as observed with the 5,000 mg/L NaCl column, samples taken at the beginning of each storm were local minima and likely due to denitrification. Effluent nitrate was greatest at 14.8 m applied water, with a maximum concentration of 3.3 mg-N/L. After the third high salt event, effluent nitrate slightly decreased by the fourth and fifth baseline storms, with effluent concentrations around 2.0 mg-N/L, but after the fourth high salt event, effluent concentrations remained above 2.0 mg-N/L.

After the first 5,000 mg/L NaCl application, nitrate effluent remained below 1.5 mg-N/L until the fifth baseline storm, where it increased to 2.5 mg-N/L (Figure 22). Effluent from the next set of salt and baseline storms remained below 1.1 mg-N/L. However, effluent from the last three sets of salt and baseline storms were greater than 1.5 mg-N/L, with the exception of samples taken at the beginning of each

storm. Nitrate concentrations from the first samples were less than 1.0 mg-N/L, which are likely a result from denitrification occurring between storm events in microsites and root zones, as discussed below (Dietz and Clausen 2006; Denich et al. 2013).

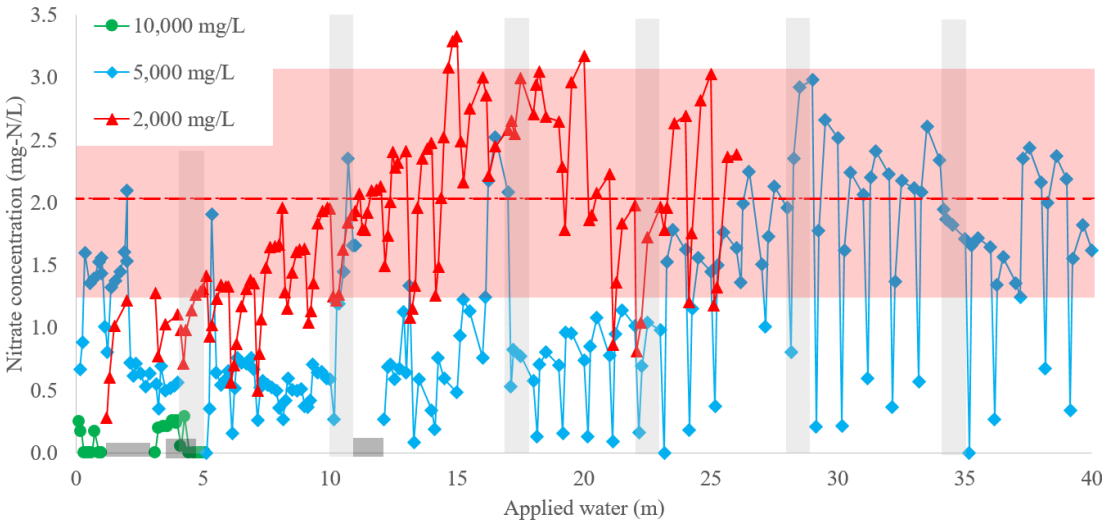

Figure 22. Nitrate in effluent from the 10,000, 5,000, and 2,000 mg/L NaCl bioretention columns. High salt events occurred every sixth event, indicated by gray boxes. Intermediate baseline events contained 20 mg/L NaCl. Influent nitrate ranged from 1.2 – 3.1 mg-N/L, with an average of 2.0 mg-N/L. Missing data are due to chloride peak interference on the IC and are represented by black boxes at the bottom of the figure. Applied velocity was 16.7 cm/hour to all columns.

In addition to micropores supporting anaerobic conditions for denitrification (Li and Davis 2014), plant roots zones may support biological communities capable of denitrification (Davis et al. 2009). Periodically throughout the study, the aluminum foil was peeled back and continuous growth of *Juncus* roots were observed. Upon planting, the *Juncus* roots were approximately 15 cm in length, but by the end of the studies, the roots had visibly grown through the BSM layer and into the sand layer in both columns. Biomass growth of the plants was not measured, although the root growth was assumed to signify salt tolerance. Although no specific studies have demonstrated the potential salt tolerance of *J. effuses*, other studies investigating salt

tolerant plants and nitrogen removal have found *Juncus* plants capable of nitrate removal at concentrations up to 23,400 mg/L NaCl (Szota et al. 2015).

While *J. effuses* root zones could have supported denitrification, the increase in effluent nitrate concentrations in the 2,000 and 5,000 mg/L NaCl columns suggests denitrification became inhibited. Lancaster et al. (2016) observed in roadside wetlands inhibition of denitrification with chloride loadings greater than 2,500 mg/L Cl^-, but noted the decrease in denitrification rates was not significant for roadside wetlands historically exposed to elevated chloride concentrations. In a laboratory setting, effluent nitrate concentrations from bioretention columns were found to decrease with salt concentrations, ranging from 80 to 935 mg/L Cl^- (Endreny et al. 2012). A nometric multidimensional scaling analysis of bacterial communities from the bioretention columns revealed distinctive communities from the high salt samples compared to the lower salt treatments. However, community composition analyses were not performed and it is unknown how the proportion of denitrifiers changed in response to increased salt concentrations. A better understanding of the composition of denitrifying communities in the 2,000 and 5,000 mg/L NaCl mesocosms may be able to support adaptations to denitrifying communities observed by Lancaster et al. (2016) and provide a better understanding as to why effluent nitrate increased in the 5,000 mg/L NaCl column.

As mentioned previously, temperature in the greenhouse did not remain constant, despite the temperature controls set at 24 °C. Denitrification rates are lower under colder conditions (Hunt et al. 2012), as Stanford et al. (1975) note that denitrification rates in soil “abruptly” decline between 10 and 15 °C in contrast to

rates between 15 and 35 °C. Although denitrification rates increase with increased temperature, bioretention laboratory and field studies (Blecken et al. 2010; Manka et al. 2016) have reported increased NO_x concentrations (maximum concentrations reported as 3.76 and 0.43 mg/L, respectively) at temperatures greater than 20 °C as a result of increased nitrification since optimum nitrification temperatures are around 20 – 35 °C.

Since influent and effluent synthetic stormwater averaged greater than 20.0 °C (Appendix D-1), it was hypothesized that the nitrate effluent concentrations would increase as a result of the increased nitrification. While a regression analysis between effluent temperature and nitrate concentration from the 2,000 and 5,000 mg/L NaCl columns revealed a slight negative correlation, the correlation coefficients were not significant (R^2 = 0.08 and 0.17 for the 2,000 and 5,000 mg/L NaCl columns, respectively Appendix E-4). Temperature may have impacted nitrate concentrations by increasing nitrification rates, but since ammonium data are unavailable for the 2,000 and 5,000 mg/L NaCl columns, the data are insufficient to support the findings by Blecken et al. (2010 and Manka et al. (2016). Since no significant relationship was found between effluent temperature and nitrate, additional factors may be the dominant driving force in denitrification, such as the addition of salt.

Nitrate mass balances were calculated for the 2,000 and 5,000 mg/L NaCl columns (Figure 23). A nitrate mass balance for the 10,000 mg/L NaCl column was not calculated since nitrate effluent data are missing after the high salt event. Influent nitrate loading rates for the 2,000 and 5,000 mg/L NaCl columns were similar, with nitrate inputs by the end of the studies equivalent to 1,415 and 2,255 mg-N for the

respective columns. The 2,000 mg/L NaCl column exported 908 mg-N by the 26th m applied water, resulting in a 35.9% nitrate mass removal efficiency. The 5,000 mg/L NaCl column exported 1,040 mg-N by 40 m applied water, and the nitrate mass removal efficiency was 53.9%.

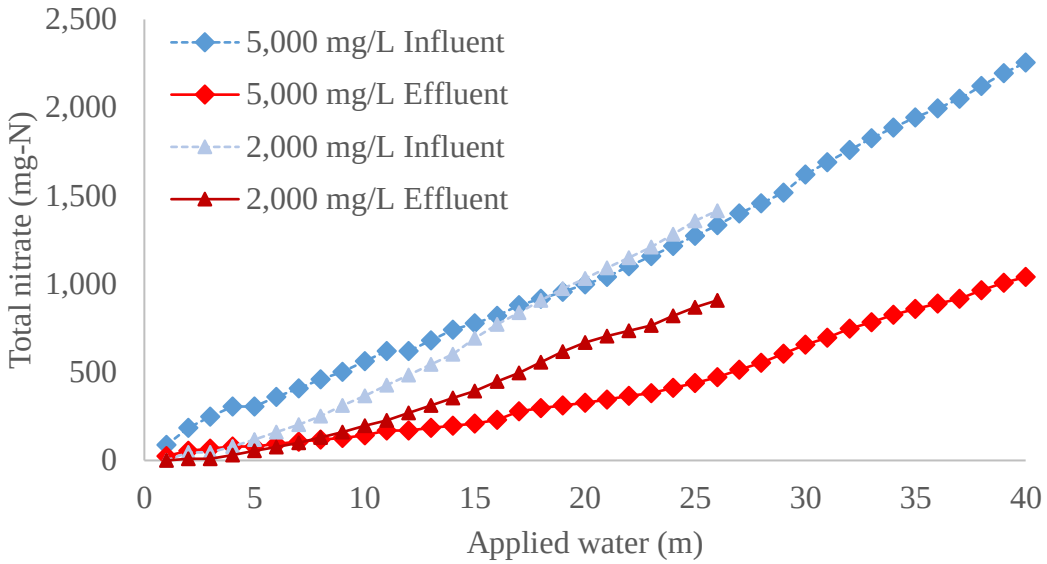

Figure 23. Nitrate mass balances for the 5,000 and 2,000 mg/L NaCl bioretention columns. High salt events occurred every six storm events. Intermediate baseline events contained 20 mg/L NaCl. Average influent nitrate was 2.0 mg-N/L. Applied velocity was 16.7 cm/hour to all columns. Storm events continued until 26 and 40 m applied water for the 2,000 and 5,000 mg/L NaCl columns, respectively.

Nitrate EMCs for the 2,000 and 5,000 mg/L NaCl columns were 1.8 and 1.3 mg-N/L. Based on the EMCs, it is not surprising that the 5,000 mg/L NaCl column retained more nitrate than the 2,000 mg/L NaCl column. The cause for the greater nitrate removal is unknown, even though the nitrate loading rates are the same for both columns. However, it is hypothesized that the denitrifying bacteria community in the 5,000 mg/L NaCl column was more resilient than the 2,000 mg/L NaCl column to the high salt events. After the second high salt event at 10 m applied water, the mass removal rates for the 2,000 and 5,000 mg/L NaCl columns diverge (Appendix

E-5), and the nitrate removal rate of the 5,000 mg/L NaCl column becomes less than that of the 2,000 mg/L NaCl column. Perhaps by the second high salt event in the 5,000 mg/L NaCl column, the denitrifying communities became better adapted to saline conditions. However, bacterial communities from both columns were not assessed for presence and activity of denitrifiers and further investigation is needed to understand denitrifier resilience to high concentrations of NaCl.

3.5.4 N Summary

During the 2,000 and 5,000 mg/L NaCl high salt events, most of the effluent TN was DN. The primary mechanisms responsible for TN release are likely cation exchange between sodium and ammonium ions, mobilization of organic N, and inhibition of denitrification. Despite elevated effluent TN concentrations, TN was retained in all columns due to water retention in the columns (Appendix D-1). Based on the duration of the 2,000 and 5,000 mg/L NaCl column studies, TN capture is possible during and after deicer applications.

3.6 Phosphorus Results

Influent TP ranged from 0.1 – 0.5 mg-P/L, with an average of 0.3 mg-P/L across all columns (Figure 24). Individual average influent concentrations for each column ranged from 0.3 to 0.4 mg-P/L with standard deviations from 0.1 to 0.2 mg-P/L (Table 18). However, the salt used apparently contained P since influent TP during high salt events was approximately 0.8 mg-P/L. Average effluent TP for individual columns ranged from 0.4 to 0.7 mg-P/L, with standard deviations from 0.4 to 0.9 mg-P/L. Effluent TP for the baseline storms for the 5,000 mg/L NaCl column

were statistically different than the baseline effluent from the control and 2,000 mg/L NaCl columns. Therefore, effluent observations within the 0 – 4 m were made relative to the respective column. Effluent control TP data are from the bioretention study conducted by Owen (2016), and long-term effluent TP is extrapolated and assumed to be <0.1 mg-P/L. Effluent DP was consistently greater than 75% of TP for all storms. All effluent from the 0 – 4 m baseline storms were less than 0.6 mg-P/L, with over 97% of all samples less than 0.3 mg-P/L.

Table 19. Summary of influent and effluent TP for the 2,000, 5,000, and 10,000 mg/L NaCl columns, with units in mg-P/L.

	2,000 mg/L NaCl		**5,000 mg/L NaCl**		**10,000 mg/L NaCl**	
	Influent	**Effluent**	**Influent**	**Effluenet**	**Influent**	**Effluent**
Average	0.3	0.4	0.4	0.5	0.3	0.7
Standard deviation	0.1	0.4	0.2	0.6	0.2	0.9

As with effluent patterns observed for N, TSS, turbidity, and TOC, sawtooth patterns were observed after high salt events for all effluent samples. O'Neill and Davis (2012) similarly observed effluent TP sawtooth patterns bioretention mesocosms. Davis et al. (2009) summarize that wet and dry periods result in variable redox conditions that may be conducive to nutrient removal, and therefore rewetting BSM at the beginning of the storm may alter redox conditions that occurred between storms.

During the 10,000 mg/L NaCl salt application, influent TP remained less than 0.2 mg-P/L (Figure 24). Following the high salt event, effluent TP increased to 3.0 mg-P/L by 5.6 m applied water. Between 5.0 and 5.6 m applied water, over half of the 242,000 mg NaCl from the high salt event had been washed out of the column;

surprisingly, the high effluent TP concentration did not coincide with the timing of large NaCl masses exiting the column during the storm immediately after the high salt event. A second and third TP peak occurred during the next storm events, which may be related to wet and dry periods. By the end of the 7.2 m applied water, effluent TP was around 0.5 mg-P/L. Notably DP comprised over 50% of TP for effluent samples following the high salt event, and of the DP, DOP comprised over 60% in effluent samples. By the 6th m applied water, DOP was between 30 and 50% of DP in all samples.

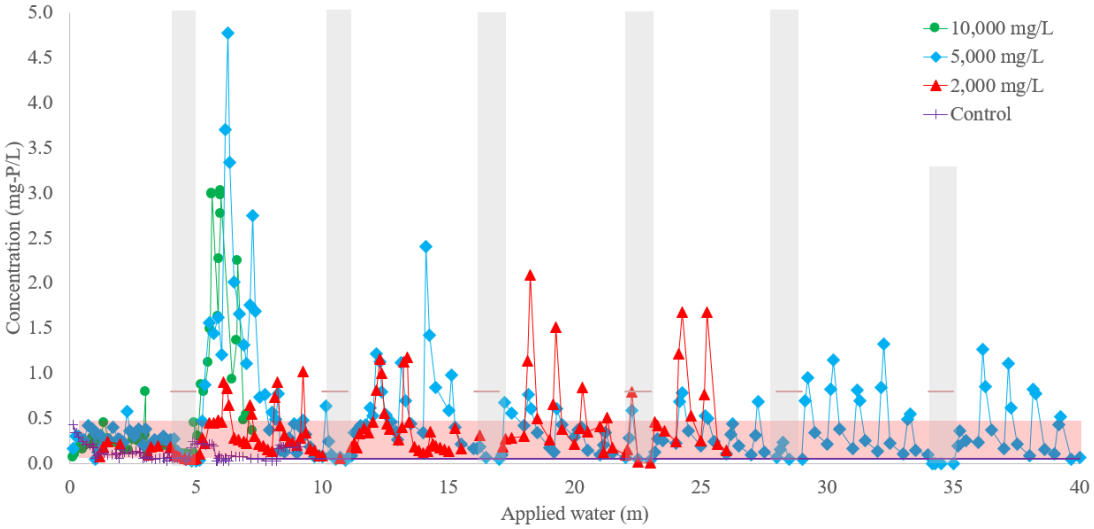

Figure 24. TP in effluent from the 10,000, 5,000, and 2,000 mg/L NaCl bioretention columns. Data for the control column are from Owen (2016), and effluent data after 8 m is extrapolated. High salt events occurred every sixth event, indicated by gray boxes. Intermediate baseline events contained 20 mg/L NaCl. Influent TP for baseline storms ranged from 0.1 – 0.5 mg-P/L, with an average of 0.3 mg-P/L, and influent TP for high salt events was around 0.8 mg-P/L. Applied velocity was 16.7 cm/hour to all columns.

Similar to the 10,000 mg/L NaCl column, the TP peak of 6.2 mg-P/L did not coincide with large masses of NaCl exiting the 5,000 mg/L NaCl column but instead occurred at 6.2 m applied water (Figure 24). After the first high salt event, effluent TP

exhibited similar sawtooth patterns during all baseline storms, with the local maxima occurring during the second sampling event. By the end of the first set of salt/five baseline storms, equivalent to 5 m applied water, effluent TP was less than 0.5 mg-P/L. The second high salt event caused an increase in effluent TP concentrations, and the greatest TP concentration was 2.4 mg-P/L. The third and fourth sets of salt/baseline storms did not release TP greater than 0.8 mg-P/L, although effluent TP sawtooth peaks increased to around 1.2 mg-P/L by the fifth and sixth sets.

The first two baseline storms following a high salt event in the 5,000 mg/L NaCl column had over 70% of TP as DP. DP represented greater than 50% of TP in effluent from the next three baseline storms. After the 30^{th} m applied water, effluent DP consistently remained above 75%. DOP data are not available after the 5^{th} m applied water, but DOP comprised around 50% of DP during the high salt event, which is a reduction from around 80% during baseline storms.

As with the 5,000 and 10,000 mg/L NaCl columns, the maximum effluent concentration from the 2,000 mg/L NaCl column after the salt application occurred during the second baseline storm, with a concentration of 0.9 mg-P/L (Figure 24). The effluent exhibited sawtooth patterns, although the magnitude of the peaks of the sawtooths remained around 1.0 mg-P/L during the first set of salt/baseline storms. During the second set of salt/baseline storms, effluent sawtooth peaks were 1.2 mg-P/L and declined to 0.3 mg-P/L during the remaining two baseline storms. Effluent sawtooth peaks increased during the second and third sets of salt/baseline storms, with peaks reaching concentrations of 2.1 and 1.7 mg-P/L, respectively. By the end of

each set of salt/baseline storms, effluent TP remained greater than influent TP, although effluent from the first three high salt events were less than 0.1 mg-P/L.

The DP dominance of TP are similarly observed in the 2,000 mg/L NaCl column. During the last 3 m applied water, DP was over 75% of TP. However, DOP declined from 80 to 65% of DP during the high salt event whereas DOP made up as much as 83% at the beginning of baseline storms and declined to 35%.

Since DP dominated TP throughout most of the events in the 2,000 and 5,000 mg/L NaCl columns, the dominant mechanism of TP release in effluent is likely tied to DP mobilization. DP mobilization may have occurred by similar mechanisms that resulted in high turbidity discharge since DP and turbidity are strongly correlated (R^2 = 0.72 and 0.70 for the 2,000 and 5,000 mg/L NaCl columns, respectively, Appendix F-1). As previously stated, salt alters the composition of exchange sites on clays (Kaiser et al., 1996; Wiklander, 1975; Wong et al., 2010), which may result in release of TP as DOP and SRP. Relationships between ionic strength and effluent copper (Bäckström et al. 2004; Zehetner et al. 2009; Tedoldi et al. 2016) serve as a basis to postulate that the effect of increased ionic strength on effluent TP, although further investigation is needed to determine the nature of the relationships. For instance, (Kakuturu and Clark 2015b) observed greater P losses in stormwater filter media columns using 1,200 mg/L NaCl than 150 mg/L NaCl. Effluent TP sawtooth peaks following the first salt event were higher in the 5,000 mg/L NaCl column (4.8 mg-P/L) than the 2,000 mg/L NaCl column (0.9 mg-P/L, Figure 24). The lesser effluent sawtooth peak observed in the 10,000 mg/L NaCl column (3.0 mg-P/L) may be related to the media clogging, which may have limited TP release.

DP and TOC are not strongly correlated (R^2 = 0.60 and 0.40 for the 2,000 and 5,000 mg/L NaCl columns, respectively, Appendix F-2), which suggests TOC and DOP removal mechanisms do not entirely account for DP washouts. However, a correlation between DOP and TOC is unavailable due to limited DOP data. Similar to how salt affects organic matter as a solvent (Kaiser et al., 1996; Wiklander, 1975; Wong et al., 2010), DOP release may be tied to organic matter mobility under high salt conditions. Since adsorption is the major removal mechanism for phosphate in BSM (LeFevre et al. 2014), anion exchange between phosphate and chloride may cause phosphate desorption and subsequent release in effluent. Although long-term SRP and DOP data are unavailable, bioretention effluent samples collected by Denich et al. (2013) following applications of runoff equivalent to 2 years' salt loading (2,430 g of a local salt mix) were consistently dominated by SRP, and chloride retention was observed after flushing columns with DI 10 times. Salt mass balances for the 2,000 and 5,000 mg/L NaCl columns likewise found salt retention, as discussed in the TSS section. The residual chloride may prevent readsorption of SRP after high salt events.

3.6.1 Phosphorus Mass Balance

TP mass balances were calculated for all mesocosms. TP was retained in the 10,000 mg/L NaCl column, with an estimated retention of 45 mg-P out of 72 mg-P (Figure 25). The likely cause for TP retention is due to the decrease in effluent flow rate, from 1.2 mL/s prior to the high salt event to less than 0.1 mL/s by the end of the study, as the media clogged. However, by the end of the experiments, TP was observed to be exported from the 2,000 and 5,000 mg/L NaCl columns.

After 7 m applied water, the 5,000 mg/L NaCl column began to export TP (Figure 25). Beyond 29 m applied water, differences between input TP and output TP masses per storm event were ±12.4 mg-P. By the time the experiment concluded, essentially equal masses of P had entered and exited the column (384 and 388 mg-P, respectively).

After 26 m applied water, TP added to the 2,000 mg/L NaCl column was 191 mg-P and TP that had exited the column was 198 mg-P/L (Figure 25). Until 26 m applied water, the column had demonstrated TP retention. Future work is needed in order to determine whether the TP release is temporary beyond 26 m applied water, although this work indicates TP export is possible under lower salt concentrations.

After 9.1 m applied water, 99.9 mg-P had been applied to the control column and 30.3 mg-P had exited the column (Owen 2016, Figure 25). Assuming a linear relationship between TP mass and applied water, it was estimated that by 40 m applied water, 436 mg-P would have been applied and 123 mg-P would have exited the column.

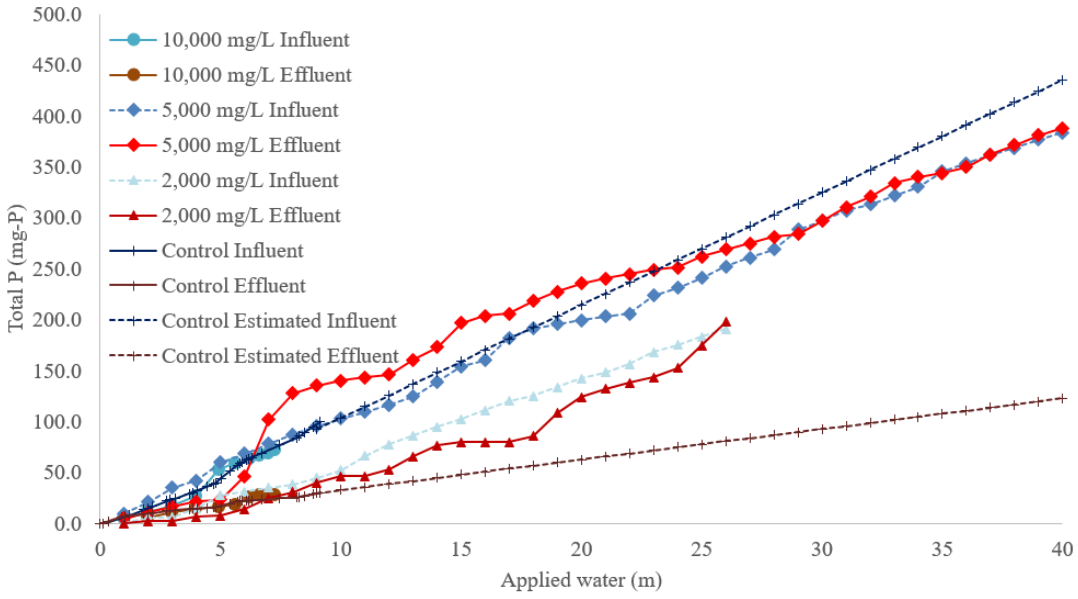

Figure 25. TP mass balances for influent and effluent for the control, 10,000, 5,000, and 2,000 mg/L NaCl bioretention columns. High salt events occurred every six storm events. Intermediate baseline events contained 20 mg/L NaCl. Influent TP for baseline storms ranged from 0.1 – 0.5 mg-P/L, with an average of 0.3 mg-P/L. Influent TP for high salt events was 0.8 mg-P/L. Applied velocity was 16.7 cm/hour to all columns. Storm events continued until 9, 26, 40, and 7 m applied water for the control, 2,000, 5,000, and 10,000 mg/L NaCl columns, respectively. Data for the control column are from Owen (2016) and after 9 m applied water, influent and effluent data for the control column are extrapolated assuming a linear relationship between TP mass and applied water.

Despite mesocosms retaining stormwater during storm events, TP was exported in the 2,000 and 5,000 mg/L NaCl columns. As discussed in the TSS mass balance section, the 2,000 and 5,000 mg/L NaCl columns received the equivalent of 1 year and 4 months and 2 years of applied MD rainfall, respectively. TP EMCs are 0.1, 0.4, 0.5, 0.3 mg-P for the control, 2,000, 5,000, and 10,000 mg/L NaCl columns, respectively. Unsurprisingly, the maximum EMC is associated with the 5,000 mg/L NaCl column that exported P earlier than the other columns in the study.

It is hypothesized that a threshold NaCl mass accumulated in the media exists, and the threshold is the difference between P export and retention. By 1 year and 4 months equivalent rainfall, the 2,000 mg/L NaCl column exported P with approximately 45,900 mg NaCl accumulated in the media. P export occurred at a rainfall equivalent of 4 months equivalent rainfall in the 5,000 mg/L NaCl column with approximately 56,000 mg NaCl accumulated. Since the masses of NaCl retained are of the same magnitude, perhaps the hypothesized threshold is dependent upon occupancy of adsorption sites by sodium and resulting displacement of phosphate.

Bioretention mesocosm and BSM studies have similarly observed increases in effluent TP following salt applications (Denich et al. 2013; Kakuturu and Clark 2015b). TP export from mesocosms loaded with 2- and 15-years worth of road salt as

NaCl was also observed by Denich et al. (2013), and it was noted that TP mass leaching with increased collection time. Although the 2-years' loading of 2,430 g of a salt mix is more than 2.5 times the amount of NaCl applied in this study, long-term P export in bioretention systems exposed to deicers may occur. However, no bioretention field studies investigating the capacity of P removal as a result of deicer application could be found at the time of this study. Field evidence to support limited or no P removal in bioretention systems may better inform placement of SCMs relative to roadways and local and state bioretention system performance evaluations and recommendations.

3.6.2 P Summary

Most of the effluent TP from all columns was DP, of which a majority of DP was assumed as DOP. DP may have been released as a result of anion exchange between chloride and phosphate ions in addition to P release associated with organic matter mobility. As a result of analytical limitations, understanding of the DP partitioning between DOP and SRP is limited and it remains inconclusive as to whether anion exchange or organic matter mobility is the primary mechanism responsible for TP release. Based on the duration of the 2,000 and 5,000 mg/L NaCl column studies, no significant P removal during and after deicer applications may occur in bioretention systems.

3.7. Mass Balance Summary

TN, TP, TSS, and NaCl accumulated mass balance summaries are provided in Table 19 for the control, 2,000, 5,000, and 10,000 mg/L NaCl columns at 9 m and 26

m applied water. The 26 m estimates for the control column are based on a linear relationship between mass and applied water. TN, TP, and TSS masses are presented as mass that had exited each column.

At 9 m and 26 m applied water, the control column had the most TN exiting in the effluent (541 and 1,480 mg-N, respectively). The 10,000 mg/L NaCl column had the least TN mass by 9 m (98.4 mg-N), which is related to the decreased effluent flow rate due to the column clogging. By the 26 m applied water, similar masses of TN had exited the control and 2,000 mg/L NaCl column (1,480 and 1,420 mg-N, respectively) whereas 1,290 mg-N had exited the 5,000 mg/L NaCl column. Despite increased effluent concentrations following high salt events, overall TN masses exiting the 2,000 and 5,000 mg/L NaCl columns remained less than that of the control column. Therefore, the periodic high salt events did not impair TN mass removal.

The control column consistently had the least TP mass compared to the 2,000 and 5,000 mg/L NaCl columns (Table 20), but the effluent mass at 9 m is comparable to that of the 10,000 mg/L NaCl column (27.9 mg-P). As stated before, the effluent mass from the 10,000 mg/L NaCl column is likely due to media clogging. Among the control, 2,000, and 5,000 mg/L NaCl columns, the greatest effluent TP masses at 9 and 26 m applied water were from the 5,000 mg/L NaCl column, followed by the 2,000 mg/L NaCl column. As a result of anion exchange and organic matter mobilization due to salt applications, increased concentrations of NaCl resulted in greater effluent TP mass and did not result in mass removal.

Table 20. TN, TP, TSS, and NaCl mass balance summaries for the control, 2,000, 5,000, and 10,000 mg/L NaCl columns. Summaries are provided for 9 m and 26 m applied water, which corresponds to when the control and 2,000 mg/L NaCl column experiments were terminated. Control data are from Owen (2016) and data after 9 m applied water are extrapolated assuming a linear relationship between mass and applied water. TSS data for the control column are unavailable. Data for the 10,000 mg/L NaCl column are unavailable for 26 m applied water.

	TN (mg-N) at 9 m		**TN (mg-N) at 26 m**		**TP (mg-P) at 9 m**		**TP (mg-P) at 26 m**	
	Influent	**Effluent**	**Influent**	**Effluent**	**Influent**	**Effluent**	**Influent**	**Effluent**
Control	564 - 1,110	541	2,460 - 3,250	1,480	45.0 - 100	30.3	191 - 281	80.8
2,000 mg/L		317		1,420		40.2		198
5,000 mg/L		487		1,290		135		269
	NaCl (mg) accumulated at 9 m		**NaCl (mg) accumulated at 26 m**		**TSS (mg) at 26 m**			
	Influent	**Effluent**	**Influent**	**Effluent**	**Effluent**			
Control	75,500 - 157,000	N/A	274,000 - 568,000	N/A	N/A			
2,000 mg/L		9,120		45,900	54,300			
5,000 mg/L		53,900		129,000	45,000			

3.8 Deicer Recommendations

NaCl, $CaCl_2$, and $MgCl_2$ are the most widely-used roadway deicers since they are relatively low cost, easy to use, and safe for the applicator and road user (National Cooperative Highway Research Program 2013). Considering human safety, KCl, LiCl, and NaF may be toxic to human organ systems, such as the nervous and reproductive systems (ScienceLab 2013a; b; c). Additionally, NaBr is cited as an irritant in the case of skin contact and of inhalation (ScienceLab 2013d).

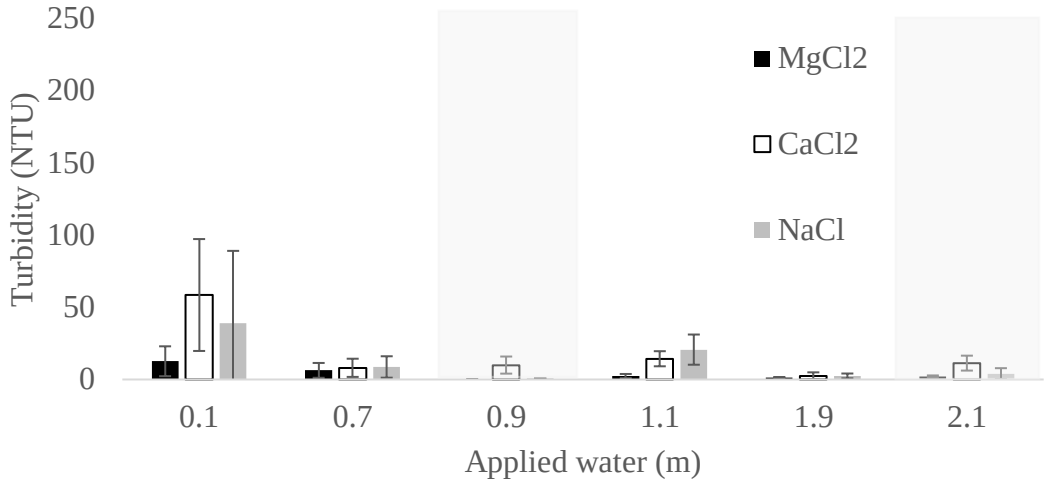

Figure 26. Average effluent TSS from the NaCl, $CaCl_2$, and $MgCl_2$ mini columns. High salt events occurred every 1 m applied water, indicated by gray boxes. Intermediate baseline events contained 20 mg/L NaCl. Effluent data during the first high salt event from the $MgCl_2$ mini columns are unavailable. Applied velocity was 16.7 cm/hour to all columns.

In contrast, the commonly used deicers are reported to be slightly hazardous in case of skin contact or of inhalation (ScienceLab 2013e; f; g), and of the three, effluent turbidity from the $MgCl_2$ column was statistically less than the $CaCl_2$ and NaCl columns immediately after the high salt event. Effluent turbidity from the remaining storm events (1.1 – 2.1 m) were statistically similar among the NaCl,

$CaCl_2$, and $MgCl_2$ mini columns (Figure 26). Additionally, $MgCl_2$ and NaCl demonstrated statistically similar TN release (2.3 – 2.4 mg-N/L, Figure 27) following the first high salt application in comparison to $CaCl_2$, which was significantly greater, with an average of 4.3 mg-N/L.

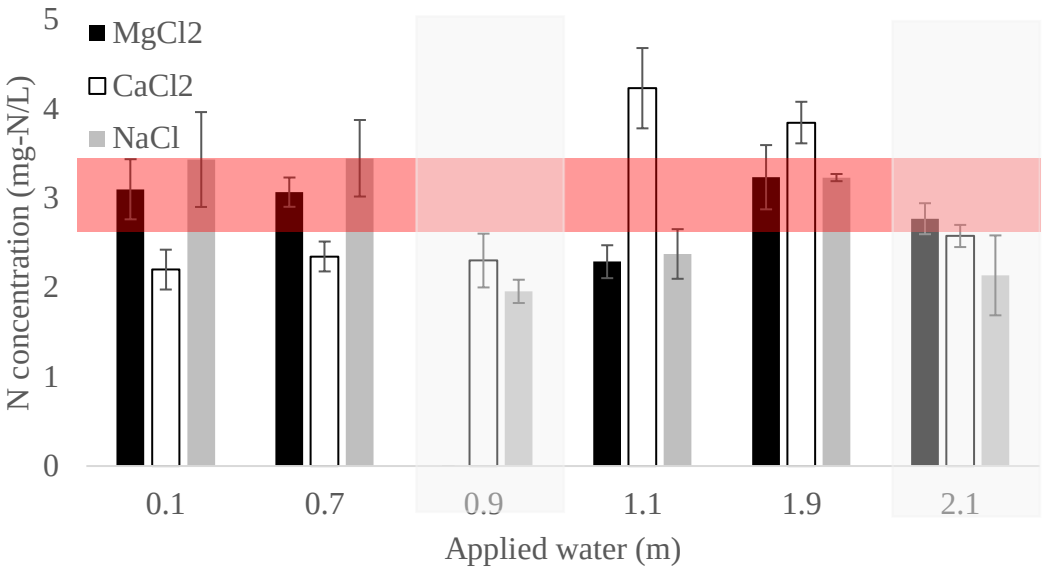

Figure 27. Average effluent TN from the NaCl, $CaCl_2$, and $MgCl_2$ mini columns. High salt events occurred every 1 m applied water, indicated by gray boxes. Intermediate baseline events contained 20 mg/L NaCl. Effluent data during the first high salt event from the $MgCl_2$ mini columns are unavailable. Applied velocity was 16.7 cm/hour to all columns.

Although not statistically different, average TP effluent from NaCl mini columns increased to 0.3 mg-P/L following the first salt event (Figure 28). In comparison, TP effluents from the $CaCl_2$ and $MgCl_2$ columns consistently remained less than 0.1 mg-P/L between high salt events. Although P speciation was not performed on effluent from mini columns, application of $CaCl_2$ may result in phosphate precipitating with calcium and subsequent removal via filtration (LeFevre et al. 2014).

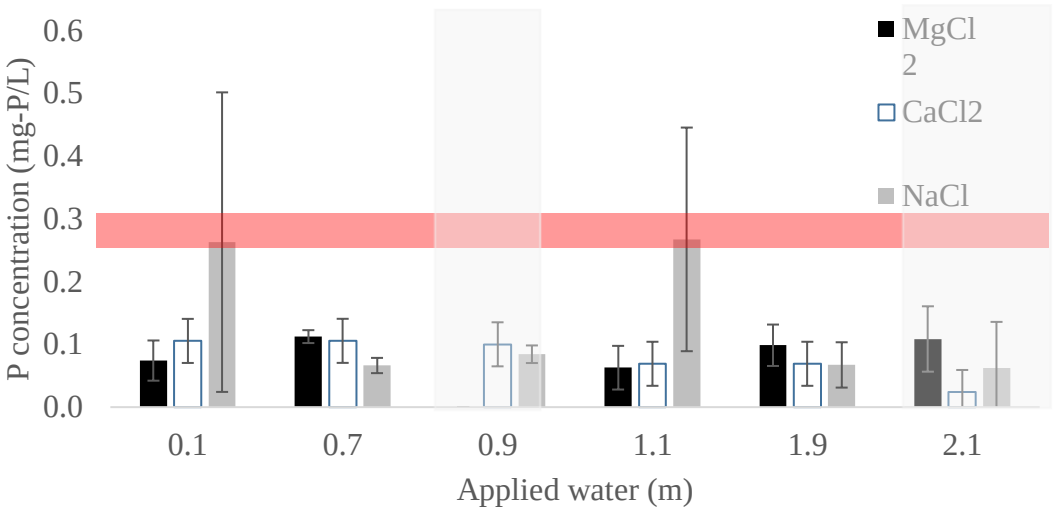

Figure 28. Average effluent TP from the NaCl, $CaCl_2$, and $MgCl_2$ mini columns. High salt events occurred every 1 m applied water, indicated by gray boxes. Intermediate baseline events contained 20 mg/L NaCl. Effluent data during the first high salt event from the $MgCl_2$ mini columns are unavailable. Applied velocity was 16.7 cm/hour to all columns.

Based on the comparisons of the three salts, $MgCl_2$ performance was the best in that effluent concentrations from the columns were the lowest recorded. $MgCl_2$ and NaCl salts may be preferred in areas that drain into waterbodies that do not meet N TMDLs, as with the preference of $CaCl_2$ and $MgCl_2$ salts and areas that do not meet P TMDLs.

The US EPA (2010) summarizes that $CaCl_2$, $MgCl_2$, and other deicer alternatives are not vastly better for the environment than NaCl, although non-chloride based deicers should be used in areas with chloride sensitivities. Additionally, regard for road safety should be taken into account when selecting deicers. The US EPA (2010) recommends selecting appropriate deicers based on environmental conditions and constraints, such as outdoor winter temperatures, since melting points vary among deicers. Therefore, continued use of salt brine mixes

containing NaCl, $CaCl_2$, and $MgCl_2$ may still be used, with the fractional composition of each dependent upon local water quality concerns and road safety.

Chapter 4: Conclusions

Three individual bioretention mesocosms were subjected to storm events, with 20 mg/L NaCl acting as a baseline concentration and interspersed with 2,000, 5,000, and 10,000 mg/L NaCl events every six storms. Influent and effluent were tested for TN, TP, and their various species. In order to understand N, P, and metals mobilization from the media, TSS, turbidity, and TOC were also evaluated.

Increased concentrations of NaCl resulted in soil deflocculation and subsequent high concentrations of effluent TSS and turbidity. After high salt events, NaCl removal from mesocosms was observed during baseline storms and by the fifth baseline storm after a high salt application, the media's SAR decreased from values greater than 10, which is classified as a very sodic soil, to less than 3, which is classified as a non-sodic soil (Sumner et al. 1998). As a result of the media returning to non-sodic conditions, the decreased effluent TSS concentrations and turbidity provide evidence that soil deflocculation ceased by the following high salt event.

2,000, 5,000, and 10,000 mg/L NaCl applications to bioretention mesocosms resulted in episodic washouts of N, P, copper, and zinc. The primary mechanisms of mobilization were due to cation exchange and mobilization of organic matter as a result of increased chloride concentrations. With the exception of the 10,000 mg/L NaCl column, which clogged after the first high salt event, the concentrations of N, P, and metals released from 2,000 and 5,000 mg/L NaCl mesocosms were dependent upon ionic strength. Increased ionic strength typically resulted in increased pollutant concentrations in effluent. Therefore, the 5,000 mg/L NaCl column tended to release higher concentrations of TN and TP than the 2,000 mg/L NaCl column and the influent. Although effluent metal concentrations typically were less than influent

concentrations, the 5,000 mg/L NaCl column tended to release higher concentrations of heavy metals than the 2,000 mg/L NaCl olumn.

By the end of the experiments, the 2,000 and 5,000 mg/L NaCl columns had received an equivalent of 1 year and 4 months, and 2 years of Maryland applied rainfall, respectively. Overall mass TP release was 3.8% and 1.1% greater than applied TP mass for the 2,000 and 5,000 mg/L NaCl columns, respectively, which suggests that the columns were a source of TP. Due to the greater ionic strength, the 5,000 mg/L NaCl column exported P earlier than the 2,000 mg/L NaCl column (17^{th} versus 26^{th} m applied water). However, heavy metal concentrations rarely exceeded influent concentrations and both columns exhibited copper (74.3% and 65.4% for the 2,000 and 5,000 mg/L NaCl column, respectively) and zinc mass reductions (76.5% and 79.5% for the 2,000 and 5,000 mg/L NaCl column, respectively). Additionally, both columns demonstrated similar performances of mass TN reduction, with the 2,000 and 5,000 mg/L NaCl columns retaining 42.3% and 43.3% of input TN by mass, respectively.

Based on nutrient performance observed from mini columns studies, effluent from NaCl, $CaCl_2$, and $MgCl_2$ columns resulted in comparable TN and TP concentrations and turbidities. Overall, $MgCl_2$ consistently performed the best in that the effluent nutrient concentrations were the minimum among the three salts. Regardless, the US EPA (2010) recommends selecting appropriate deicers based on environmental conditions, such as outdoor winter temperatures, and constraints, such as areas with chloride sensitivities. Since $CaCl_2$ and $MgCl_2$ are not vastly better for the environment than NaCl, further investigation into non-chloride based deicer

alternatives and nutrient performance is necessary to accommodate deicer applications to chloride-sensitive areas.

From this study, it is recommended to minimize NaCl applications in order to prolong nutrient release from bioretention systems. Although TN export was not a concern, TP export was observed under 2,000 and 5,000 mg/L NaCl events. Since TP export was observed from both mesocosms, relationships relating applied NaCl mass, applied water, and expected P release may be used to estimate amendment additions in order to improve DP removal. Based on isotherm relationships between adsorbed P and amendments such as water treatment residual (WTR), the mass of BSM amendment may be estimated in order to result in a desired DP mass removal. Previous studies have used WTR to improve DP removal (Liu and Davis 2014), although the use of WTR in combination with high concentrations of road salt has not been investigated. In addition to more research investigating long-term effects of deicers on pollutant retention performance, previously studied BSM amendments to improve retention, such as WTR (Liu and Davis 2014), activated carbon (Björklund and Li 2017), and fly ash (Youngblood et al. 2017), should be studied as a mitigation strategy to heavy metal, N, and P mobilization due to deicers.

Appendices

Appendix A: Bioretention Soil Media Specifications

Table Appendix A-1. BSM Specifications (Maryland State Highway Administration 2017b).

<table>
<tr><th colspan="7">COMPOSITION- BIORETENTION SOIL MIX (BSM)</th></tr>
<tr><th>TEST PROPERTY</th><th>TEST [1] METHOD</th><th colspan="5">TEST VALUE</th></tr>
<tr><td>Weeds</td><td>—</td><td colspan="5">Free of seed and viable plant parts of species in 920.06.02(a)(b)(c) when inspected.</td></tr>
<tr><td>Debris</td><td>—</td><td colspan="5">No observable content of cement, concrete, asphalt, crushed gravel or construction debris.</td></tr>
<tr><td>Hardwood Mulch</td><td>—</td><td colspan="5">20% of the loose volume of BSM when inspected.</td></tr>
<tr><td rowspan="5">Textural Analysis</td><td rowspan="5">T-88</td><td colspan="2">Particle</td><td colspan="3">% Passing by Weight</td></tr>
<tr><td>Size</td><td>mm</td><td>Minimum</td><td colspan="2">Maximum</td></tr>
<tr><td>Sand</td><td>2.0 – 0.050</td><td>79</td><td colspan="2">94</td></tr>
<tr><td>Silt</td><td>0.050 – 0.002</td><td>4</td><td>20</td><td rowspan="2">Combined Silt and Clay 21</td></tr>
<tr><td>Clay</td><td>less than 0.002</td><td>1</td><td>10</td></tr>
<tr><td>Soil pH</td><td>ASTM D 4972</td><td colspan="5">pH of 5.7 to 7.4.</td></tr>
<tr><td>Organic Matter</td><td>T-267</td><td colspan="5">Minimum 1.5 % by weight.</td></tr>
<tr><td>Soluble Salts</td><td>EC 1:2 (V:V)</td><td colspan="5">500 ppm (0.78 mmhos/cm) or less.</td></tr>
<tr><td>Harmful Materials</td><td>—</td><td colspan="5">920.01.01(a).</td></tr>
<tr><td colspan="7">Note:
[1] Materials Standards and Materials Testing 356 (MSMT 356) has been superseded by OMT Landscaping Soils Eligibility List. Test methods not defined herein shall be as per visual inspection or methods defined by the Landscape Operations Division.</td></tr>
</table>

Appendix B: Related TSS and Turbidity Data

Figure Appendix B-1. Clogging of the 10,000 mg/L NaCl bioretention mesocosm during the first storm after the high salt spike. The column was terminated at 7.2 m applied water due to clogging.

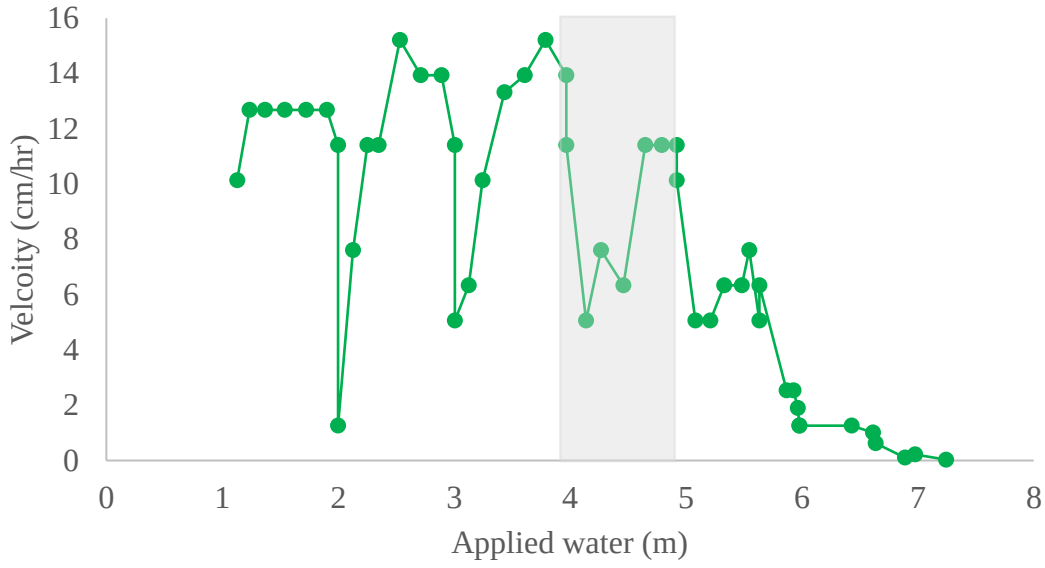

Figure Appendix B-2. Effluent velocity from the 10,000 mg/L NaCl bioretention column. The high salt event is indicated by gray box. Intermediate baseline events contained 20 mg/L NaCl. Applied velocity was 16.7 cm/hour to the column. The column was terminated at 7.2 m due to clogging.

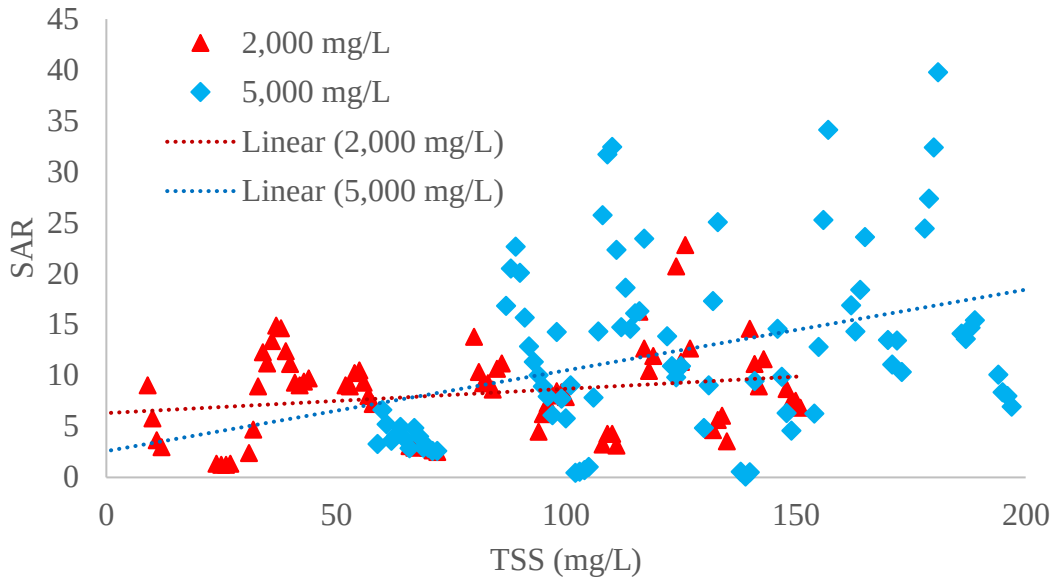

Figure Appendix B-3. Correlations between effluent TSS and SAR for the 2,000 and 5,000 mg/L NaCl columns. For the 2,000 and 5,000 mg/L NaCl columns, the correlation coefficients were 0.05 and 0.13, respectively.

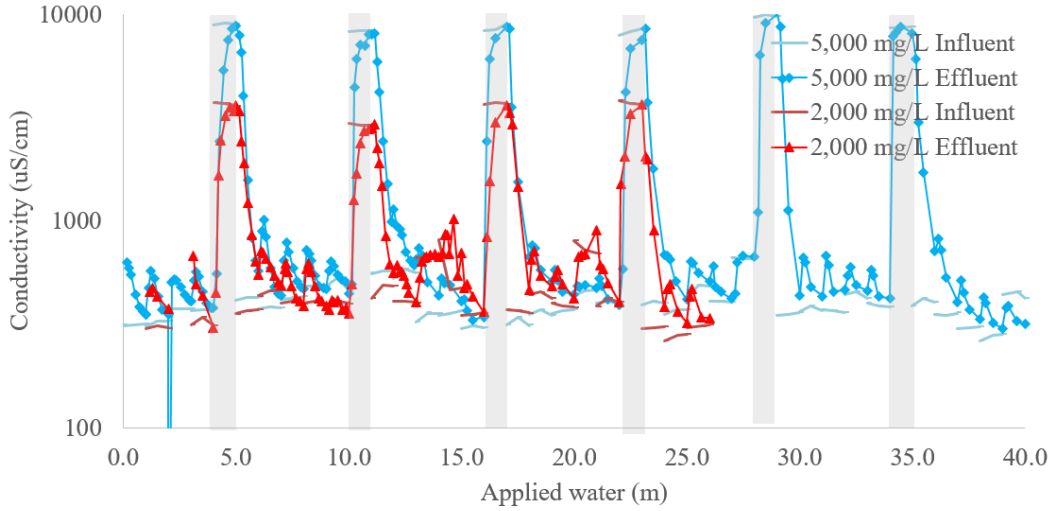

Figure Appendix B-4. Effluent conductivity from the 5,000 and 2,000 mg/L NaCl bioretention columns. High salt events occurred every sixth event, indicated by gray boxes. Intermediate baseline events contained 20 mg/L NaCl. Applied velocity was 16.7 cm/hour to all columns.

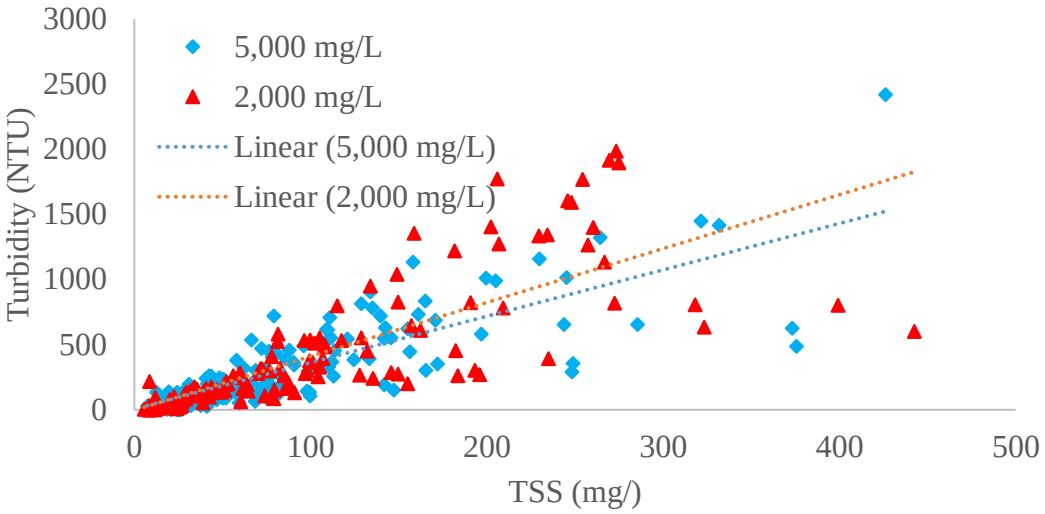

Figure Appendix B-5. Correlations between effluent TSS and turbidity for the 5,000 mg/L and 2,000 mg/L NaCl columns. For the 2,000 and 5,000 mg/L NaCl columns, the correlation coefficients were R^2 = 0.60 and 0.66, respectively.

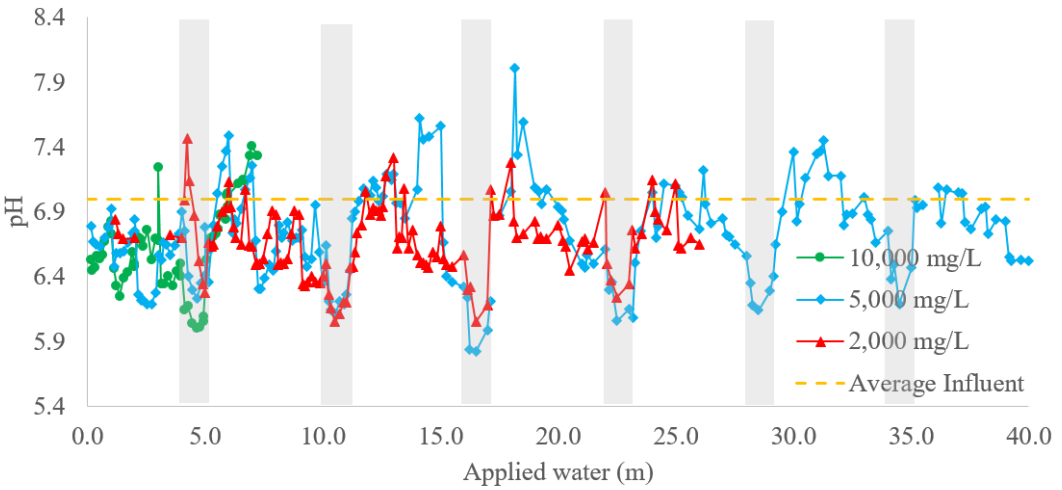

Figure Appendix B-6. Effluent pH for the 2,000 5,000, and 10,000 mg/L NaCl bioretention columns. Average influent pH was 7.0. High salt events occurred every sixth event, indicated by gray boxes. Intermediate baseline events contained 20 mg/L NaCl. Applied velocity was 16.7 cm/hour. The 10,000 mg/L NaCl column was terminated at 7.2 m due to clogging.

Appendix C: Related TOC Data

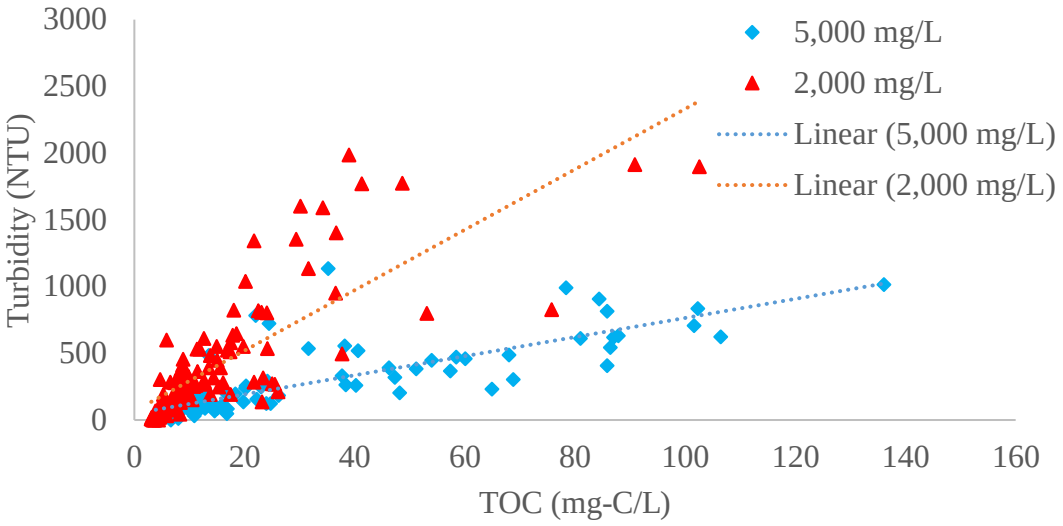

Figure Appendix C-1. Correlations between effluent TOC and turbidity for the 2,000 mg/L and 5,000 mg/L NaCl columns. For the 2,000 and 5,000 mg/L NaCl columns, the correlation coefficients were R^2 = 0.62 and 0.64, respectively.

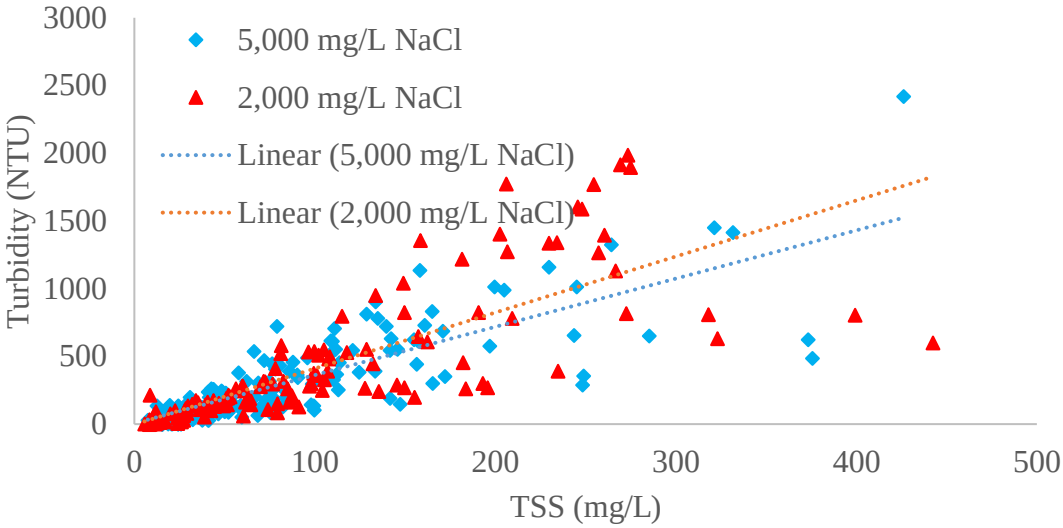

Figure Appendix C-2. Correlations between effluent TOC and TSS for the 2,000 mg/L and 5,000 mg/L NaCl columns. For the 2,000 and 5,000 mg/L NaCl columns, the correlation coefficients were R^2 = 0.60 and 0.66, respectively.

Appendix D: Related Metals Data

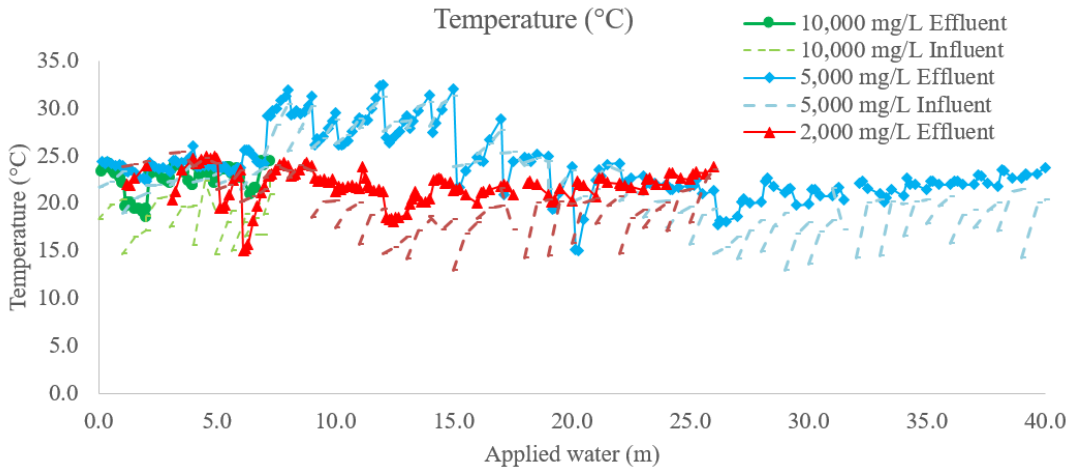

Figure Appendix D-1. Influent and effluent temperature for the 2,000 5,000, and 10,000 mg/L NaCl bioretention columns. High salt events occurred every sixth event, indicated by gray boxes. Intermediate baseline events contained 20 mg/L NaCl. Applied velocity was 16.7 cm/hour. The 10,000 mg/L NaCl column was terminated at 7.2 m due to clogging.

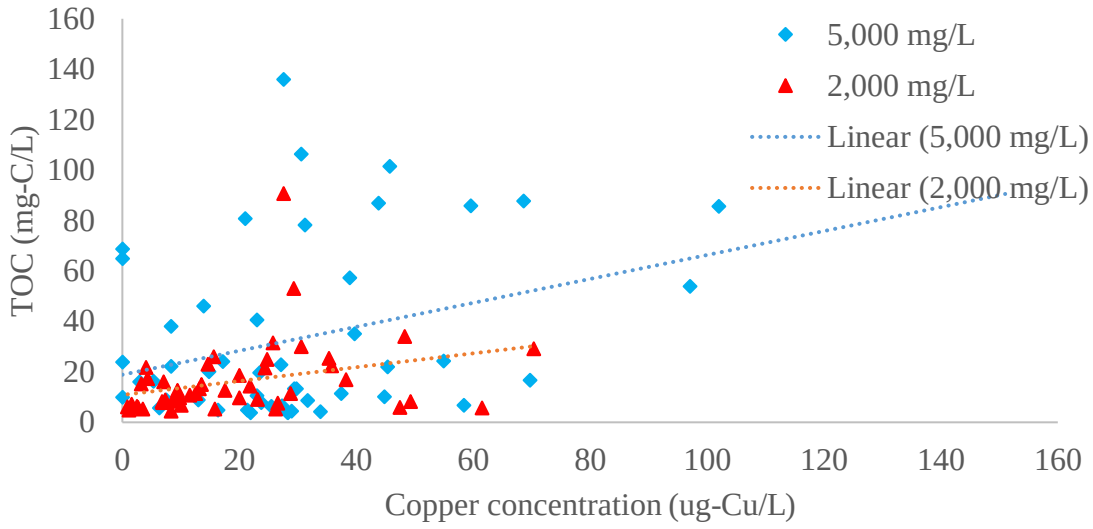

Figure Appendix D-2. Correlations between copper and TOC effluent concentrations for the 2,000 and 5,000 mg/L NaCl columns. The correlation coefficients for the 2,000 and 5,000 mg/L NaCl columns are 0.09 and 0.10, respectively.

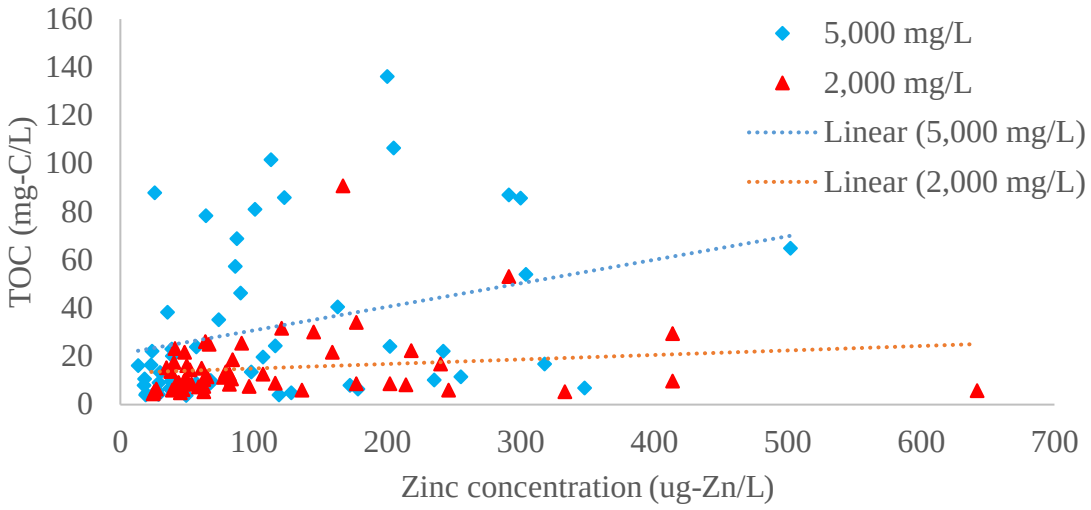

Figure Appendix D-3. Correlations between copper and TOC effluent concentrations for the 2,000 and 5,000 mg/L NaCl columns. The correlation coefficients for the 2,000 and 5,000 mg/L NaCl columns are 0.02 and 0.10, respectively.

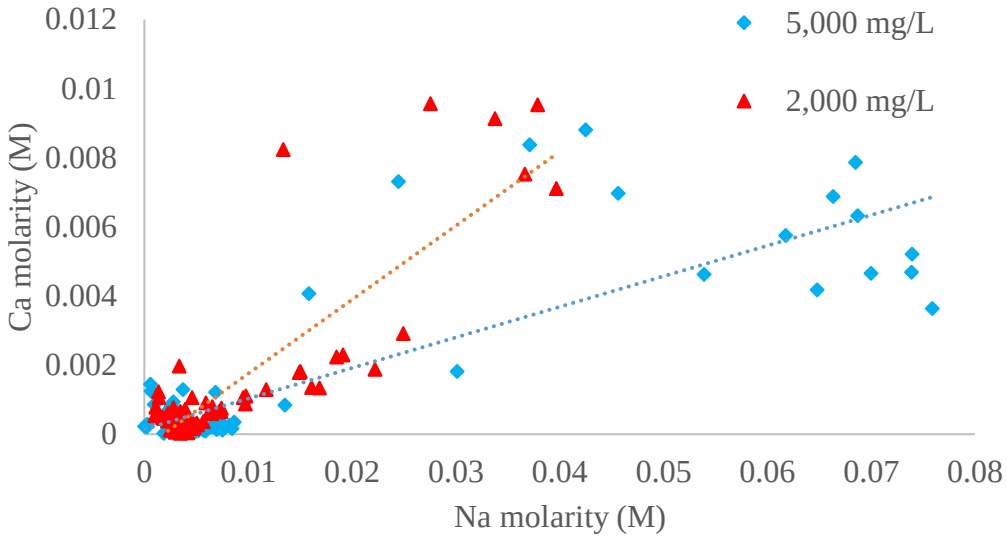

Figure Appendix D-4. Correlations between sodium and calcium effluent concentrations for the 2,000 and 5,000 mg/L NaCl columns. The correlation coefficients for the 2,000 and 5,000 mg/L NaCl columns are 0.74 and 0.70, respectively.

Appendix E: Related N Data

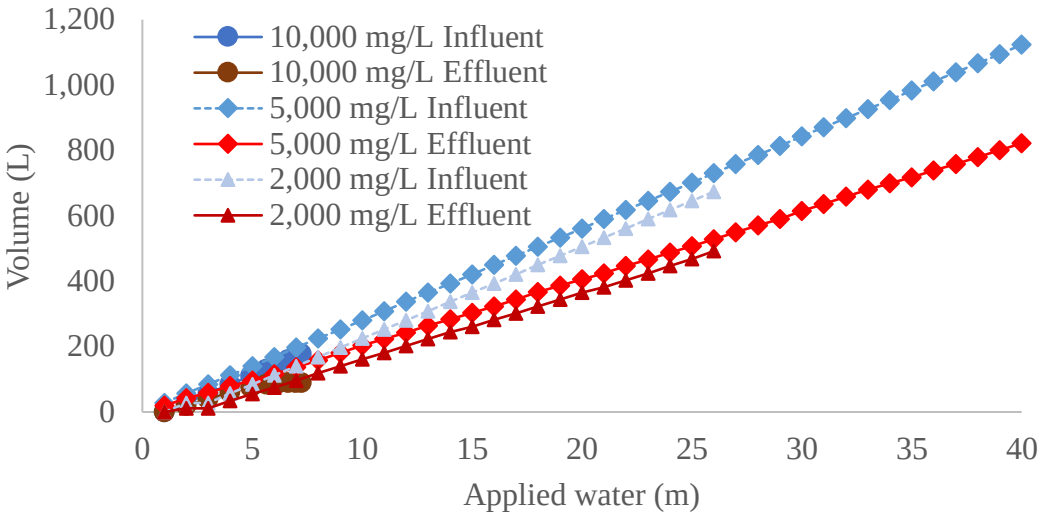

Figure Appendix E-1. Water balances for influent and effluent for the 10,000, 5,000, and 2,000 mg/L NaCl bioretention columns. High salt events occurred every six storm events. Intermediate baseline events contained 20 mg/L NaCl. Applied velocity was 16.7 cm/hour to all columns. Storm events continued until 26, 40, and 7 m applied water for the 2,000, 5,000, and 10,000 mg/L NaCl columns, respectively.

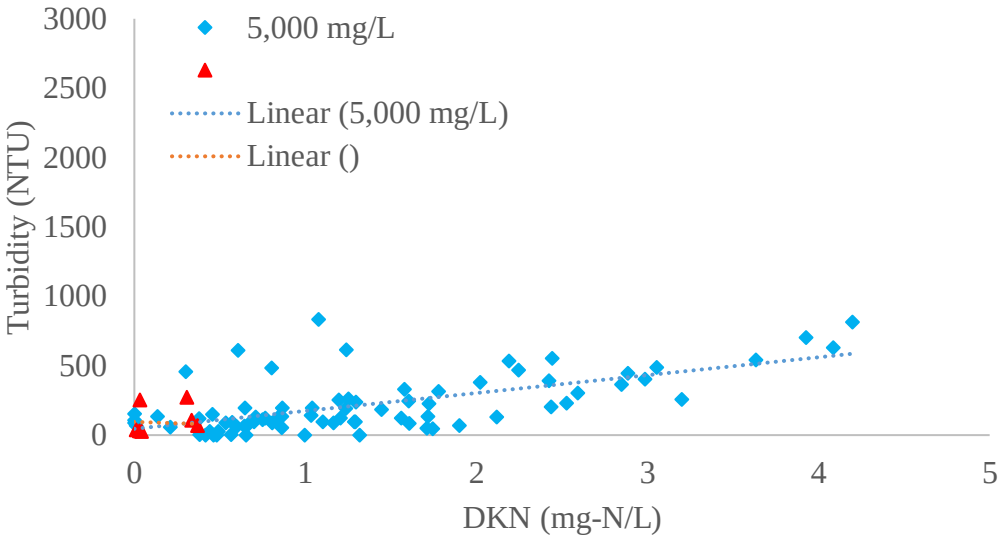

Figure Appendix E-2. Correlations between DKN and turbidity for the 2,000 and 5,000 mg/L NaCl columns. For the 2,000 and 5,000 mg/L NaCl columns, R^2 = 0.55 and 0.41, respectively.

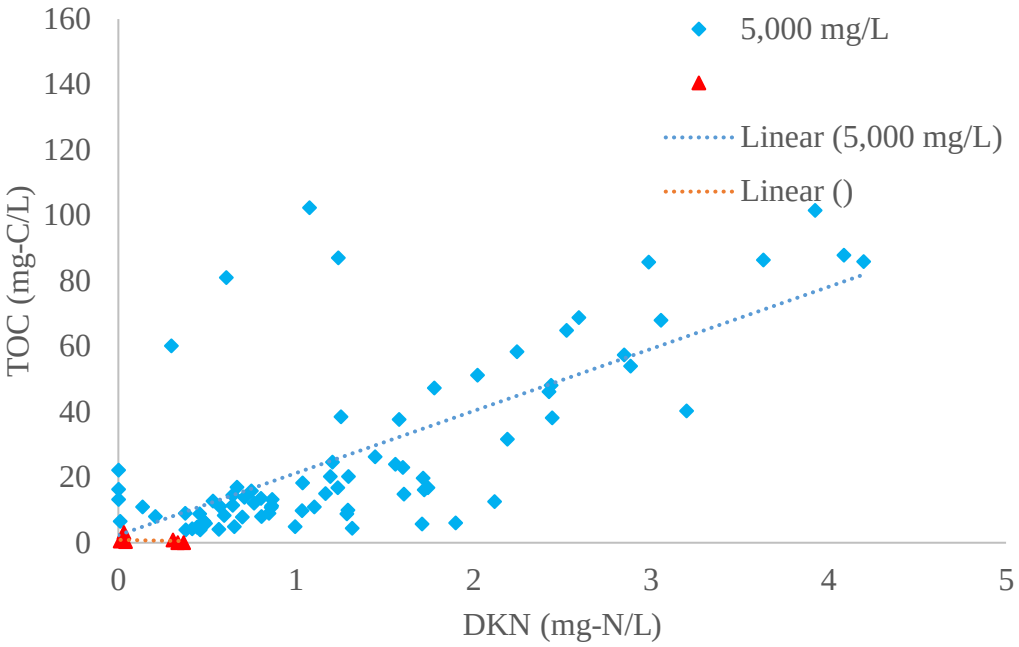

Figure Appendix E-3. Correlations between DKN and TOC for the 2,000 and 5,000 mg/L NaCl columns. For the 2,000 and 5,000 mg/L NaCl columns, R^2 = 0.21 and 0.49, respectively.

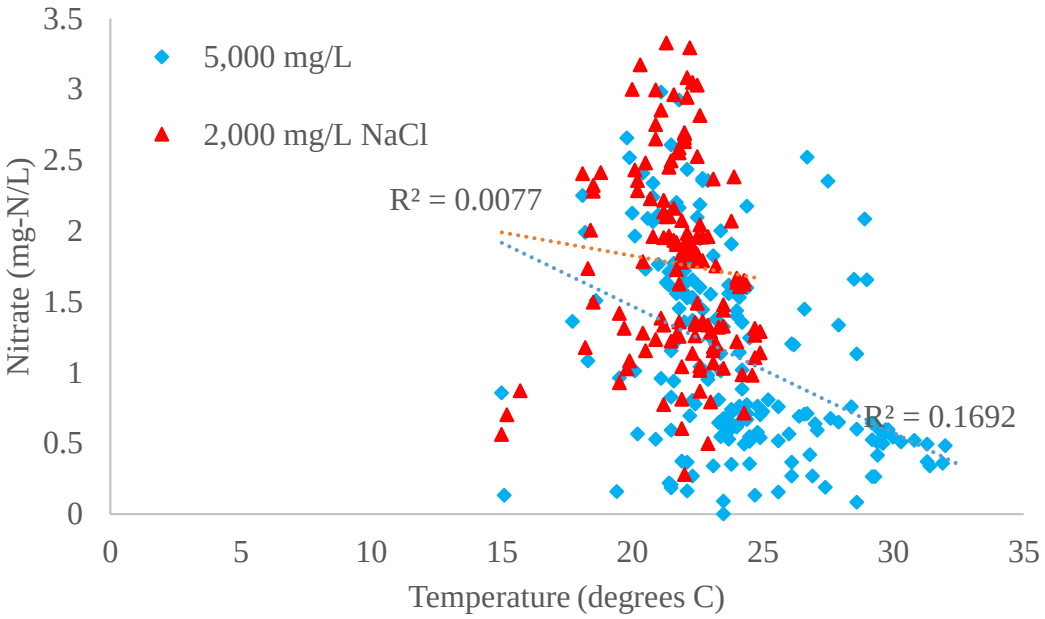

Figure Appendix E-4. Correlations between effluent temperature and nitrate for the 2,000 and 5,000 mg/L NaCl columns. For the 2,000 and 5,000 mg/L NaCl columns, R^2 = 0.07 and 0.17, respectively.

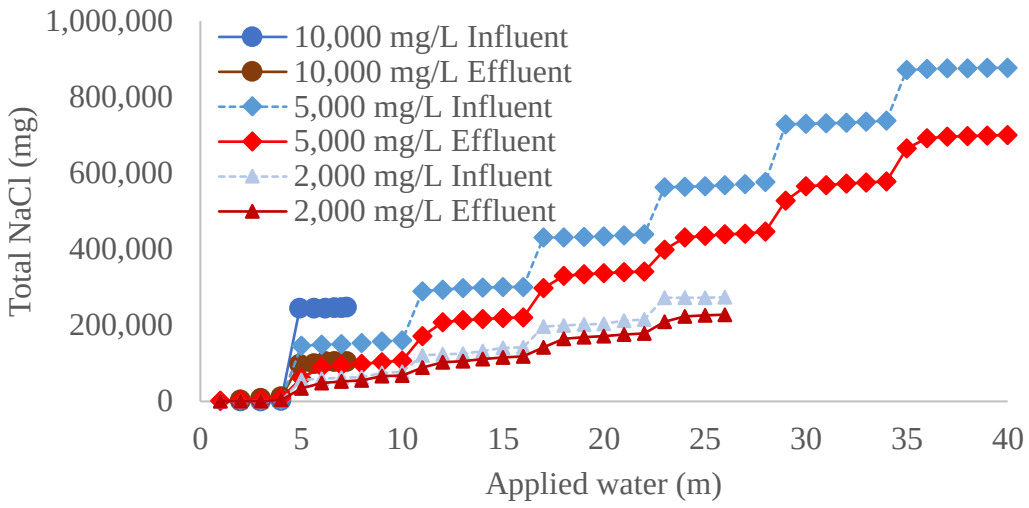

Figure Appendix E-5. NaCl mass balances for the 2,000, 5,000, and 10,000 mg/L NaCl bioretention columns. High salt events occurred every six storm events. Intermediate baseline events contained 20 mg/L NaCl. Applied velocity was 16.7 cm/hour to all columns. Storm events continued until 26, 40, and 7 m applied water for the 2,000, 5,000, and 10,000 mg/L NaCl columns, respectively.

Appendix F: Related P Data

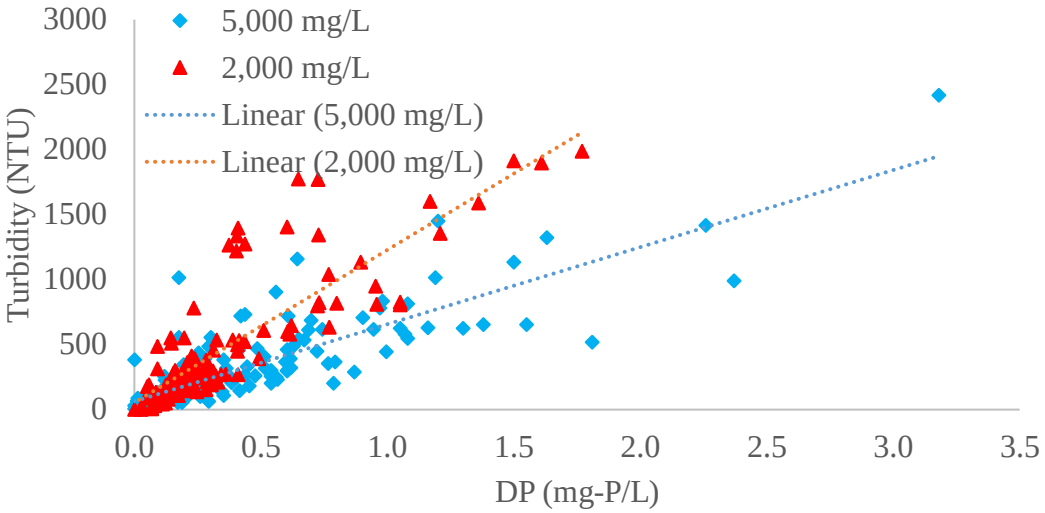

Appendix F-1. Correlations between DP and turbidity for the 2,000 and 5,000 mg/L NaCl columns. For the 2,000 and 5,000 mg/L NaCl columns, R^2 = 0.72 and 0.70, respectively.

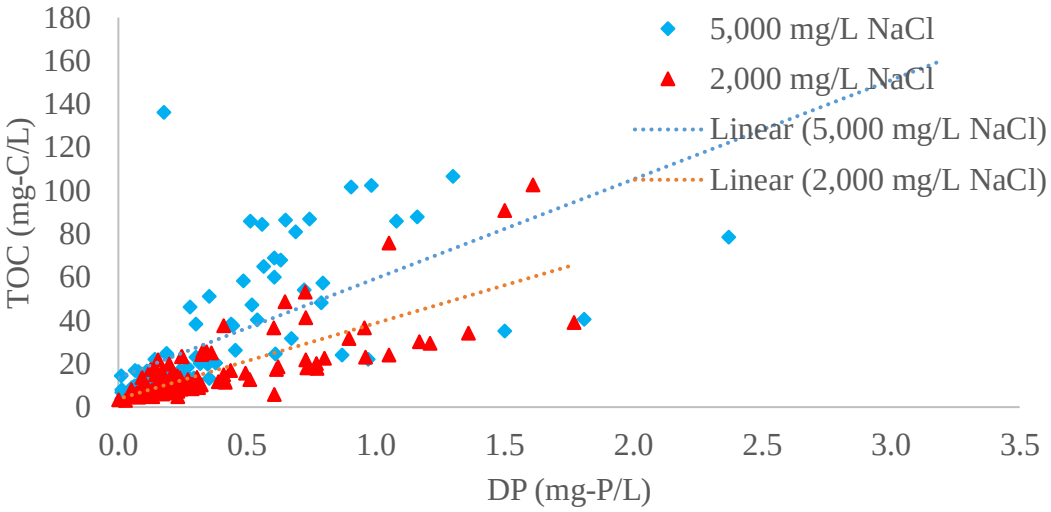

Figure Appendix F-2. Correlations between DP and TOC for the 2,000 and 5,000 mg/L NaCl columns. For the 2,000 and 5,000 mg/L NaCl columns, R^2 = 0.60 and 0.40, respectively.

Bibliography

Amrhein, C., Strong, J. E., and Mosher, P. A. (1992). “Effect of deicing salts on metal and organic matter mobilization in roadside soils.” *Environmental Science & Technology*, 26(4), 703–709.

Bäckström, M., Karlsson, S., Bäckman, L., Folkeson, L., and Lind, B. (2004). “Mobilisation of heavy metals by deicing salts in a roadside environment.” *Water Research*, 38(3), 720–732.

Björklund, K., and Li, L. (2017). “Removal of organic contaminants in bioretention medium amended with activated carbon from sewage sludge.” *Environmental Science and Pollution Research*, 24(23), 19167–19180.

Blecken, G.-T., Zinger, Y., Deletić, A., Fletcher, T. D., Hedström, A., and Viklander, M. (2010). “Laboratory study on stormwater biofiltration: Nutrient and sediment removal in cold temperatures.” *Journal of Hydrology*, 394(3–4), 507–514.

Borst, M., and Brown, R. A. (2014). “Chloride Released from Three Permeable Pavement Surfaces after Winter Salt Application.” *JAWRA Journal of the American Water Resources Association*, 50(1), 29–41.

Bouyoucos, G. J. (1962). “Hydrometer Method Improved for Making Particle Size Analyses of Soils1.” *Agronomy Journal*, 54(5), 464–465.

Brown, R. A., and Hunt, W. F. (2012). “Improving bioretention/biofiltration performance with restorative maintenance.” *Water Science and Technology; London*, 65(2), 361–367.

Davis, A., Hunt, W., Traver, R., and Clar, R. (2009). "Bioretention Technology: Overview of Current Practice and Future Needs." *Journal of Environmental Engineering*, 135(3), 109–117.

Davis, A. P., Traver, R. G., and Hunt, W. F. (2010). "Improving Urban Stormwater Quality: Applying Fundamental Principles." *Journal of Contemporary Water Research & Education,* 146(1), 3–10.

Denich, C., and Bradford, A. (2008). "Cold climate issues for bioretention: Assessing impacts of salt and aggregate application on plant health, media clogging, and groundwater quality." *LID for Urban Ecosystem and Habitat Protection, Seattle, Washington, EWRI of ASCE*.

Denich, C., Bradford, A., and Drake, J. (2013). "Bioretention: assessing effects of winter salt and aggregate application on plant health, media clogging and effluent quality." *Water Quality Research Journal of Canada*, 48(4), 387–399.

Dietz, M. E. (2007). "Low Impact Development Practices: A Review of Current Research and Recommendations for Future Directions." *Water, Air, and Soil Pollution*, 186(1–4), 351–363.

Dietz, M. E., and Clausen, J. C. (2006). "Saturation to Improve Pollutant Retention in a Rain Garden." *Environmental Science & Technology*, 40(4), 1335–1340.

Doan, L. N., and Davis, A. P. (2017). "Bioretention–Cistern–Irrigation Treatment Train to Minimize Stormwater Runoff." *Journal of Sustainable Water in the Built Environment*, 3(2), 04017003.

Drake, J., Bradford, A., and Van Seters, T. (2014). "Stormwater quality of spring–summer-fall effluent from three partial-infiltration permeable pavement

systems and conventional asphalt pavement." *Journal of Environmental Management*, 139, 69–79.

Eaton, A. E., Clesceri, L. S., Rice, E. W., and Greenberg, A. E. (2005a). "5310-B Total Organic Carbon." *Standard Methods for Examination of Water and Wastewater: Centennial Edition*, American Public Health Association, Baltimore, 5-21-5–23.

Eaton, A. E., Clesceri, L. S., Rice, E. W., and Greenberg, A. E. (2005b). "3030-E NitricAcid Digestion." *Standard Methods for Examination of Water and Wastewater: Centennial Edition*, American Public Health Association, Baltimore, 3-8-3–9.

Eaton, A. E., Clesceri, L. S., Rice, E. W., and Greenberg, A. E. (2005c). "4500-N-C Persulfate Method." *Standard Methods for Examination of Water and Wastewater: Centennial Edition*, American Public Health Association, Baltimore, 4-105-4–107.

Eaton, A. E., Clesceri, L. S., Rice, E. W., and Greenberg, A. E. (2005d). "4500-NH3-F Phenate Method." *Standard Methods for Examination of Water and Wastewater: Centennial Edition*, American Public Health Association, Baltimore, 4–114.

Eaton, A. E., Clesceri, L. S., Rice, E. W., and Greenberg, A. E. (2005e). "4500-NO2 Colorimetric Method." *Standard Methods for Examination of Water and Wastewater: Centennial Edition*, American Public Health Association, Baltimore, 4-118-4–119.

Eaton, A. E., Clesceri, L. S., Rice, E. W., and Greenberg, A. E. (2005f). "In-Line UV/Persulfate Digestion and Flow Injection Analysis for Total Phosphorus." *Standard Methods for Examination of Water and Wastewater: Centennial Edition*, American Public Health Association, Baltimore, 4-159-4–160.

Endreny, T., Burke, D. J., Burchhardt, K. M., Fabian, M. W., and Kretzer, A. M. (2012). "Bioretention Column Study of Bacteria Community Response to Salt-Enriched Artificial Stormwater." *Journal of Environment Quality*, 41(6), 1951–1959.

Gao, X., Ito, T., Nasukawa, H., and Kitamura, S. (2016). "Application of Fertilizer Made of Steelmaking Slag in the Recovery of Paddy Fields Damaged by the Tsunami of 2011." *ISIJ International*, 56(6), 1103–1110.

Géhéniau Nicolas, Fuamba Musandji, Mahaut Valérie, Gendron Mario R., and Dugué Marie. (2015). "Monitoring of a Rain Garden in Cold Climate: Case Study of a Parking Lot near Montréal." *Journal of Irrigation and Drainage Engineering*, 141(6), 04014073.

Green, S. M., and Cresser, M. S. (2008). "Nitrogen Cycle Disruption through the Application of De-icing Salts on Upland Highways." *Water, Air, and Soil Pollution*, 188(1–4), 139–153.

Heiri, O., Lotter, A. F., and Lemcke, G. (2001). "Loss on ignition as a method for estimating organic and carbonate content in sediments: reproducibility and comparability of results." *Journal of Paleolimnology*, 25(1), 101–110.

Hunt, W. F., Davis, A. P., and Traver, R. G. (2012). "Meeting Hydrologic and Water Quality Goals through Targeted Bioretention Design." *Journal of Environmental Engineering*, 138(6), 698–707.

Ilyas, M., Qureshi, R. H., and Qadir, M. A. (1997). "Chemical changes in a saline-sodic soil after gypsum application and cropping." *Soil Technology*, 10(3), 247–260.

Kaiser, K., Guggenberger, G., and Zech, W. (1996). "Sorption of DOM and DOM fractions to forest soils." *Geoderma*, 74(3–4), 281–303.

Kakuturu, S. P., and Clark, S. E. (2015a). "Clogging Mechanism of Stormwater Filter Media by NaCl as a Deicing Salt." *Environmental Engineering Science*, 32(2), 141–152.

Kakuturu, S. P., and Clark, S. E. (2015b). "Effects of Deicing Salts on the Clogging of Stormwater Filter Media and on the Media Chemistry." *Journal of Environmental Engineering*, 141(9), 04015020.

Khorsha, G., and Davis, A. P. (2017). "Ammonium Removal from Synthetic Stormwater using Clinoptilolite and Hydroaluminosilicate Columns." *Water Environment Research: A Research Publication of the Water Environment Federation*, 89(6), 564–575.

Kreeb, D., L. B. (2003). "Hydrologic efficiency and design sensitivity of bioretention facilities." Honors Research Thesis, University of Maryland, College Park, MD.

Lancaster, N. A., Bushey, J. T., Tobias, C. R., Song, B., and Vadas, T. M. (2016). "Impact of chloride on denitrification potential in roadside wetlands." *Environmental Pollution*, 212, 216–223.

LeFevre, G. H., Paus, K. H., Natarajan, P., Gulliver, J. S., Novak, P. J., and Hozalski, R. M. (2014). "Review of dissolved pollutants in urban storm water and their removal and fate in bioretention cells." *Journal of Environmental Engineering*, 141(1), 04014050.

Li, L., and Davis, A. P. (2014). "Urban Stormwater Runoff Nitrogen Composition and Fate in Bioretention Systems." *Environmental Science & Technology*, 48(6), 3403–3410.

Liu, J., and Davis, A. P. (2014). "Phosphorus Speciation and Treatment Using Enhanced Phosphorus Removal Bioretention." *Environmental Science & Technology*, 48(1), 607–614.

Manka, B. N., Hathaway, J. M., Tirpak, R. A., He, Q., and Hunt, W. F. (2016). "Driving forces of effluent nutrient variability in field scale bioretention." *Ecological Engineering*, 94, 622–628.

Maryland Department of the Environment. (2000). "Maryland Stormwater Design Manual."

Maryland Department of the Environment. (2005). *Title 26 Department of the Environment, Subtitle 08 Water Pollution, Chapters 01-10. Code of Maryland Regulations*, 316.

Maryland State Highway Administration. (2017a). *Impervious Restoration and Coordinated Total Maximum Daily Load Implementation Plan*.

Maryland State Highway Administration. (2017b). “Landscaping Soils Eligibility List.”

Maryland State Highway Administration. (n.d.). “Chesapeake Bay and Local Waterway Restoration.” <http://www.roads.maryland.gov/m/index.aspx?PageId=333> (May 18, 2018).

Mehlich, A. (1984). “Mehlich 3 soil test extractant: A modification of Mehlich 2 extractant.” *Communications in Soil Science and Plant Analysis*, 15(12), 1409–1416.

Murphy, J., and Riley, J. P. (1962). “A modified single solution method for the determination of phosphate in natural waters.” *Analytica Chimica Acta*, 27, 31–36.

Muthanna, T. M., Viklander, M., Gjesdahl, N., and Thorolfsson, S. T. (2007). “Heavy Metal Removal in Cold Climate Bioretention.” *Water, Air, and Soil Pollution*, 183(1–4), 391–402.

National Cooperative Highway Research Program. (2013). *Strategies to Mitigate the Impacts of Chloride Roadway Deicers on the Natural Environment*. Synthesis 449, Transportation Research Board of the National Academies.

Nelson, P., and Oades, J. M. (1998). “Organic matter, sodicity and soil structure.” *Sodic soils. Distribution, processes, management and environmental consequences*, Oxfod University Press, New York, 51–75.

Nelson, S. S., Yonge, D. R., and Barber, M. E. (2009). "Effects of Road Salts on Heavy Metal Mobility in Two Eastern Washington Soils." *Journal of Environmental Engineering*, 135(7), 505–510.

Norrström, A. C. (2005). "Metal mobility by de-icing salt from an infiltration trench for highway runoff." *Applied Geochemistry*, 20(10), 1907–1919.

Norrström, A. C., and Bergstedt, E. (2010). "The Impact of Road De-Icing Salts (NaCl) on Colloid Dispersion and Base Cation Pools in Roadside Soils." 281–299.

O'Neill, S. W., and Davis, A. P. (2012). "Water Treatment Residual as a Bioretention Amendment for Phosphorus. II: Long-Term Column Studies." *Journal of Environmental Engineering*, 138(3), 328–336.

Owen, D. (2016). "Nutrient Leaching from Bioretention Amended with Source-Separated Compost." Master's Thesis, University of Maryland.

Papenfuse, E. (2016). "Maryland Weather." *Msa.maryland.gov*, <https://msa.maryland.gov/msa/mdmanual/01glance/html/weather.html> (May 23, 2018).

Parameswaran, T. G., and Sivapullaiah, P. V. (2017). "Influence of Sodium and Lithium Monovalent Cations on Dispersivity of Clay Soil." *Journal of Materials in Civil Engineering*, 29(7), 04017042.

Paus, K. H., Morgan, J., Gulliver, J. S., Leiknes, T., and Hozalski, R. M. (2014). "Effects of temperature and NaCl on toxic metal retention in bioretention media." *Journal of Environmental Engineering*, 140(10), 04014034.

Qadir, M., and Oster, J. (2002). "Vegetative bioremediation of calcareous sodic soils: history, mechanisms, and evaluation." *Irrigation Science*, 21(3), 91–101.

Qadir, M., and Schubert, S. (2002). "Degradation processes and nutrient constraints in sodic soils." *Land Degradation & Development*, 13(4), 275–294.

Rengasamy, P., and Olsson, K. (1991). "Sodicity and soil structure." *Australian Journal of Soil Research*, 29(6), 935.

Robinson, H. K., Hasenmueller, E. A., and Chambers, L. G. (2017). "Soil as a reservoir for road salt retention leading to its gradual release to groundwater." *Applied Geochemistry*, Urban Geochemistry, 83, 72–85.

ScienceLab. (2013a). "Lithium Chloride MSDS." <http://www.sciencelab.com/> (May 17, 2018).

ScienceLab. (2013b). "Potassium Chloride MSDS." <http://www.sciencelab.com/> (May 17, 2018).

ScienceLab. (2013c). "Sodium Fluoride MSDS." <http://www.sciencelab.com/> (May 17, 2018).

ScienceLab. (2013d). "Sodium Bromide MSDS." <http://www.sciencelab.com/> (May 17, 2018).

ScienceLab. (2013e). "Sodium Chloride MSDS." <http://www.sciencelab.com/> (May 17, 2018).

ScienceLab. (2013f). "Calcium Chloride MSDS." <http://www.sciencelab.com/> (May 17, 2018).

ScienceLab. (2013g). "Magnesium Chloride MSDS." <http://www.sciencelab.com/> (May 17, 2018).

Shainberg, I., Sumner, M. E., Miller, W. P., Farina, M. P. W., Pavan, M. A., and Fey, M. V. (1989). "Use of Gypsum on Soils: A Review." *Advances in Soil Science*, B. A. Stewart, ed., Springer US, New York, NY, 1–111.

Søberg, L. C., Viklander, M., and Blecken, G.-T. (2014). "The influence of temperature and salt on metal and sediment removal in stormwater biofilters." *Water Science & Technology*, 69(11), 2295.

Søberg, L. C., Viklander, M., and Blecken, G.-T. (2017). "Do salt and low temperature impair metal treatment in stormwater bioretention cells with or without a submerged zone?" *Science of The Total Environment*, 579, 1588–1599.

Stagge, J. H., Davis, A. P., Jamil, E., and Kim, H. (2012). "Performance of grass swales for improving water quality from highway runoff." *Water Research*, 46(20), 6731–6742.

Stanford, G., Dzienia, S., and Vander Pol, R. A. (1975). "Effect of Temperature on Denitrification Rate in Soils1." *Soil Science Society of America Journal*, 39(5), 867.

Sumner, M. E., Rengasamy, P., and Naidu, R. (1998). "Sodic Soils: A Reappraisal." *Sodic Soils: Distribution, Properties, Management, and Environmental Consequences*, Oxfod University Press, New York, 3–17.

Szota, C., Farrell, C., Livesley, S. J., and Fletcher, T. D. (2015). "Salt tolerant plants increase nitrogen removal from biofiltration systems affected by saline stormwater." *Water Research*, 83, 195–204.

Tedoldi, D., Chebbo, G., Pierlot, D., Kovacs, Y., and Gromaire, M.-C. (2016). "Impact of runoff infiltration on contaminant accumulation and transport in the soil/filter media of Sustainable Urban Drainage Systems: A literature review." *Science of The Total Environment*, 569–570, 904–926.

US EPA. (2002). *Consolidataed Assessment and Listing Methodology: Toward a Compendium of Best Practices*. Washington, D.C.

US EPA. (2010). "Source Water Protection Practices Bulletin: Managing Highway Deicing to Prevent Contamination of Drinking Water." Source Water Protection Practices Bulletin.

US EPA. (2015). "Sediment-Related Criteria for Surface Water Quality."

US EPA. (2017). "Chapter 3: Water Quality Criteria." *Water Quality Standards Handbook*, US EPA.

Warren, L. A., and Zimmerman, A. P. (1994). "The influence of temperature and NaCl on cadmium, copper and zinc partitioning among suspended particulate and dissolved phases in an urban river." *Water Research*, 28(9), 1921–1931.

Wiklander, L. (1975). "The role of neutral salts in the ion exchange between acid precipitation and soil." *Geoderma*, 14(2), 93–105.

Willard, L. (2014). "Does It Pay to Be Manure? Assessing the Performance of a Bioretention Cell Seven Years Post-Construction." Master's Thesis, Virginia Polytechnic Institute and State University, Blacksburg, VA.

Winston, R. J., Davidson-Bennett, K. M., Buccier, K. M., and Hunt, W. F. (2016). "Seasonal Variability in Stormwater Quality Treatment of Permeable

Pavements Situated Over Heavy Clay and in a Cold Climate." *Water, Air, & Soil Pollution*, 227(5).

Wong, V. N. L., Greene, R. S. B., Dalal, R. C., and Murphy, B. W. (2010). "Soil carbon dynamics in saline and sodic soils: a review." *Soil Use and Management*, 26(1), 2–11.

Youngblood, S., Vogel, J., Brown, G., Storm, D., McLemore, A., and Kandel, S. (2017). "Field Studies of Microbial Removal from Stormwater by Bioretention Cells with Fly-Ash Amendment." *Water*, 9(7), 526.

Zehetner, F., Rosenfellner, U., Mentler, A., and Gerzabek, M. H. (2009). "Distribution of Road Salt Residues, Heavy Metals and Polycyclic Aromatic Hydrocarbons across a Highway-Forest Interface." *Water, Air, and Soil Pollution*, 198(1–4), 125–132.

Zhang, L., Seagren, E., Davis, A., and Karns, J. (2011). "Long-Term Sustainability of Escherichia Coli Removal in Conventional Bioretention Media." *Journal of Environmental Engineering*, 137(8), 669–677.